Systematic Engine Uprate Technology Development and Deployment for Pipeline Compressor Engines through Increased Torque

FINAL REPORT

(November 2004 - October 2005)

Prepared by:

Dennis Schmitt
Daniel Olsen

Engines and Energy Conversion Laboratory
Department of Mechanical Engineering
Colorado State University
Fort Collins, Colorado 80523-1374
CSU Project # 533822

Prepared for:

Department of Energy
Contract No. DE-FC26-04NT42270

DOE Project Manager
Richard Baker

September, 2005

DISCLAIMER

EXECUTIVE SUMMARY

Three methods were utilized to analyze key components of slow-speed, large-bore, natural gas integral engines. These three methods included the application of computational fluid dynamics (CFD), dynamic modal analysis using finite element analysis (FEA), and a stress analysis method also using FEA. The CFD analysis focuses primarily on the fuel mixing in the combustion chamber of a TLA engine. Results indicate a significant increase in the homogeneity of the air and fuel using high-pressure fuel injection (HPFI) instead of standard low-pressure mechanical gas admission valve (MGAV). A modal analysis of three engine crankshafts (TLA-6, HBA-6, and GMV-10) is developed and presented. Results indicate that each crankshaft has a natural frequency and corresponding speed that is well away from the typical engine operating speed. A frame stress analysis method is also developed and presented. Two different crankcases are examined. A TLA-6 crankcase is modeled and a stress analysis is performed. The method of dynamic load determination, model setup, and the results from the stress analysis are discussed. Preliminary results indicate a 10%-15% maximum increase in frame stress due to a 20% increase in HP. However, the high stress regions were localized. A new hydraulically actuated mechanical fuel valve is also developed and presented. This valve provides equivalent high-energy (supersonic) fuel injection comparable to a HPFI system, at 1/5th of the natural gas fuel pressure. This valve was developed in cooperation with the Dresser-Rand Corporation.

TABLE OF CONTENTS

DISCLAIMER 1
EXECUTIVE SUMMARY 2
TABLE OF CONTENTS 3
LIST OF FIGURES 4
LIST OF TABLES 7
ABBREVIATIONS AND SYMBOLS 8
1.0 Progress and Approach 9
1.1 Optical Engine Evaluations 9
1.2 Component Procurement and Fabrication 9
1.3 Uprate Systems Test Plan 10
1.4 Testing of Uprate Systems 10
2.0 Results and Discussion 11
2.1 Optical Engine Evaluations 11
2.2 Component Procurement and Fabrication 15
2.2.1 Crankshaft Modal Analysis 15
2.2.2 Crankcase Stress Analysis 21
2.3 Hydraulically Actuated Mechanical Fuel Injection System 49
2.4 Uprate Systems Test Plan 52
3.0 Conclusions 53
4.0 Summary 55
4.1 Summary of Accomplishments 55
REFERENCES 56

LIST OF FIGURES

Figure 1 Gas velocity flow field for TLA 11

Figure 2 Fuel distribution at ignition for TLA (fuel mole fraction) 12

Figure 3 Flame propagation and fuel consumption from -6º to 6º (ATDC) for TLA..... 12

Figure 4 Flame propagation and fuel consumption from 10º to 22º (ATDC) for TLA 12

Figure 5 Temperature and NO_x 0º to 30º (ATDC) for TLA 13

Figure 6 Temperature and NO_x 40º to 70º (ATDC) for TLA 13

Figure 7 Fuel gas flow comparisons 120º to 90º (BTDC) for TLA..... 14

Figure 8 Fuel gas flow comparisons 80º to 50º (BTDC) for TLA..... 14

Figure 9 Fuel gas flow comparisons 40º to 10º (BTDC) for TLA..... 15

Figure 10 TLA-6 crankshaft lumped mass approximation example 18

Figure 11 TLA-6 crankshaft modal analysis simulation setup 18

Figure 12 TLA-6 crankshaft modal analysis fringe plot..... 19

Figure 13 Frame stress analysis process flow chart..... 22

Figure 14 GMV-4TF power piston input forces for Working Model simulation..... 23

Figure 15 Working Model GMV-4TF simulation setup with results 24

Figure 16 GMV-4TF crankcase comparison of ‘accurate’ vs. ‘simplified’ models 25

Figure 17 Example of GMV-4TF meshed simplified crankcase 25

Figure 18 Working Model simulation results of GMV crankshaft bearing forces 26

Figure 19 Rosette strain gages 28

Figure 20 Omega strain gage signal conditioner 28

Figure 21 Hi-Techniques data acquisition unit..... 28

Figure 22 Strain gage hardware demonstration apparatus..... 29

Figure 23 Strain gage mounted to test shaft..... 29

Figure 24 Strain gage installation locations example 30

Figure 25 FEA stress results for a GMV-4 crankcase when cylinder 2 is at peak pressure 31

Figure 26 GMV-4 stress analysis results for crankshaft bearing #3 (upper web portion) with approximate strain gage location indicated..... 32

Figure 27 GMV-4 stress analysis results for crankshaft bearing #3 (lower web portion) with approximate strain gage location indicated..... 32

Figure 28 TLA-6 Power piston input forces (nominal) for Working Model simulation .. 34

Figure 29 TLA-6 Compressor piston input forces (nominal) for Working Model simulation..... 34

Figure 30 TLA-6 Power piston input forces (uprated) for Working Model simulation ... 35

Figure 31 TLA-6 Compressor piston input forces (uprated) for Working Model simulation..... 35

Figure 32 Working Model TLA-6 power piston simulation setup with results..... 36

Figure 33 Working Model TLA-6 power piston and compressor simulation setup with results 36

Figure 34 TLA-6 with compressors modeled in Pro Engineer - Wildfire 38

Figure 35 TLA-6 Crankcase modeling comparison..... 38

Figure 36 Mesh of the simplified TLA-6 crankcase..... 39

Figure 37 Simulation results of nominal TLA (with compressor) crankshaft bearing forces..... 40

Figure 38 Simulation results of nominal TLA crankshaft bearing forces 40

Figure 39 Simulation results of uprated TLA (with compressor) crankshaft bearing forces..... 42

Figure 40 Simulation results of uprated TLA crankshaft bearing forces..... 42

Figure 41 TLA-6 Journal bearing locations to cylinder locations 44

Figure 42 Application of loads to crankcase journal bearings..... 45

Figure 43 FEA results for bearings 2/3 with cylinder 2 at peak pressure and standard conditions..... 47

Figure 44 FEA Results for bearings 2/3 with cylinder 2 at peak pressure and uprated conditions 48

Figure 45 Reversed bending fatigue life of gray cast iron[viii] 48

Figure 46 Goodman diagram for indicating safe and unsafe fatigue zones[viii] 49

Figure 47 Cross-section view of typical TLA fuel injection valve..... 50

Figure 48 Cross-section view of new fuel injection valve..... 50

Figure 49 Hydraulically actuated mechanical fuel injection valve assembly..... 51

Figure 50 Hydraulically actuated mechanical fuel injection valve system..... 51

Figure 51 Hydraulic schematic for new fuel valve design 52

LIST OF TABLES

Table 1 Uprate systems test plan 10

Table 2 Engine parameter and modal analysis results comparison 20

Table 3 Input force data at individual cylinder peak force locations for the GMV-4TF.. 26

Table 4 Working Model dynamic force results at selected points for the GMV-4TF..... 27

Table 5 FEA results for a GMV-4 crankcase..... 30

Table 6 Force data at individual cylinder peak force locations for the nominal TLA-6 .. 39

Table 7 Working Model dynamic force results for the nominal TLA-6 with compressors..... 41

Table 8 Force Data at individual cylinder peak force locations for the uprated TLA-6... 41

Table 9 Working Model dynamic force results for the uprated TLA-6 with compressors..... 43

Table 10 FEA Results for a TLA crankcase 46

Table 11 Percent difference between results from the FEA analyses..... 47

ABBREVIATIONS AND SYMBOLS

ATDC	After Top Dead Center
BHP	Brake Horse Power
BMEP	Brake Mean Effective Pressure
BTDC	Before Top Dead Center
CAE	Computer-Aided Engineering
CFD	Computational Fluid Dynamics
CSU	Colorado State University
DOE	Department of Energy
EECL	Engines and Energy Conversion Laboratory
FEA	Finite Element Analysis
GRI	Gas Research Institute
HPFI	High-Pressure Fuel Injection
MGAV	Mechanical Gas Admission Valve
OEM	Original Equipment Manufacturer
PRCI	Pipeline Research Council International, Inc.

1.0 Progress and Approach

1.1 Optical Engine Evaluations

It was concluded that performing testing on the current optical engine (GMV combustion chamber design, 14" bore and stroke) would not provide results applicable to the TLA-6 (17" bore, 19" stroke). The costs associated with refitting the optical engine to match the bore and stroke of the TLA were prohibitive. Originally the optical engine evaluations were to examine the fuel and air mixing processes in the cylinder. Due to the incompatibility of the optical engine, this was accomplished using computational fluid dynamics (CFD). The CFD analysis software used was Star CD and the geometry imported into Star CD for mesh generation was created within PTC's Pro Engineer 3D solid modeling computer-aided engineering (CAE) software. The CFD modeling process for in-cylinder mixing has been validated by comparing modeling results with experiments for similar EECL mixing studies.

In cylinder mixing was evaluated for three different configurations, all based upon a TLA engine. The first case analyzed was for the stock condition, which uses a low-pressure mechanical gas admission valve, and a standard head and piston. The second case is the same as the first except that the enhanced mixing technology is added. The enhanced mixing technology is the high-pressure fuel injection (HPFI) system, which replaces the original MGAV system. The final configuration analyzed consisted of the HPFI system, a modified piston, and a standard head.

1.2 Component Procurement and Fabrication

Verbal donation commitments for high-pressure fuel injection (HPFI) systems from two different vendors, Hoerbiger Corporation of America and Enginuity, LLC have been secured. Altronic Corporation has offered to donate the Hoerbiger HPFI control system, a CPU-2000 spark ignition system, and an engine speed governing system. Additionally, if requested they have indicated that they will provide an add-on module to their CPU-2000 ignition system that will control diesel pilot injectors. Diesel pilot injectors and other required components for the pilot injection system are available from other and on-going research projects.

The EECL, in close collaboration with Dresser-Rand, developed a new hydraulically actuated, inwardly opening, mechanical fuel injection system design. Dresser-Rand has expressed strong interest in commercial development of this system.

1.3 Uprate Systems Test Plan

The uprate systems test plan documents a process for quantifying the engine benefits due to the installation of uprate technologies. In this plan the Clark TLA engine is quantitatively characterized by varying the equivalence ratio and the engine speed in its stock configuration. The stock configuration test measurements include standard temperatures, pressures, and emissions; from this data, combustion statistics are determined. These same measurements are also collected for a similar equivalence ratio and speed map with the implementation of the enhanced mixing technology (HPFI), HPFI and enhanced ignition, and an optimal control methodology. The final set of data measured is with the engine in its uprated condition. This is accomplished with all of the identified uprate technologies acting together while varying the load and speed of the engine up to 20% over rated power. The same measurements that are collected for the other cases are collected for this final configuration. See Table 1 for a chart of the uprate systems test plan. The test plan document was submitted to DOE previously.

Configuration	Operating Condition	Measures
Stock	Equivalence Ratio Map and Speed Map	Standard Temperature, Pressure, Combustion Statistics, HAPS, and Criteria Pollutants
Enhanced Mixing		
Enhanced Mixing & Ignition		
Optimal Control Methodology		
Uprated	Variation of Load and Speed (up to 20% increase BHP)	

Table 1 Uprate systems test plan

1.4 Testing of Uprate Systems

This is to be performed after the baseline testing is complete and the uprate hardware has been installed.

2.0 Results and Discussion

2.1 Optical Engine Evaluations

The CFD results, in lieu of the optical engine evaluations, investigated three configurations for a TLA-6. A summary of the three configurations is as follows:

- OEM TLA with mechanical gas admission valve (MGAV), standard piston, and standard head
- Enhanced mixing (HPFI), standard piston, and standard head
- Enhanced mixing (HPFI), modified crown piston, and standard head

The CFD analysis evaluated the combustion chamber gas velocity during mixing, gas distribution, flame propagation, fuel consumption, temperature distribution, NO_x generation, and a comparison of fuel gas mixing with three different configurations. The gas velocity within the cylinder at ignition can be seen in Figure 1. The velocity flow pattern is set up as a result of the scavenging system design. The flow field present at ignition is residual from the scavenging process. The flow field contains both swirl and tumble characteristics. A representation of fuel distribution at ignition can be seen in Figure 2. Clearly the fuel distribution is highly stratified. See Figure 3 and Figure 4 for images representing flame propagation and fuel gas consumption in the combustion chamber from –6º ATDC to 22º ATDC. Representations of temperature distribution and NO_x generation from TDC to 70º ATDC can be seen in Figure 5 and Figure 6. The fuel gas mixing comparison of the stock configuration vs. HPFI with the stock piston vs. HPFI with a modified piston from 120º BTDC to 10º BTDC can be seen in Figure 7 through Figure 9.

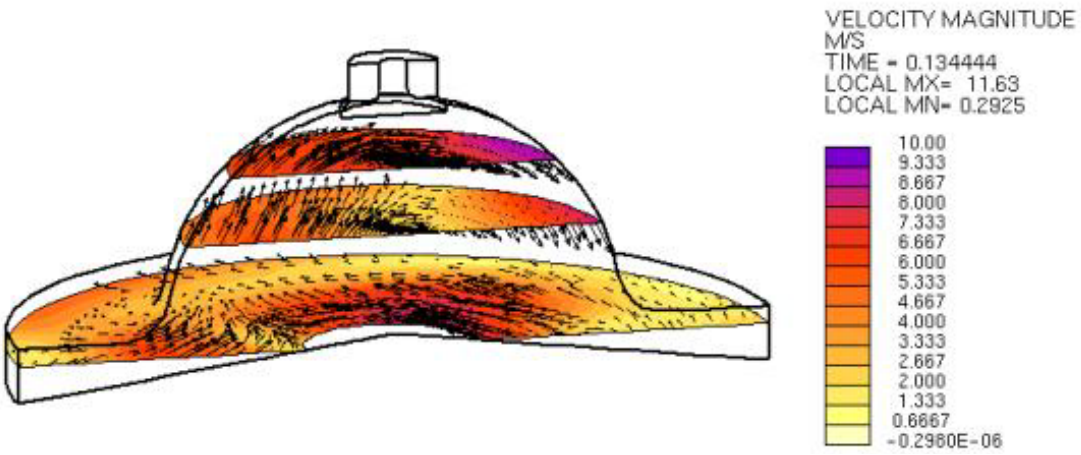

Figure 1 Gas velocity flow field for TLA

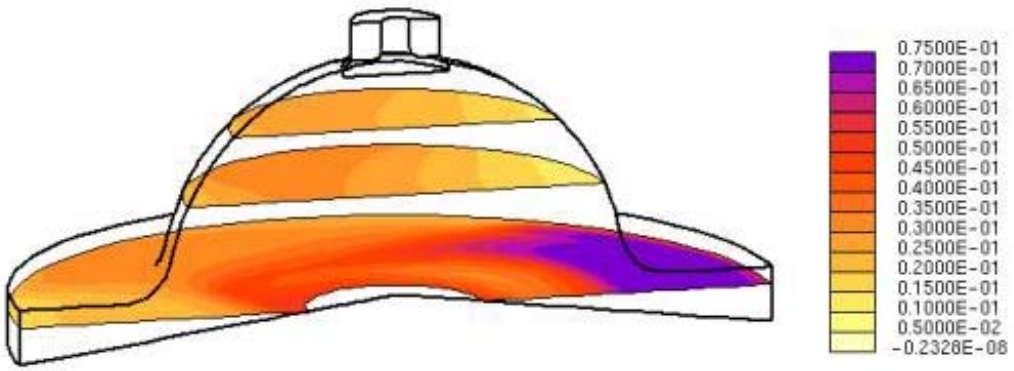

Figure 2 Fuel distribution at ignition for TLA (fuel mole fraction)

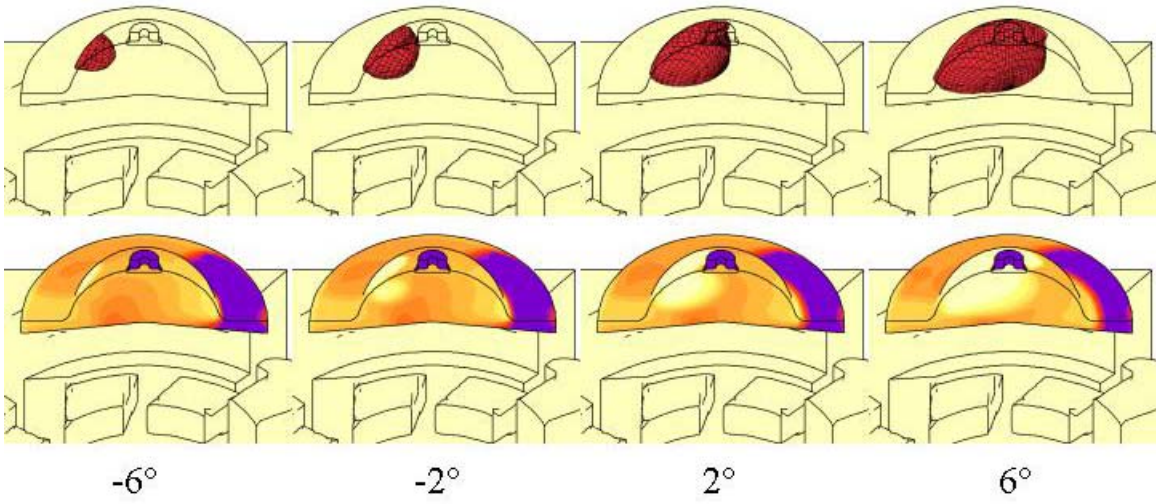

Figure 3 Flame propagation and fuel consumption from -6º to 6º (ATDC) for TLA

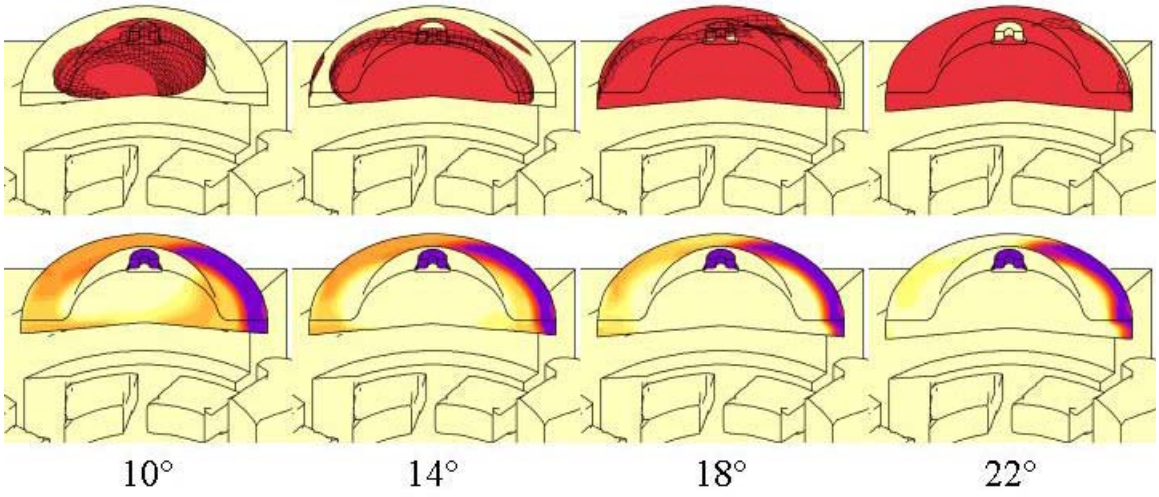

Figure 4 Flame propagation and fuel consumption from 10º to 22º (ATDC) for TLA

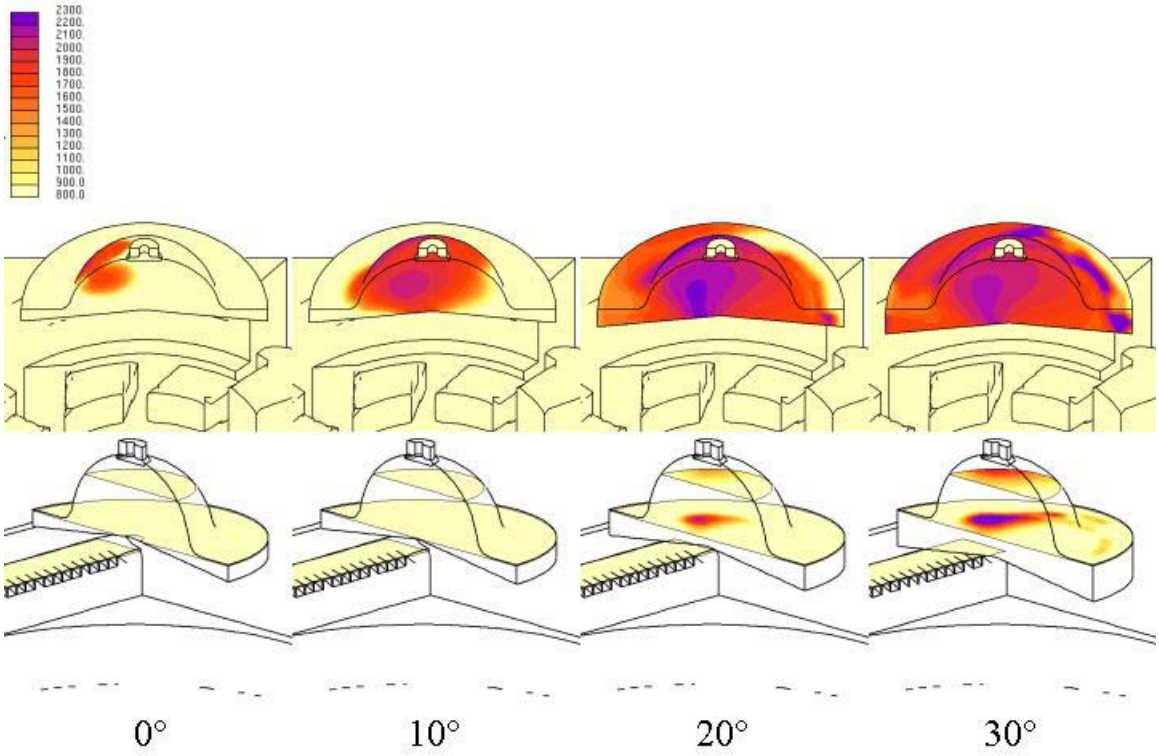

Figure 5 Temperature and NO_x 0º to 30º (ATDC) for TLA

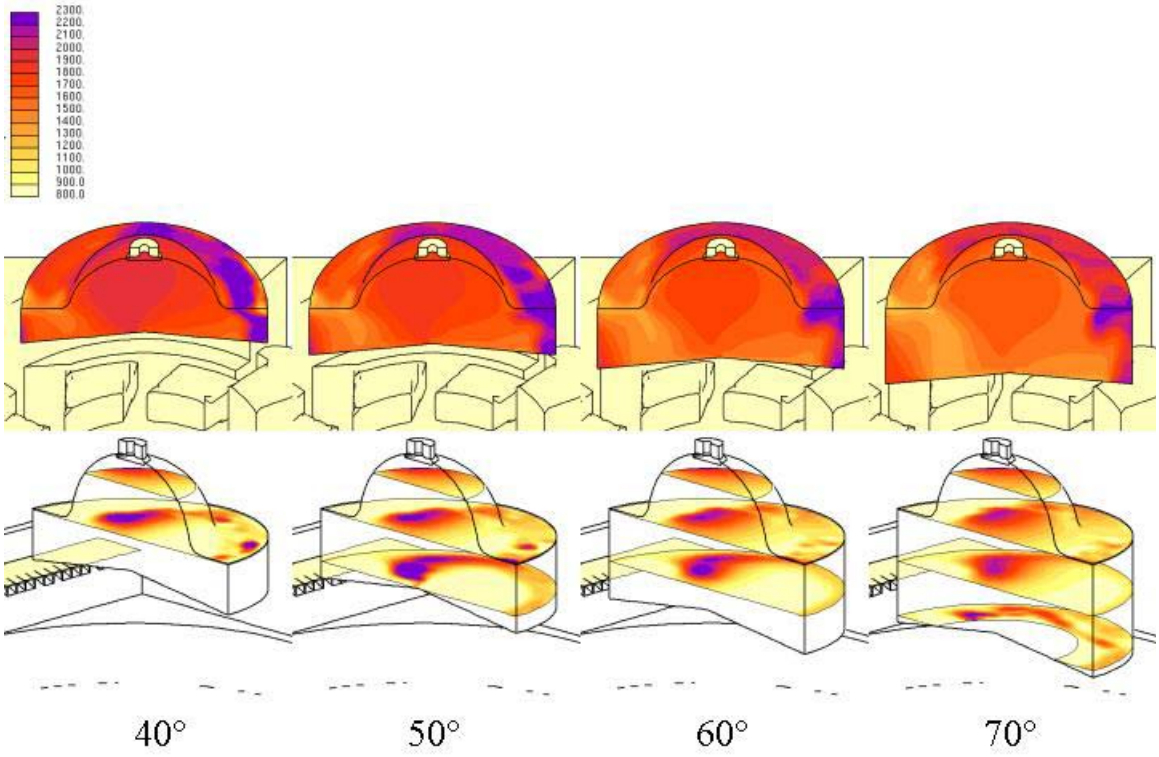

Figure 6 Temperature and NO_x 40º to 70º (ATDC) for TLA

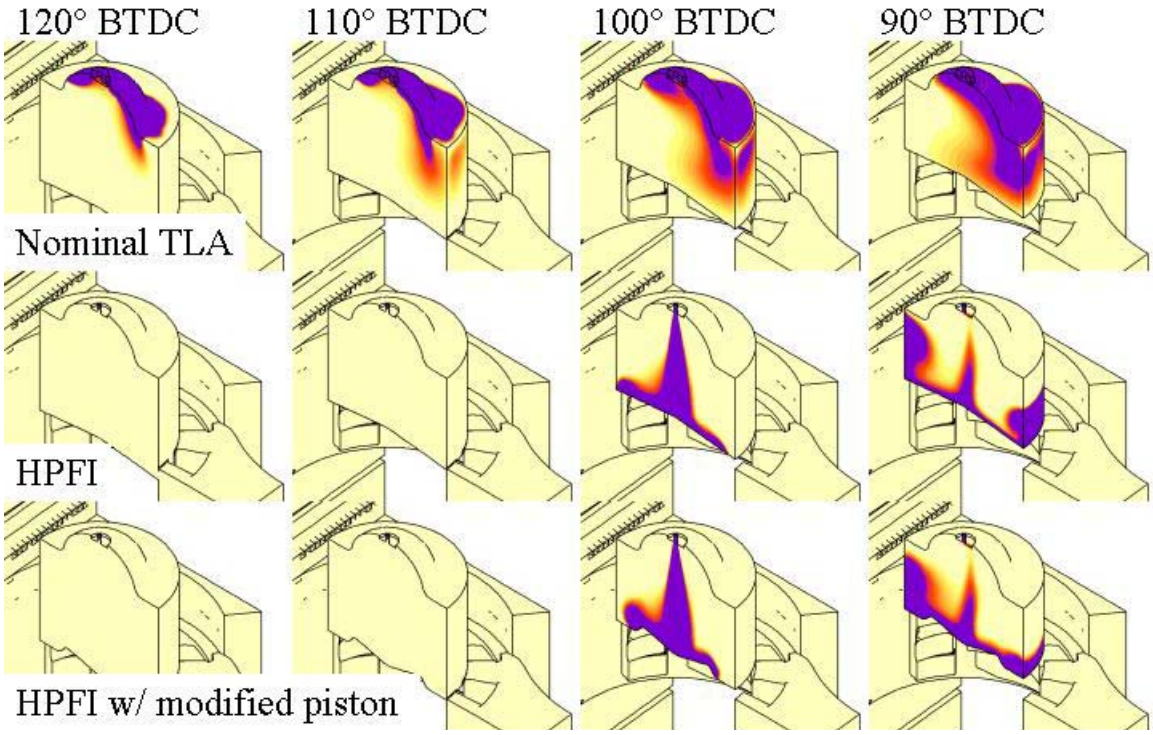

Figure 7 Fuel gas flow comparisons 120º to 90º (BTDC) for TLA

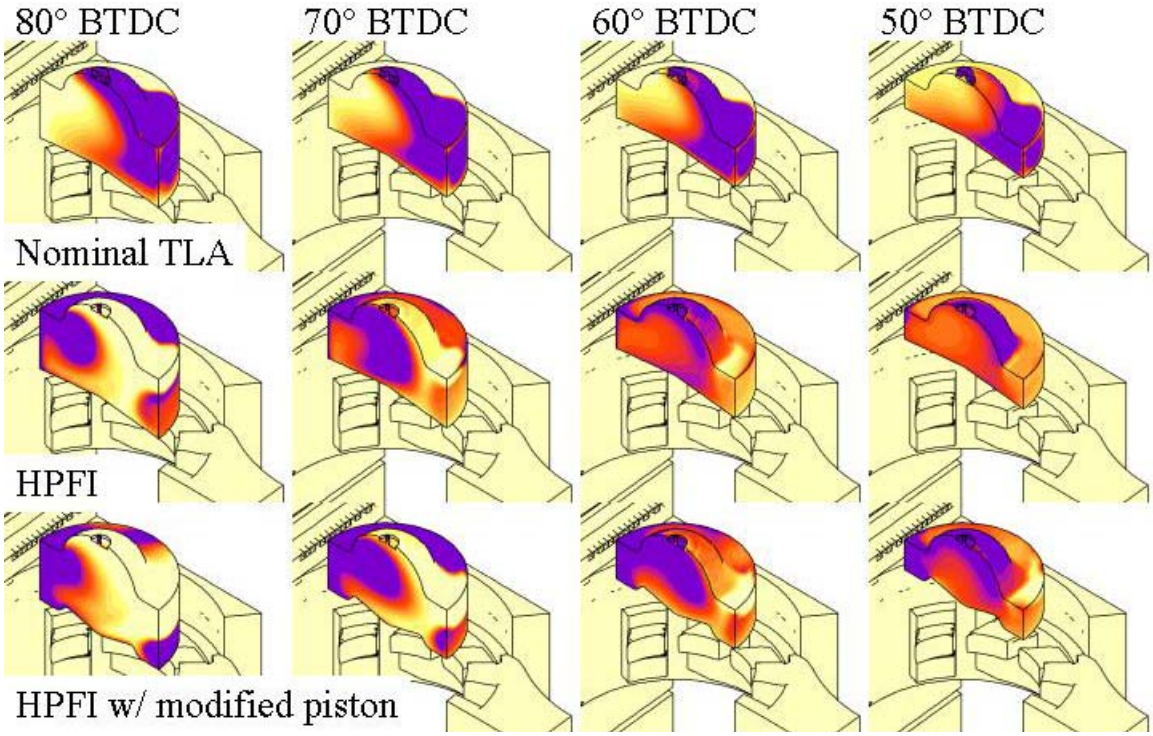

Figure 8 Fuel gas flow comparisons 80º to 50º (BTDC) for TLA

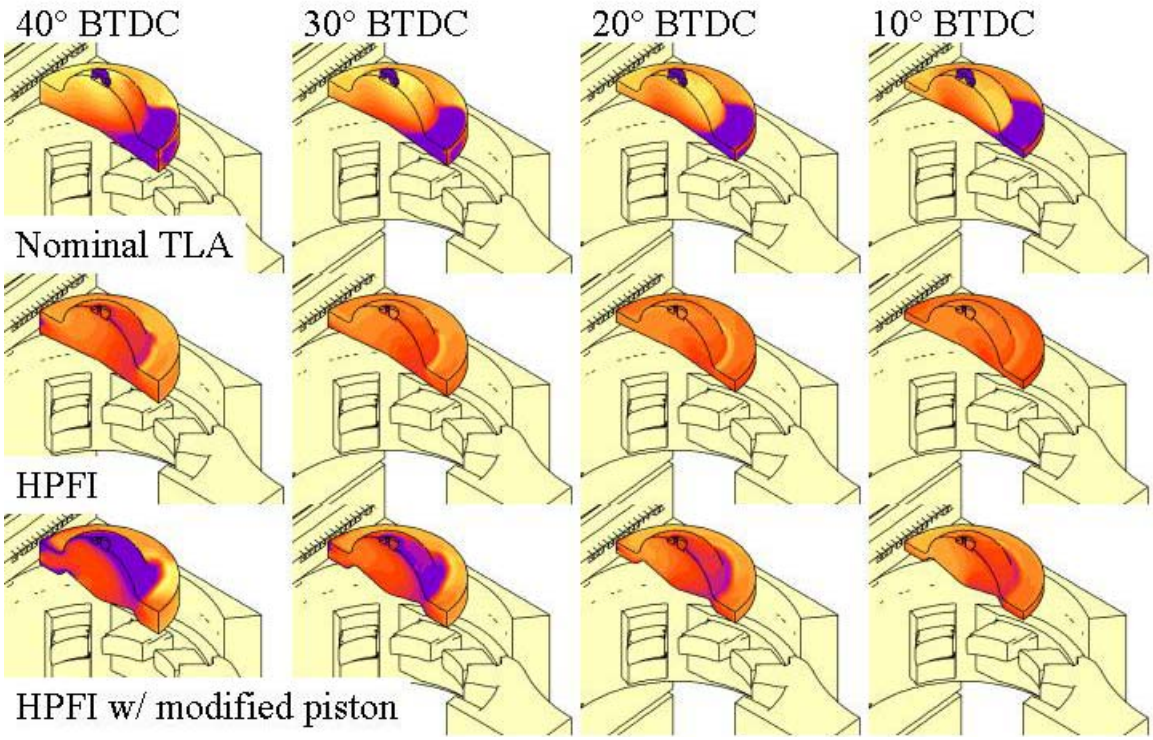

Figure 9 Fuel gas flow comparisons 40º to 10º (BTDC) for TLA

There are a number of important conclusions that can be drawn from the mixing evaluations of the three different cylinder configurations. In Figure 9 at 10°BTDC the HPFI case with the stock piston (center) is better mixed. There is still some level of stratification, but it is clearly a significant improvement over the Nominal TLA case. The modified piston (bottom case) does not improve mixing in the cylinder when compared with the HPFI case with the stock piston.

2.2 Component Procurement and Fabrication

Analysis was performed related to crankshaft speed sensitivities and crankcase stresses. Crankshaft modal analysis was performed on several crankshafts to evaluate operational speed conditions and crankcase stresses were analyzed based upon a nominal operating condition and an uprated condition.

2.2.1 Crankshaft Modal Analysis

2.2.1.1 Background

The need to get more work out of large-bore natural gas integral compressor engines is becoming more prevalent. One method previously used has been to increase the speed of

the engine. This method has been successful, but it is also well documented that there have been many premature crankshaft failures due to the increase in crankshaft stresses. It has been noted by several of the OEM's that if the engine's speed is increased there can be, on some engines, a very real potential of approaching a critical speed where resonance issues become of significant concern. Appendix A contains several OEM memos and report summaries that are in response to this concern.

It is well known and well understood that as a rotating mass approaches its natural frequency, the amplitude of the deflections can become so large that it can cause premature failure, even when below the static critical stress[i]. This is due to an increase of the fatigue effects since the crankshaft begins to deflect more than what would normally be acceptable. If an engine is allowed to run at, or even near a critical speed, these larger deflections can cause locally higher stresses, at stress concentration points, which then amplify fatigue effects, severely cutting short the life of a crankshaft.

The crankshaft is probably one of the most studied components of any internal combustion engine and as such there have been many different methods developed to try to efficiently analyze the crankshaft[ii]. Of the many different methods, there have been analytical models, computer simulation models, a combination of analytical and computer simulation models, and there have been entire computer programs developed just to analyze crankshafts[iii,iv]. Although most of the models are for determining the crankshaft stresses for automotive size engines, the fundamental engineering principles translate to slow-speed, large-bore natural gas engines. Of the varying methods developed, modal analysis methods are thought to be of most interest and benefit for this project. Although there are fewer overall studies relating directly to modal analysis of crankshafts, it is still thought that the engineering fundamentals can still translate to this application.

Solid models of crankshafts for a Clark TLA-6, Clark HBA-6, and Cooper-Bessemer GMV10 were created and studied to see if, through a modal analysis using Pro Mechanica, any insight could be gained regarding their natural frequencies.

2.2.1.2 Clark TLA-6 Crankshaft Analysis

Modal analysis was performed using Pro Engineer's Pro Mechanica Finite Element Analysis (FEA) module. A model of the TLA-6 crankshaft was created and assigned material properties for ductile steel. To account for the attached mass of the connecting rods and piston assemblies, a simplified mass assumption was created to simulate these components, see Figure 10. This 'lumped-mass' however, does not include equivalent

moment of inertia details. The flywheel was modeled and used in the final analyses, but in some of the analyses a point mass assumption was used. This point mass was assigned to the very end of the crankshaft. The crankshaft in a TLA-6 engine is constrained by the crankshaft bearings and the captive ends of the crankcase and upper block. To simulate these constraints, each crankshaft journal bearing was identified and defined as a specific surface on the crankshaft. These defined surfaces then had their respective degrees of freedom constrained. The journal bearing surface associated with the non-flywheel end of the crankshaft was allowed to rotate about the axis of the crankshaft, but was not allowed to translate in the direction of the crankshaft axis. The remaining journal bearing surfaces were allowed to rotate about the crankshaft axis and translate in the direction of the crankshaft axis. All other remaining degrees of freedom were constrained to prevent rotation or translation in the two directions normal to the crankshaft axis. An example of the flywheel and constraints setup can be seen in Figure 11.

The modal analysis results indicated that the first natural frequency of the crankshaft was 59 Hz with the flywheel geometry. This result correlates to an engine speed of approximately 3,540 rpm. Figure 12 provides a graphical representation of the distortion (exaggerated by 10%) due to the resonant condition of the crankshaft. When examining the different critical speeds, the 10^{th} order critical is 354 rpm and would in general be an indication that the crankshaft is not in jeopardy of sustaining any damaging stresses while operating at 300 rpm. At this speed, all i^{th} order critical speeds (where i = 1,2,3, etc.) are considered to be insignificant. Comparison of these results to actual measured modal data is recommended.

Although this modal analysis is approximate, the results are within the expected range when considering what historically are common resonant frequencies of these large-bore natural gas engine crankshafts. Appendix A has OEM communications and report summaries that support this historical perspective.

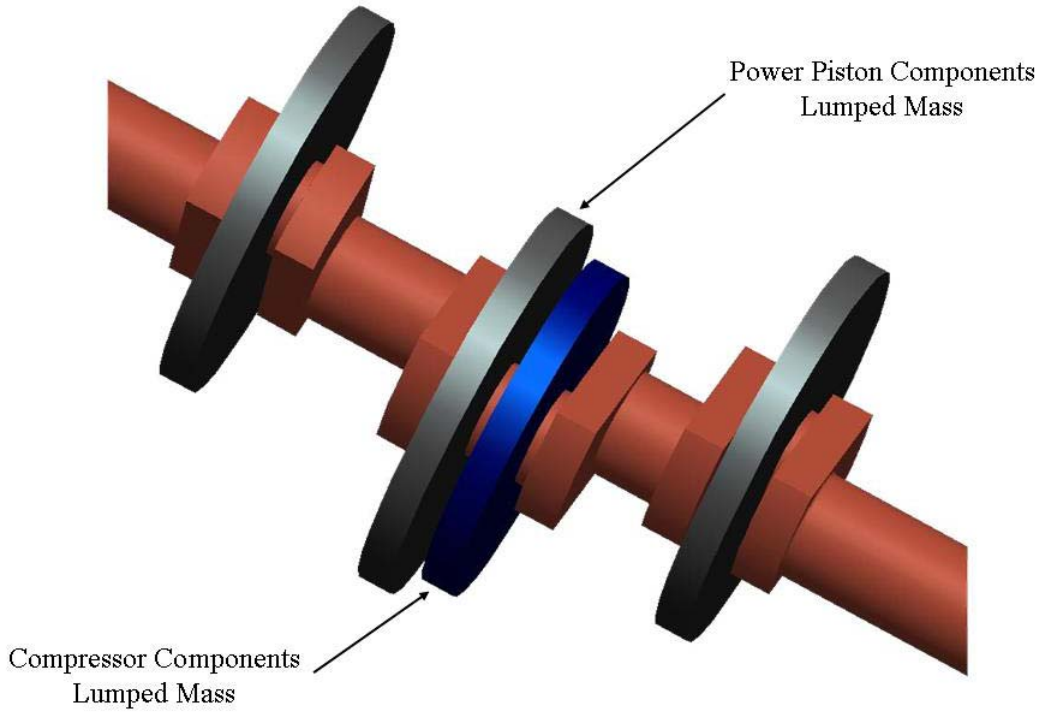

Figure 10 TLA-6 crankshaft lumped mass approximation example

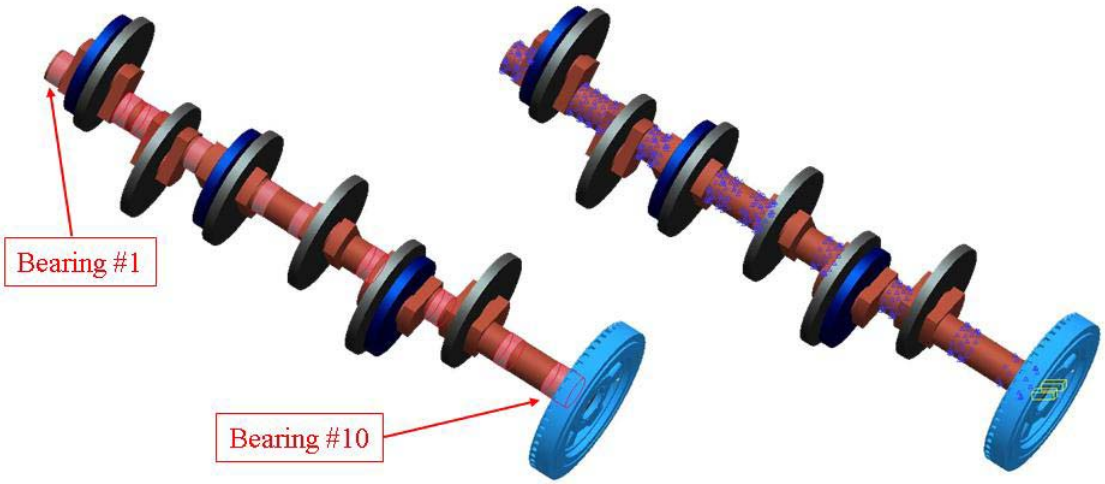

Figure 11 TLA-6 crankshaft modal analysis simulation setup

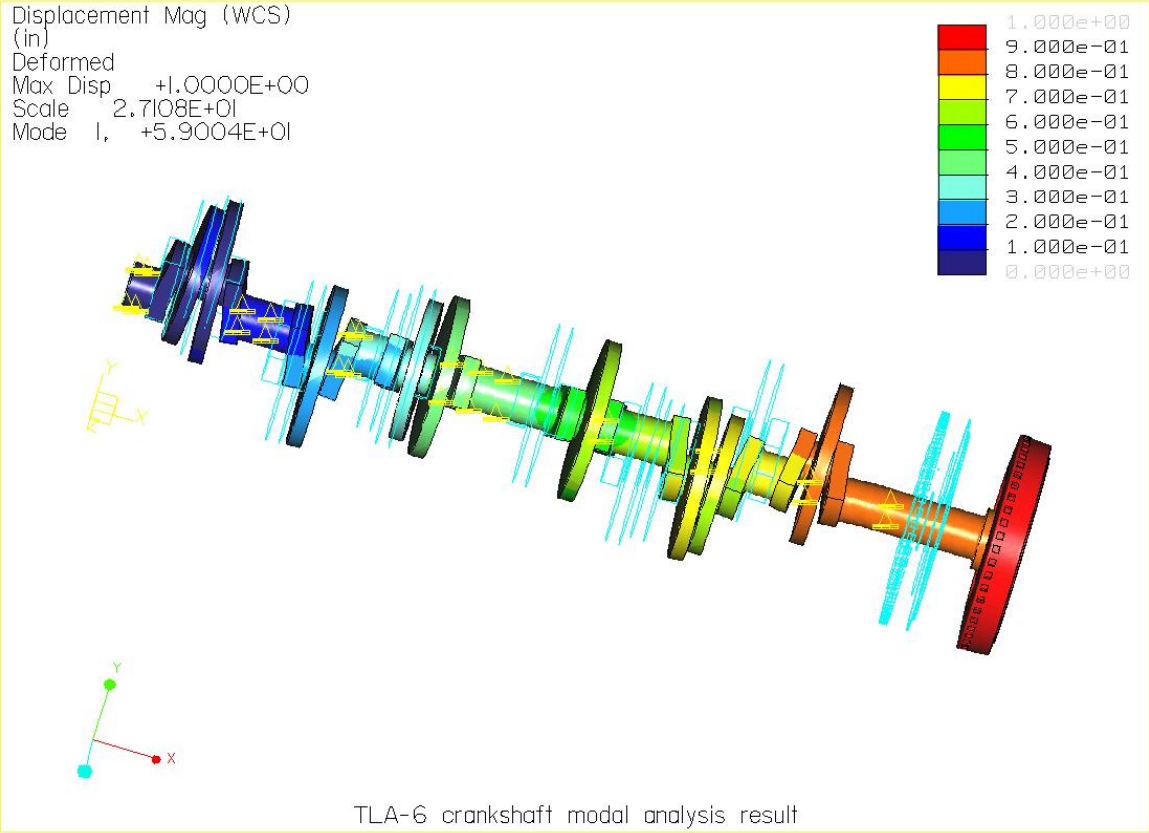

Figure 12 TLA-6 crankshaft modal analysis fringe plot

2.2.1.3 Clark HBA-6 Crankshaft Analysis

Nearly the exact same modal analysis process, as outlined in section 2.2.1.2, was applied to the Clark HBA-6 crankshaft. HBA-6 crankshaft modal analysis models included the flywheel and were compared to modal analysis results using the point mass assumption for the flywheel. The results were similar, in both modeling cases, to those of the TLA-6 analyses. HBA-6 crankshaft modal analysis results indicate that it could have a first harmonic of approximately 54 Hz, or 3,240 rpm. This result indicates that only the 10^{th} order critical, of 324 rpm, would be near the normal operation speed of 300 rpm. At this speed, all i^{th} order critical speeds (where i = 1,2,3, etc.) are considered to be insignificant. Comparison of these results to actual measured modal data is recommended.

2.2.1.4 Cooper-Bessemer GMV-10 Crankshaft Analysis

A Cooper-Bessemer GMV-10 crankshaft was modeled and the same modal analysis process, as outlined in section 2.2.1.2, was applied to this crankshaft was well. Analysis performed on this crankshaft included a point mass assumption for the flywheel as well as a simplified model of a GMV-10 flywheel. The GMV-10 modal analysis results were

similar to analysis results for the TLA and HBA. Results from these modal analyses indicated that the first harmonic was approximately 56 Hz, or 3,360 rpm. This result indicates that the 10^{th} order critical speed would be 336 rpm. This is significantly above the normal operation speed of 300 rpm. All i^{th} order critical speeds (where i = 1,2,3, etc.) above 10 are considered to be insignificant. This suggests the engine could be operated at higher speeds. For this model engine some industry data was available for comparison. From this data (February 14, 2003 Cooper Energy Services Memo in Appendix A), the first harmonic was determined to be at approximately 30 Hz, or 1,785 rpm. This is significantly different than our results. As a point of comparison the Holzer method[v], a well accepted closed form crank shaft analysis technique, predicts 61 Hz for the first harmonic. The Holzer method result supports the Pro Mechanica analysis method. Additionally, the memo states that the 6^{th} order critical speed is 297 rpm. This is surprising since the nominal operating speed is 300 rpm. In our opinion the analysis results given in the February 14^{th} 2003 memo are inconsistent.

2.2.1.5 Analysis Results and Model Comparison

A summary of engine parameters and modal analysis results can be seen in Table 2. The fundamental frequency determined for each crankshaft is listed as well as the flywheel weights, spacing between crankshaft journal bearings and the total lumped mass weights per cylinder. In the case of the TLA-6, cylinders 2, 4, and 6 have a simplified lumped component weight of 1,900 lbs. and 3,300 lbs. for cylinders 1, 3, 5. In the case of the HBA-6 engine, cylinders 1 and 3 have a simplified lumped component weight of 3,084 lbs., cylinders 2 and 5 have a weight of 2,288 lbs., and cylinders 4 and 6 have a weight of 3,332 lbs. The percent difference between the manufacturer's published weights and modeled weights are compared. The GMV-10 assembly was approximately 6% underweight, the TLA-6 assembly was less than 1% overweight, and the HBA-6 was approximately 2% underweight.

	f_n (Hz)	Flywheel Weight (lb)	Bearing Spacing (in)	Total Lumped Mass Weight per Cyl. (lb)	% Diff. for Ass'y Weight (Model vs. Actual)
GMV-10	56	5,380	25.5	2,473	-5.96
TLA-6	52	5,400	31.0	1,900/3,300	0.67
HBA-6	54	5,400	30.0	3,084/2,288/3,332	-2.05

Table 2 Engine parameter and modal analysis results comparison

2.2.2 Crankcase Stress Analysis

2.2.2.1 Background Information

One of the significant concerns regarding uprating many older two-stroke natural gas integral engines is the potential for an increase in component failures. This concern is generally larger for the target engines of this project since they tend have some of the lowest BMEP ratings compared to the rest of the engines in the field today. Traditionally, low BMEP engines also have lighter crankcases compared to later generation engines of similar families (e.g. GMV vs. GMVH). Because of this concern, the internal frame stresses were analyzed to explore the level of internal stresses at nominal conditions compared to that of an uprated condition. This analysis looked at the magnitude, distribution, and location of the stresses within the crankcase. This process is outlined in the following sections. The general process and an accompanying flowchart (see Figure 13) are given below:

- Identify a target engine of interest
- Determine power piston and compressor piston forces, usually from pressure trace data (either from industry input or other engine modeling software)
- Perform dynamic force analysis using the input force data
- Create a solid model of the target engine crankcase
- Input load results from dynamic force analysis into an FEA program (e.g. Pro Mechanica)
- Perform stress analysis
- Analyze results

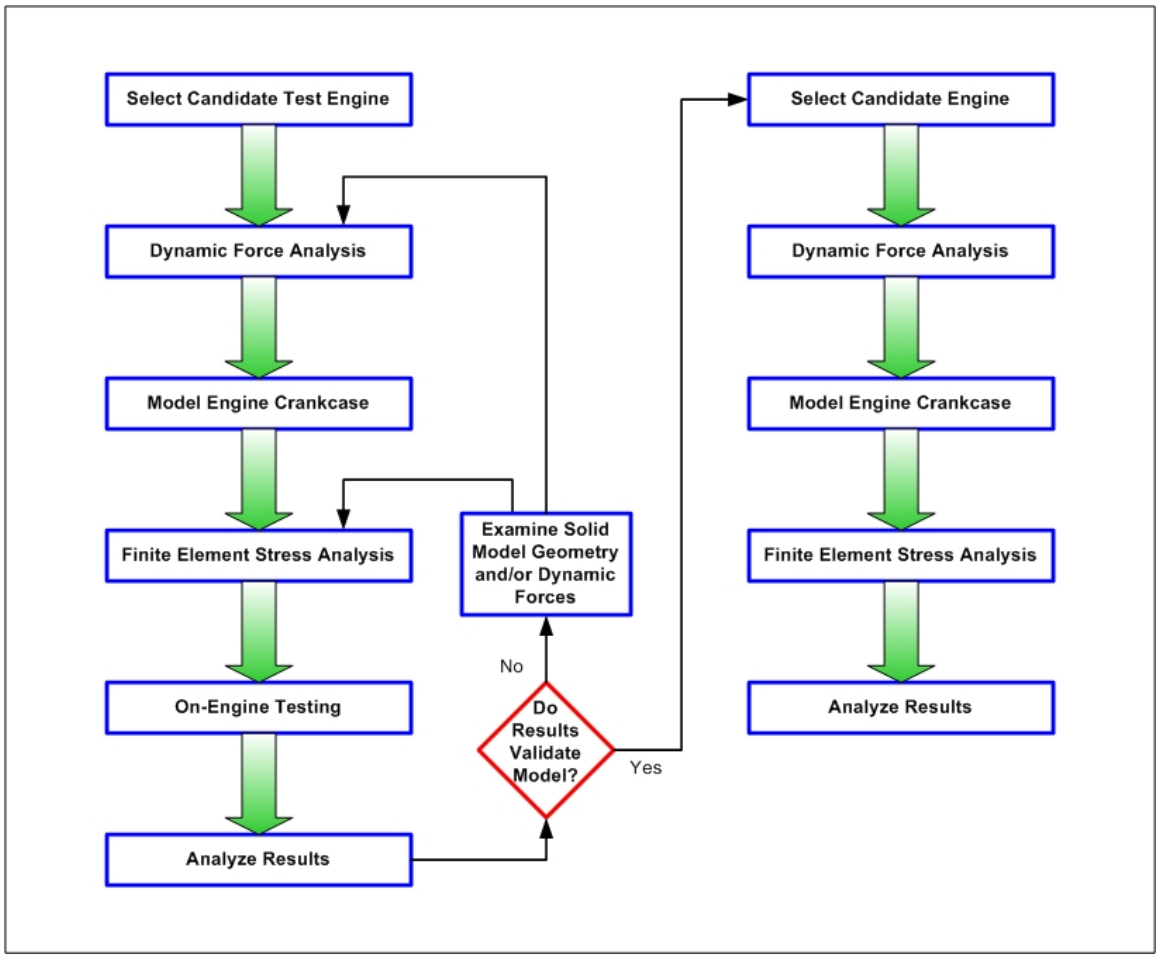

Figure 13 Frame stress analysis process flow chart

The process outlined above is for the crankcase stress measurements; it will be validated with on-engine strain measurements and then correlated to the modeling predictions. The validation process will be performed using the EECL's GMV-4TF and is addressed in the following section.

2.2.2.2 Cooper-Bessemer GMV-4TF Crankcase Analysis

Dynamic Model Analysis

A dynamic analysis of a modeled GMV-4TF engine without compressors, but under a dynamometer load, was performed so that the main bearing forces on the crankcase could be determined. This modeling was performed using MSC Working Model 2D version 5.0 software. The input power piston forces were determined from actual GMV pressure traces that were collected at the EECL during engine testing. The GMV was run with MGAV fuel injection at a nominal, sea level conditions simulated with a boost of 7.5" Hg gage (3.7 psig) from a supercharger and an exhaust backpressure valve. The pressure traces were converted to input force traces and the locations of peak-pressure (peak force)

were maintained at 18° ATDC for each cylinder. The input force profile can be seen in Figure 14. The Working Model simulation takes into account the weights of the components that move and rotate, but all of the geometries are simplified. The pin/bearing diameters of the connecting rods and crank pins were entered and coefficients of friction were also added. The values for the coefficients of friction were set to 0.05. For full hydrodynamic bearings, with the given engine speed, the coefficient of friction probably could have been set to as high as 0.10[vi]. The Working Model GMV simulation setup can be seen in Figure 15. Although the EECL GMV engine does not have the compressors attached to the engine, the crosshead is still attached to the crankshaft and is included in the Working Model simulation setup.

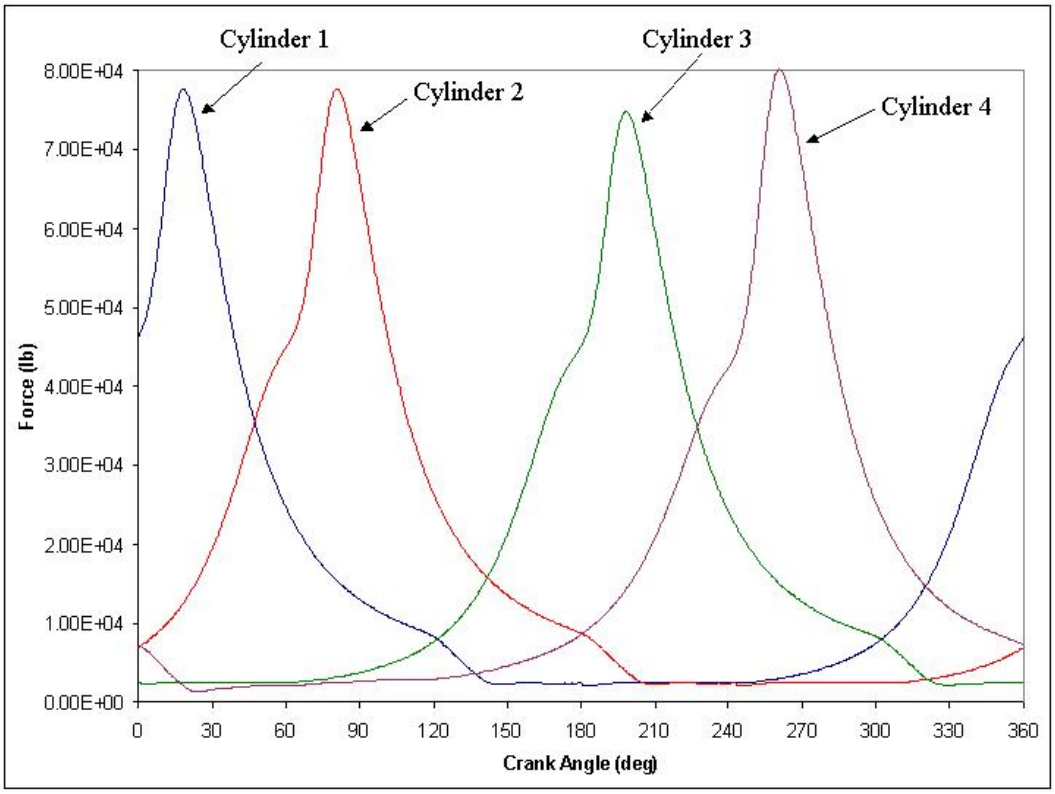

Figure 14 GMV-4TF power piston input forces for Working Model simulation

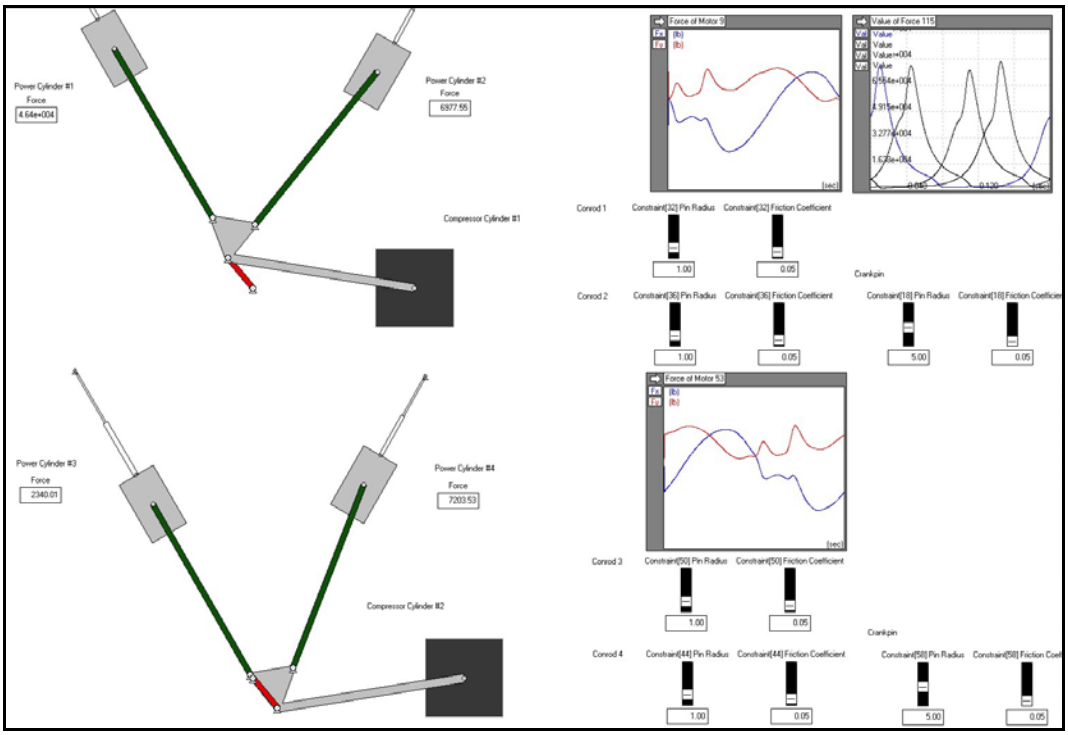

Figure 15 Working Model GMV-4TF simulation setup with results

Finite Element Stress Analysis

A solid model of the GMV-4TF crankcase was created using Pro Engineer Wildfire 3-D solid modeling CAE software. Although no engineering drawings were available initially, the model of the GMV crankcase was approximated according to on-engine measurements and assumptions. Dimensions were then verified or updated once the engineering drawings were received (see left image in Figure 16). The external covers and crankcase end caps were modeled (not shown) and put in place as if they were rigidly connected (bolted) so as to create a more accurate model for stress analysis. Simplification efforts that went into the GMV crankcase model attempted to maintain a majority of the geometric detail, but some superfluous details were removed. This simplification is to assist the meshing process, but not at a cost of stress analysis accuracy. This was achieved by modifying some of the more complex features, specifically related to the crankcase outer structure and some detail of the internal web strengtheners and ribs. See Figure 17 for an example of the meshed crankcase.

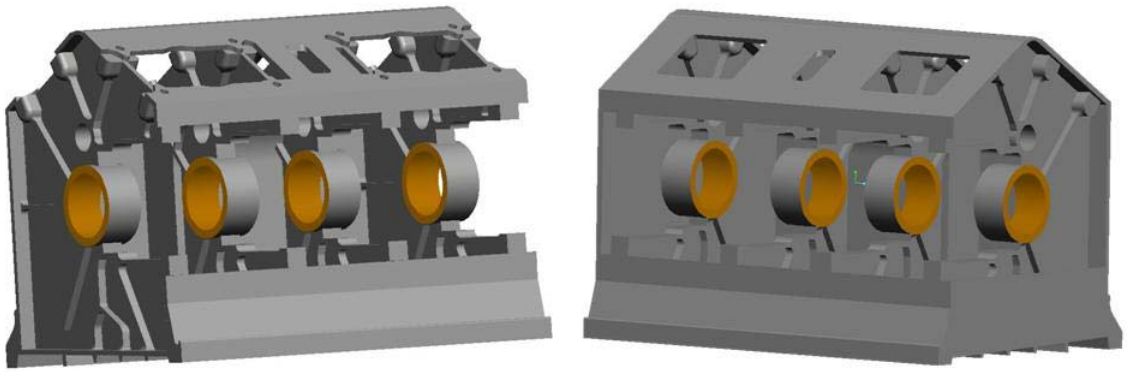

Figure 16 GMV-4TF crankcase comparison of 'accurate' vs. 'simplified' models

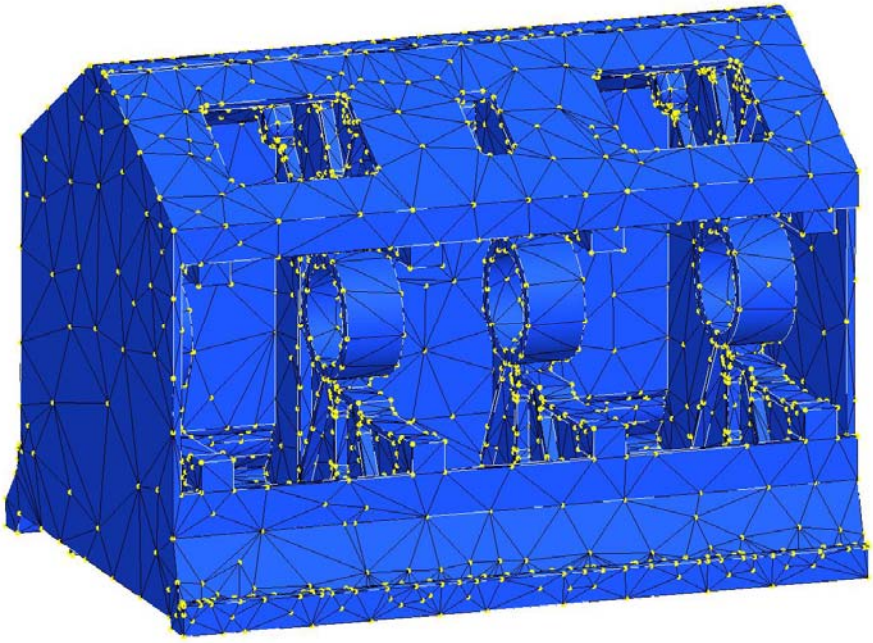

Figure 17 Example of GMV-4TF meshed simplified crankcase

The crankcase material properties that were entered into the FEA software were based upon gray cast iron. Table 3 lists the forces applied to the power pistons at a moment when each of the pistons was at peak pressure (peak force). These were initially the moments in time of primary interest for investigating the internal crankcase stress distributions. Figure 18 illustrates the resulting dynamic forces on the crankshaft journal bearings, where the results are in terms of the forces in the x and y directions. The results are the combined effects of cylinders 1 and 2 together and cylinders 3 and 4 together. The orientation of the +x and +y directions correlates to the model setup in Working Model. These directions are then correlated to the +x and +y directions in Pro Engineer and modified accordingly, if necessary.

The moments in time that were of primary interest for FEA, as stated earlier, occur when each of the power pistons is at peak pressure. After analyzing the graphical results, this was expanded to include four more points of interest that may provide additional insight as to the magnitude and location of critical stresses within the GMV crankcase. The x and y components of these forces for all of the points of interest can be seen in Table 4. These forces listed have had their direction reversed from the data in Figure 18, since they are reaction forces on the crankcase not the crankshaft. The results provided from Working Model are only the reaction forces on the crankshaft, so a transformation is necessary to setup the stress analysis model properly in Pro Mechanica.

		Cylinder Forces (lb)				
Run	Location (CAD)	# 1	# 2	# 3	# 4	Notes
1	18.0	77,630	12,410	2,459	2,082	Cylinder 1 @ P.P.
2	85.5	14,020	73,590	3,417	2,558	Cylinder 2 @ P.P.
3	198.0	2,463	3,931	74,780	14,140	Cylinder 3 @ P.P.
4	260.5	2,971	2,463	15,030	80,100	Cylinder 4 @ P.P.

Table 3 Input force data at individual cylinder peak force locations for the GMV-4TF

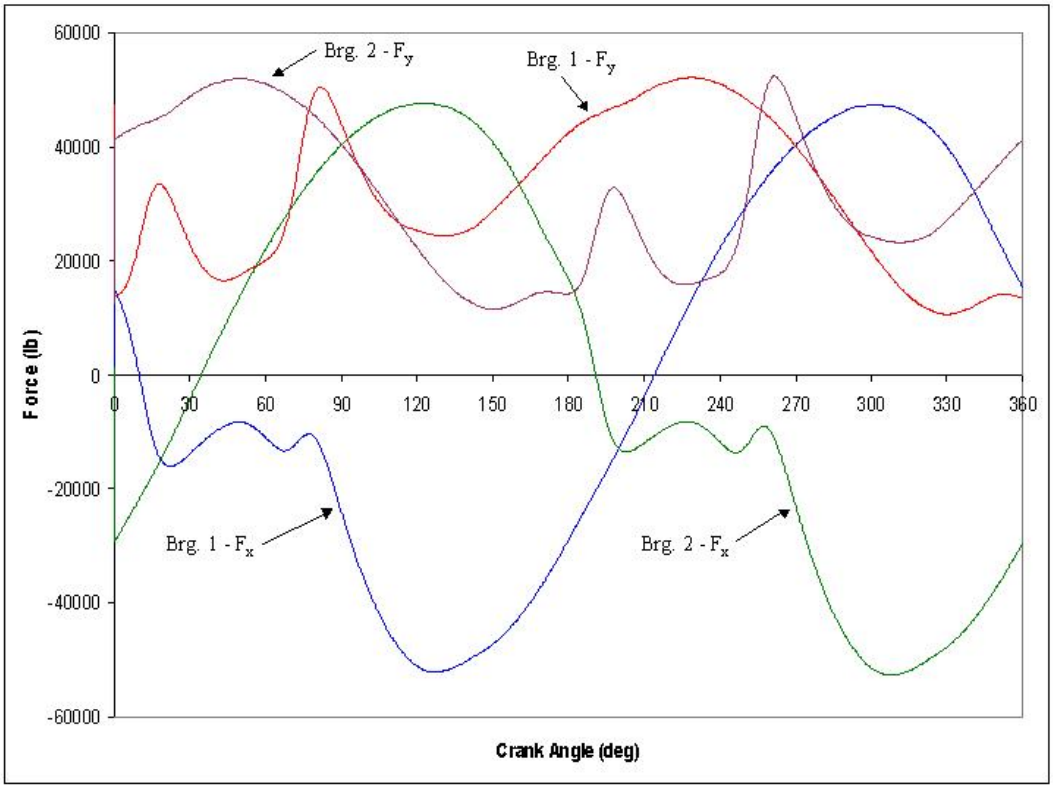

Figure 18 Working Model simulation results of GMV crankshaft bearing forces

		Crankcase Bearing Saddle Forces (lb)				
		# 1 (Cyl's 1&2)		# 2 (Cyl's 3&4)		Notes
Run	Location (CAD)	x-dir	y-dir	x-dir	y-dir	
1	18.0	14,420	-33,430	15,300	-45,090	Cylinder 1 @ P.P.
2	85.5	17,280	-48,700	-38,120	-42,720	Cylinder 2 @ P.P.
3	198.0	14,590	-46,840	11,670	-32,760	Cylinder 3 @ P.P.
4	260.5	-35,580	-44,770	10,170	-52,030	Cylinder 4 @ P.P.

Table 4 Working Model dynamic force results at selected points for the GMV-4TF

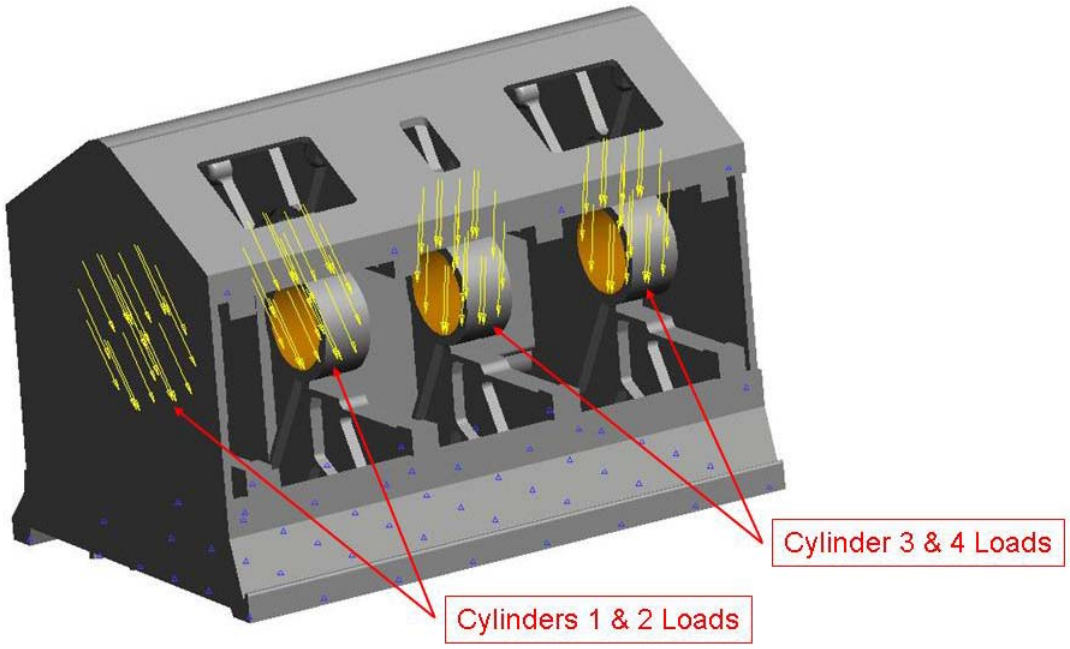

The crankcase stress analysis was performed using Pro Engineer's FEA module, Pro Mechanica. For each moment in time to be investigated, the bearing loads on the crankcase were entered into the model. Constraints for the overall crankcase were also applied. This allowed for accounting for the grouting and anchoring of the engine to an engine skid. It should be noted that, although the engine is constrained based upon near-real world engine support schemes, the software treats this as an idealized case and does not account for the degradation of grout pads and other anchoring systems. Other preliminary loads were added to the crankcase model as well, such as the weights of the cylinder/head assembly for each power piston.

On-Engine Testing

The crankcase FEA results are to be used as a guide for locating the strain gages on the crankcase for the on-engine model verification measurements. Rosette style strain gages

(see Figure 19) and a signal-conditioning unit (see Figure 20) were purchased for the on-engine testing, which will interface with the data acquisition unit (see Figure 21). Prior to the on-engine testing, a test device was fabricated to verify operation and to provide insight to any calibration needs that may arise from the use of the strain gages (i.e. temperature compensation, voltage offsets, etc.). A simple cantilevered tube with a predetermined torque and bending moment was used to verify system operation and identify any calibration issues, shown in Figure 22 and Figure 23.

GMV-4 FEA results were analyzed and then higher stress locations that were determined by FEA were compared to actual engine geometry and access. It was determined that due to limited access, the strain gages would be located on the thin-walled, vertically oriented portion of the crankcase webs either above or below the crankshaft journal bearing, identified in Figure 24. This allowed for two rosettes per journal bearing to be installed, for a total of eight rosettes. Two rosettes, or one journal bearing location, can be measured at a time during data collection.

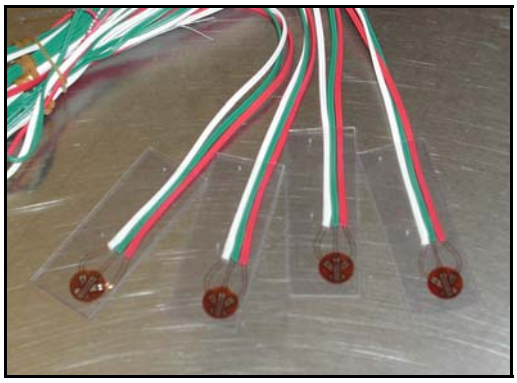

Figure 19 Rosette strain gages

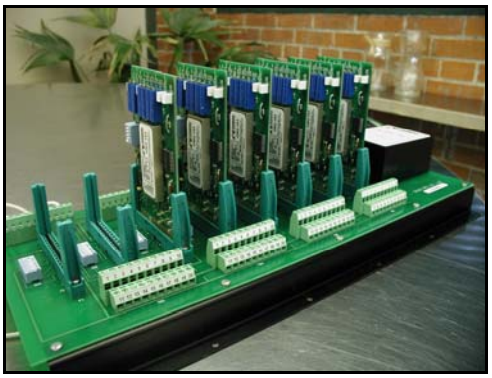

Figure 20 Omega strain gage signal conditioner

Figure 21 Hi-Techniques data acquisition unit

Figure 22 Strain gage hardware demonstration apparatus

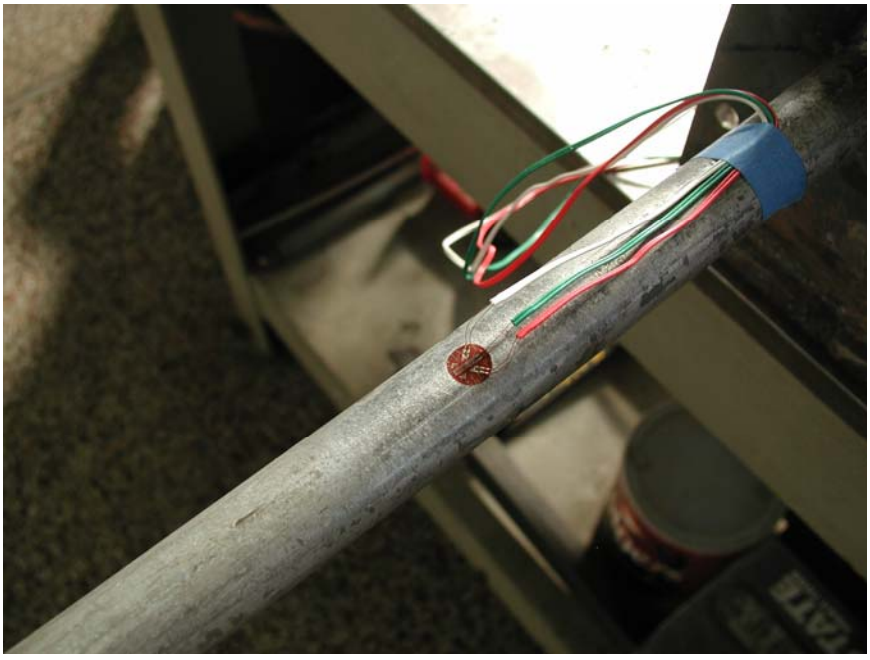

Figure 23 Strain gage mounted to test shaft

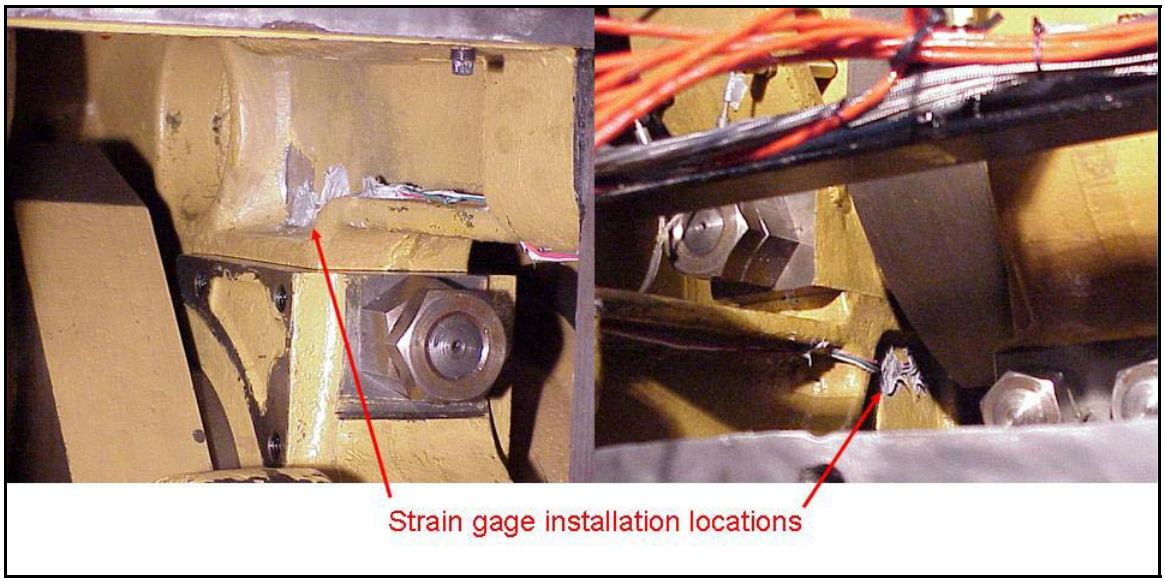

Figure 24 Strain gage installation locations example

Finite Element Stress Analysis Results vs. On-Engine Testing Results

FEA results indicated that the stresses within the crankcase are significant but only in localized regions. These locations of high stress are also worth evaluating since modeled geometry does not always represent actual geometry exactly. Table 5 summarizes the results from the four cases that were examined. The values of stress are the von Mises stress and the maximum principle stress. The maximum stress was a principal stress of -39,285 psi and is predicted to occur when cylinder 2 is at peak pressure. The negative sign indicates a direction relative to the world coordinate system within Pro Engineer. Crankcase stress results can be seen graphically in Figure 25. This figure represents the stress distributions within the crankcase when cylinder 2 is at peak pressure. The stress range has been reduced (0 to 4,000 psi) to provide a graphical representation that provides better resolution for the lower stress regions.

Stress (psi)	Cylinder 1 @ P.P	Cylinder 2 @ P.P	Cylinder 3 @ P.P	Cylinder 4 @ P.P
V.M.	21,742	28,649	24,109	24,122
Max. Principal	-27,822	-39,285	-33,110	-27,508

Table 5 FEA results for a GMV-4 crankcase

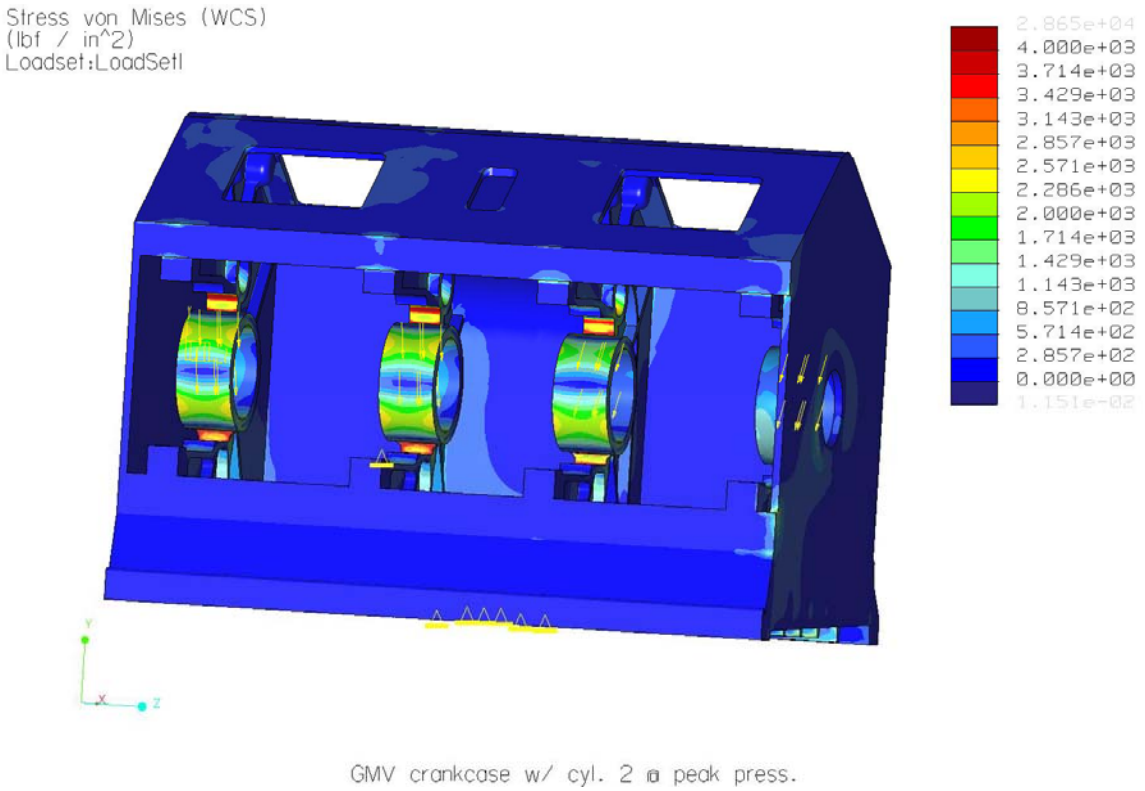

Figure 25 FEA stress results for a GMV-4 crankcase when cylinder 2 is at peak pressure

Since the high stress regions are localized and modeled geometry closely, but not exactly, represents actual geometry, FEA results can help provide a method for a more conservative, worst case, analysis. In order to determine the accuracy of the method, strain gages will be used to capture actual stress data. As presented earlier, the strain gages were mounted above and below each main crankshaft bearing, on the vertical portion of the crankcase webs. Figure 26 and Figure 27 show stress analysis results of the corresponding modeled regions where the strain gages are installed (approximately) on the GMV crankcase. The strain gage testing was not able to be completed on this project because of funding constraints. However, it was completed as part of a student Masters Thesis by Schmitt. The results are presented in detail in that work. The testing showed that for 13 out of 16 measurements above the bearings and 12 out of 16 measurements below the bearings the finite element model under predicted stress when compared with the measured values. The average percent difference between measured and modeled stress values for the upper and lower bearings was 58% and 33%, respectively. Although the differences are considerable, the crank case FEA is still extremely valuable in identifying key regions where reinforcement is needed. Caution is advised, however, when using the results to arrive at operational safety factors.

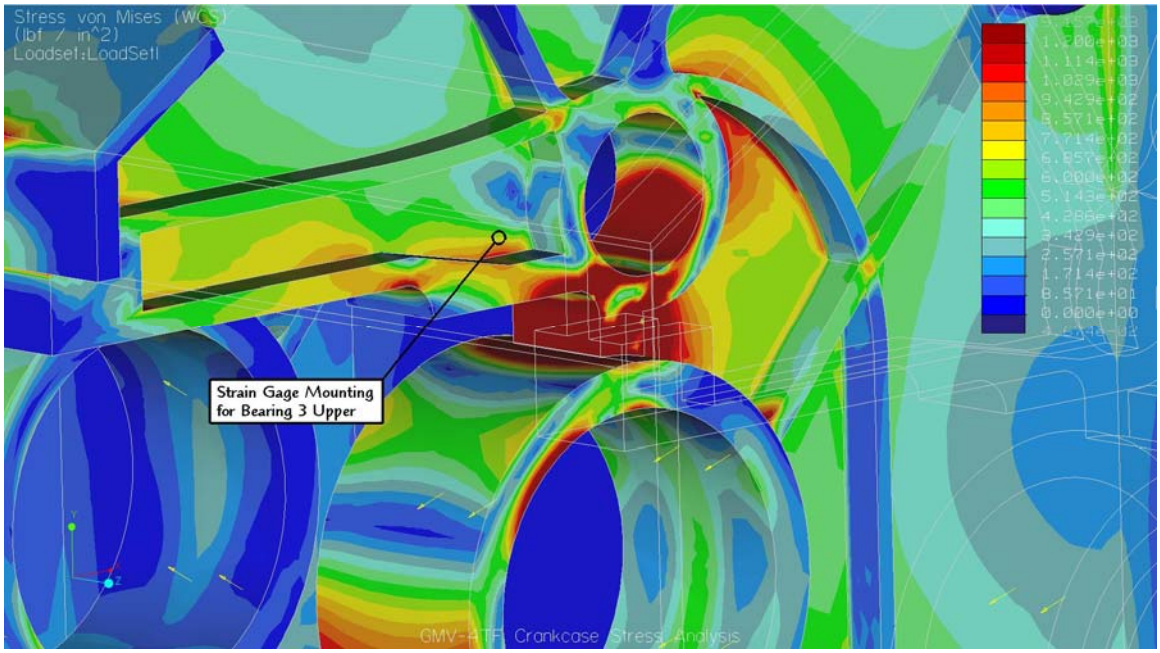

Figure 26 GMV-4 stress analysis results for crankshaft bearing #3 (upper web portion) with approximate strain gage location indicated

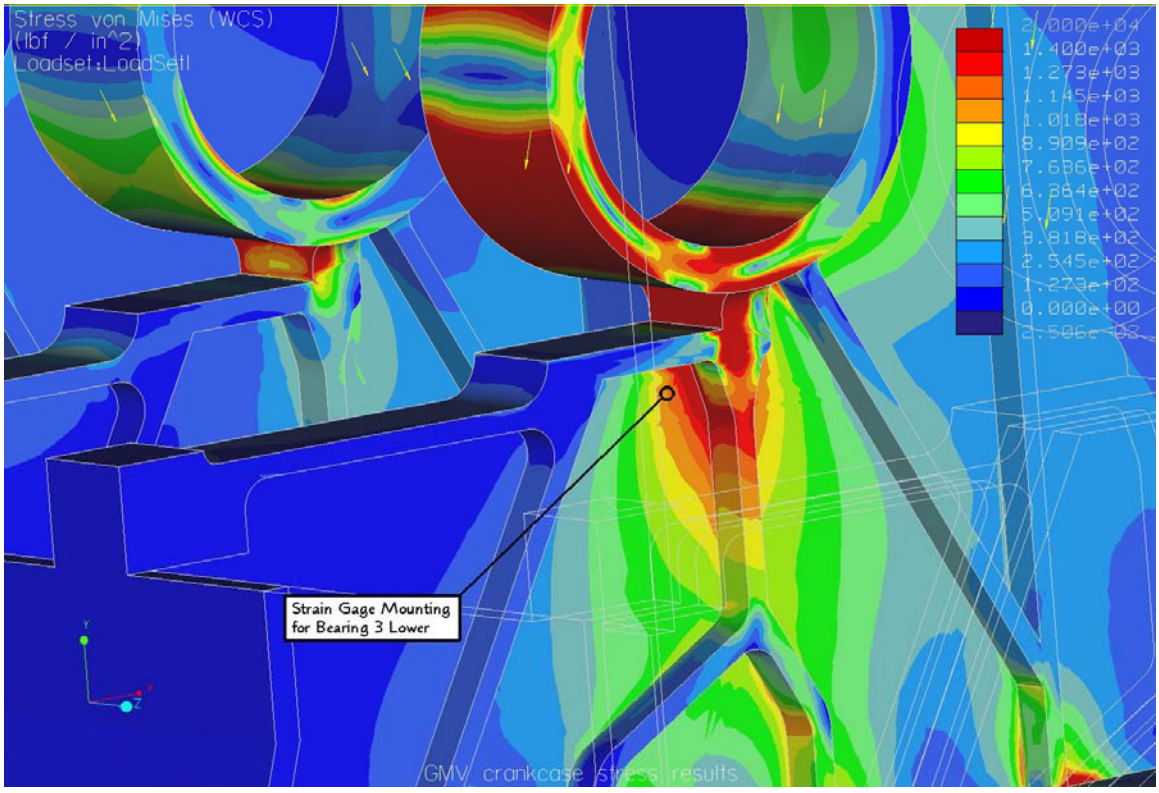

Figure 27 GMV-4 stress analysis results for crankshaft bearing #3 (lower web portion) with approximate strain gage location indicated

2.2.2.3 Clark TLA-6 Frame Stress Analysis

Dynamic Model Analysis

A dynamic analysis of a modeled Clark TLA-6 engine with three compressors was performed so that the extent of the increase in main bearing forces due to increased load (via torque) could be better understood. Two modeling scenarios were run and compared to each other, one with the pressure trace at nominal conditions and the second with the pressure trace at an uprated condition. This modeling was performed using MSC Working Model 2D version 5.0 software and the Ricardo Wave Model. The Wave Model software provided a pressure trace based upon the engine's parameters and operating conditions. The pressure trace data maintained the location of the peak pressure at 18° ATDC. The pressure trace data was determined at a standard boost pressure of 20 psi and at an increased (uprated) boost pressure of 24 psi, a 20% increase[vii]. The Working Model software then was provided power piston force data, calculated from the pressure trace data; the input force profiles can be seen in Figure 28 and Figure 30. The Working Model software was also provided the compressor piston force data, which was calculated from industry data for inlet and suction gas pressures and assumed pressure transition profiles. The compressor input force data can be seen in Figure 29 and Figure 31[viii]. The Working Model simulation takes into account the weights of the components that move and rotate, but all of the geometries are simplified. The pin/bearing diameters of the connecting rods and crank pins were entered and coefficients of friction were also added. The values of the coefficients of friction for the wrist pin and crank journal bearings were set to 0.05. The value of the coefficient of friction for the piston rings on the cylinder wall was set to 0.15. For full hydrodynamic bearings, at the given engine speed, the coefficient of friction probably could have been set to as high as 0.10[vi]. The TLA model also included the piston ring frictional effects by approximating this with a slot friction element. The Working Model TLA-6 simulation setup can be seen in Figure 32 and Figure 33. The results from this modeling indicate that, as expected, the forces would increase with an increase in load, which would result from higher peak cylinder pressures.

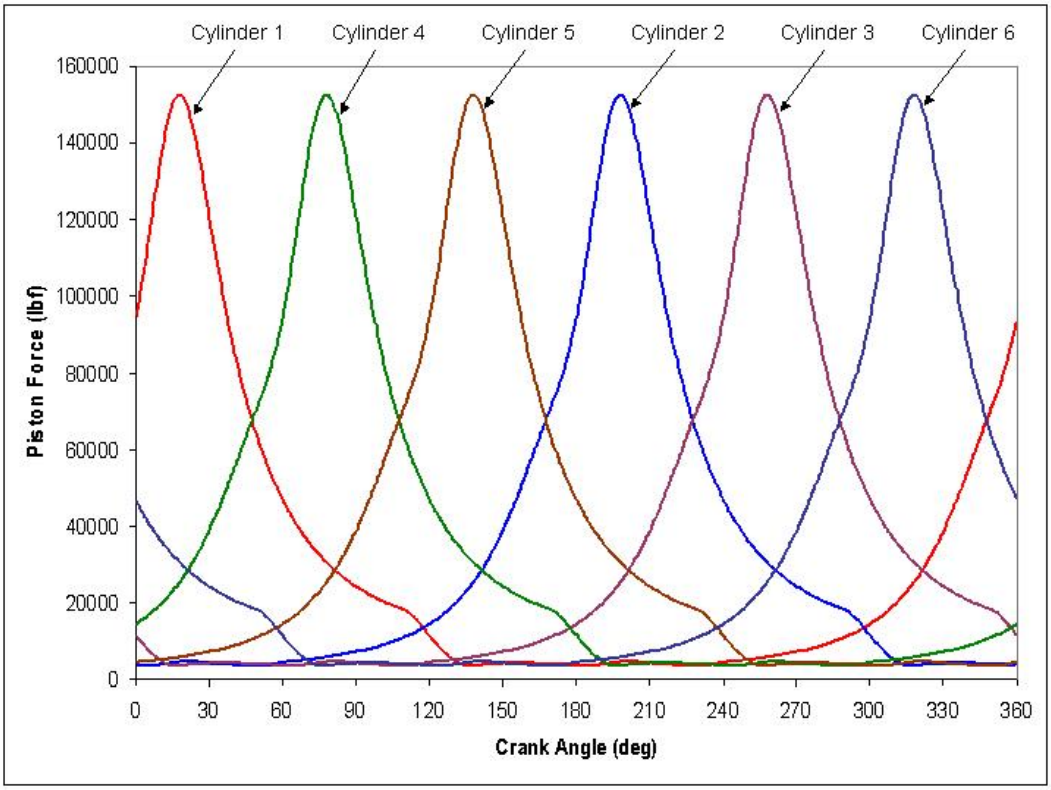

Figure 28 TLA-6 Power piston input forces (nominal) for Working Model simulation

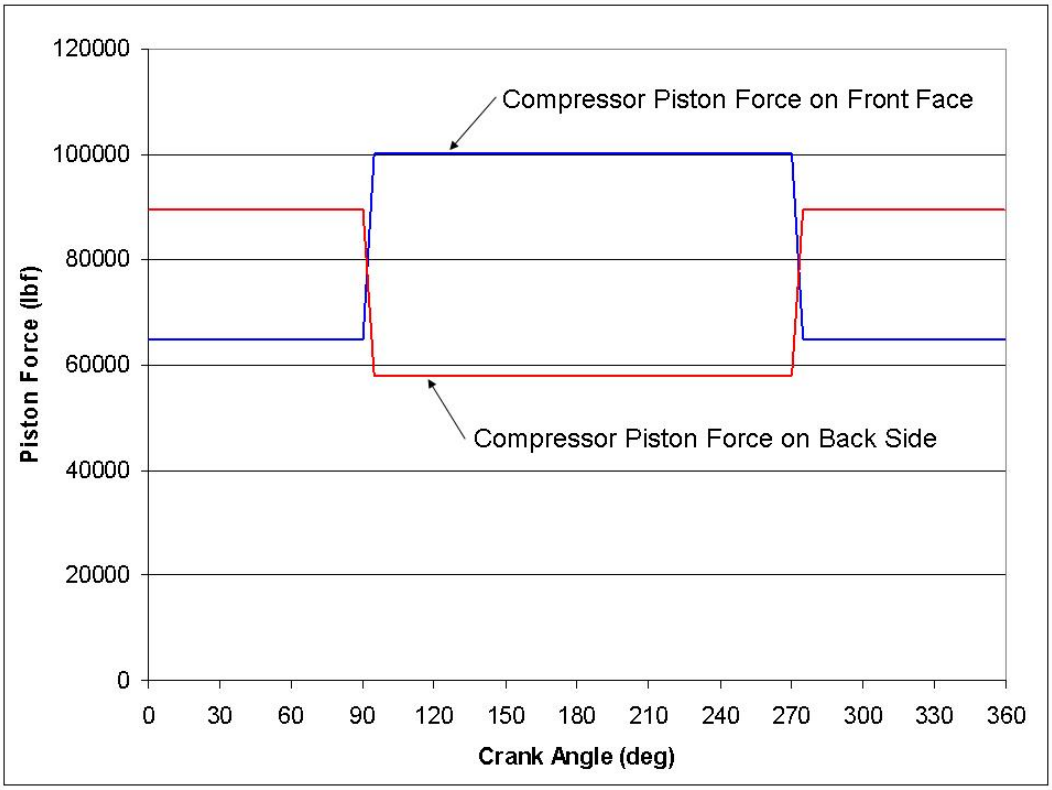

Figure 29 TLA-6 Compressor piston input forces (nominal) for Working Model simulation

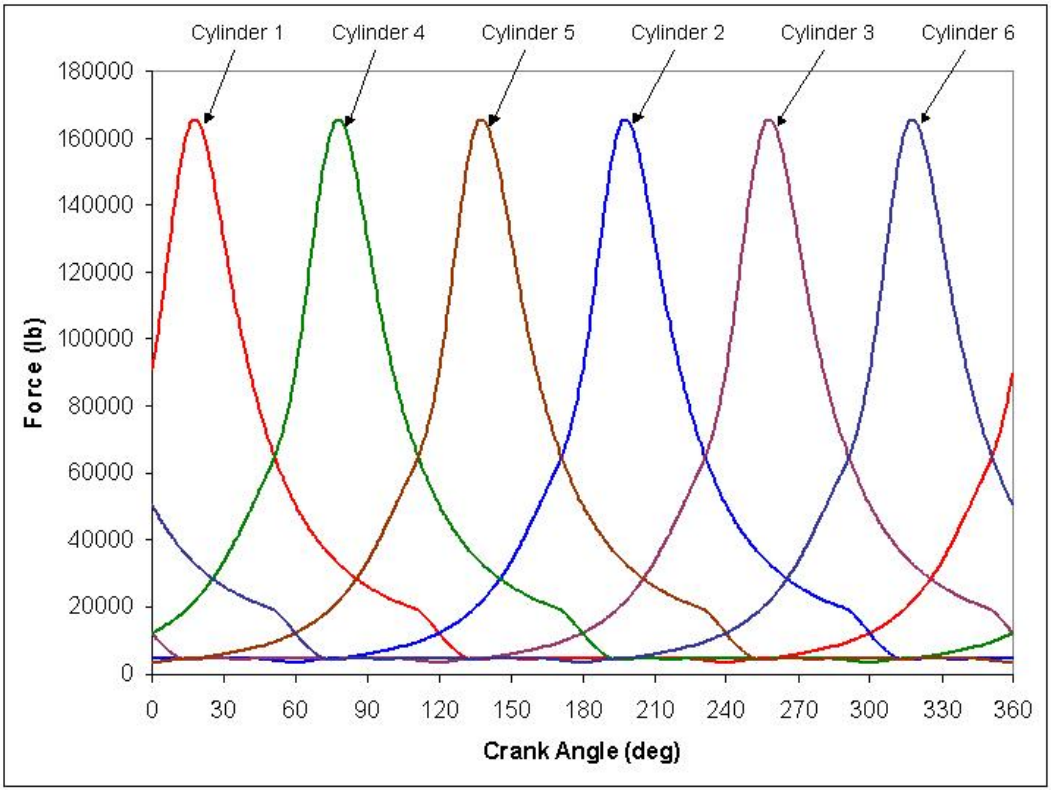

Figure 30 TLA-6 Power piston input forces (uprated) for Working Model simulation

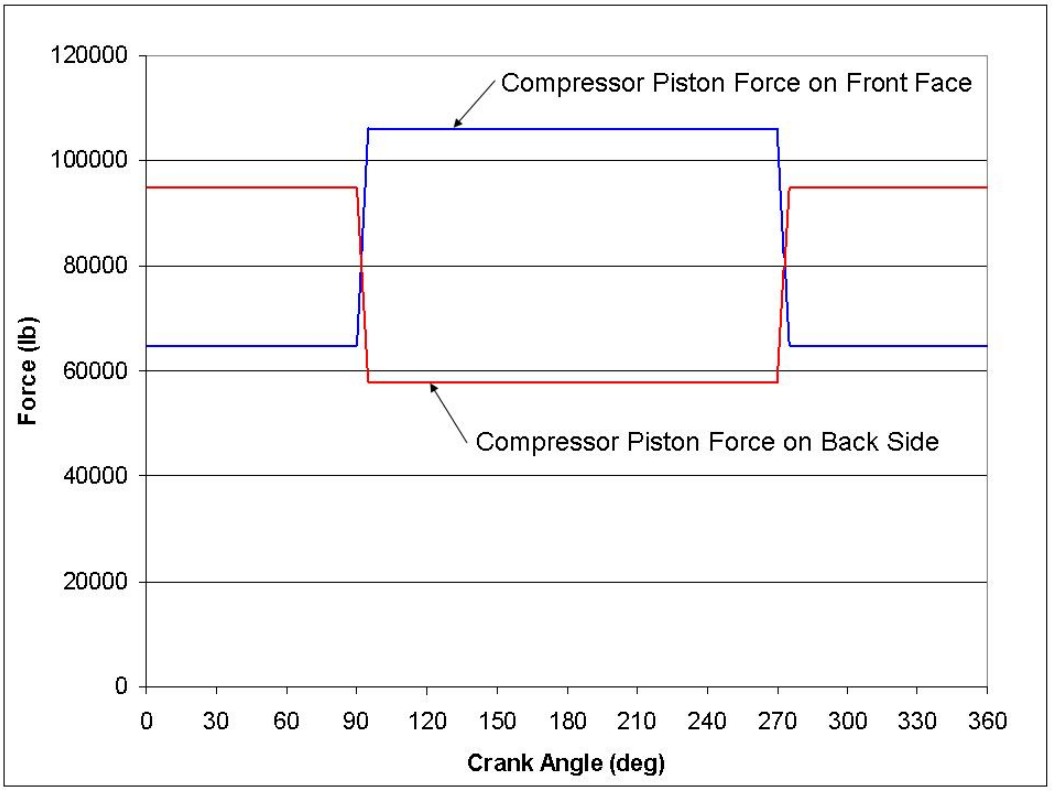

Figure 31 TLA-6 Compressor piston input forces (uprated) for Working Model simulation

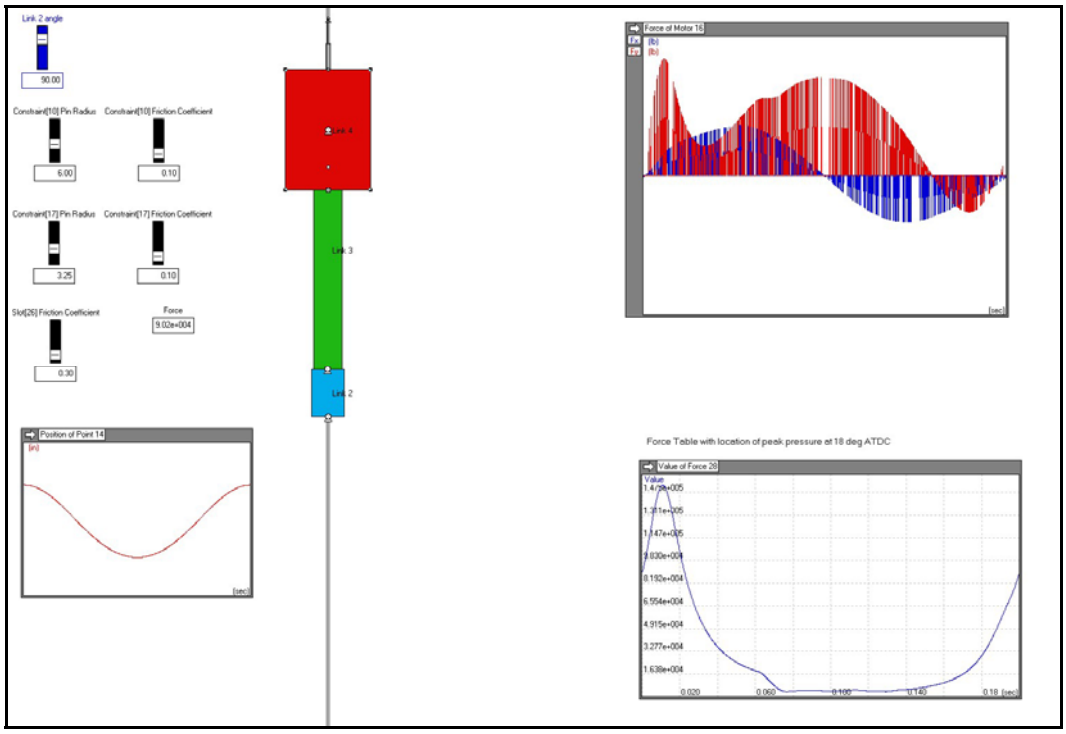

Figure 32 Working Model TLA-6 power piston simulation setup with results

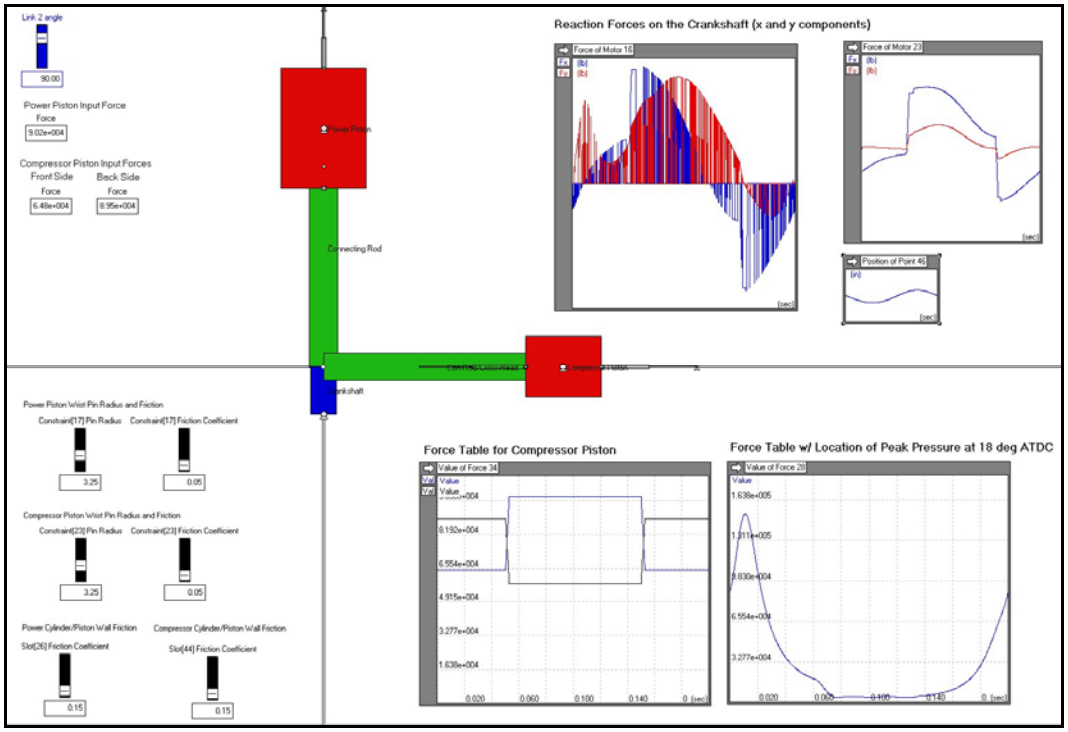

Figure 33 Working Model TLA-6 power piston and compressor simulation setup with results

Finite Element Stress Analysis

A solid model of the entire Clark TLA-6 engine, with three compressors, was created using Pro Engineer Wildfire 3-D solid modeling CAE software (see Figure 34). The crankcase that was created from engineering drawings was too complicated for Pro Mechanica to create a successful mesh, so a simplified model was created (see Figure 35 and Figure 36). A significant amount of effort went into the simplified model such that it was not so oversimplified that potentially critical stresses would be neglected during the stress analysis. This was achieved by modifying some of the complex internal features, specifically related to the crankcase web strengtheners or ribs. The overall thickness of the crankcase webs was modified such that the total volume of material was essentially the same without the ribs as compared to the original volume of the webs with the ribs. It is recognized that these simplifications could be critical and the crankcase model may need to be refined to replace some detail, however, depending upon the results, this may not be necessary. The crankcase material properties that were entered into the software were based upon gray cast iron. Pro Mechanica treats the solid model as if it were made from an ideal, isotropic material. Table 6 lists the forces applied to each of the power pistons, for the nominal condition, at a moment when a piston of interest (e.g. cylinder #1) is at peak pressure (peak force). Figure 37 illustrates the resulting nominal condition dynamic forces on the crankshaft journal bearings, where the results are in terms of the forces in the x and y directions. This result includes the effects of the compressor forces. Figure 38 illustrates the resulting dynamic forces on the crankshaft journal bearings, but without the effects of the compressors. Table 7 summarizes the results from the dynamic analysis for the nominal condition. These forces listed in Table 7 are the forces that will be used to create the load-set for the crankcase stress FEA. The orientation of the +x and +y directions correlates to the model setup in Working Model. These directions are then correlated to the +x and +y directions in Pro Engineer and the signs are modified accordingly, if necessary.

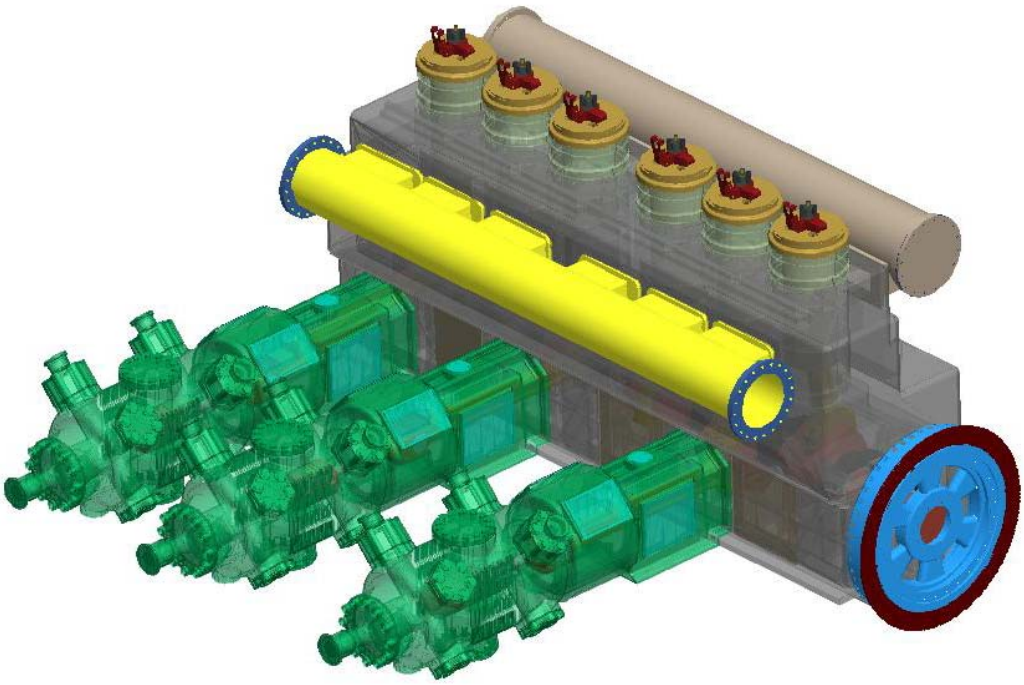

Figure 34 TLA-6 with compressors modeled in Pro Engineer - Wildfire

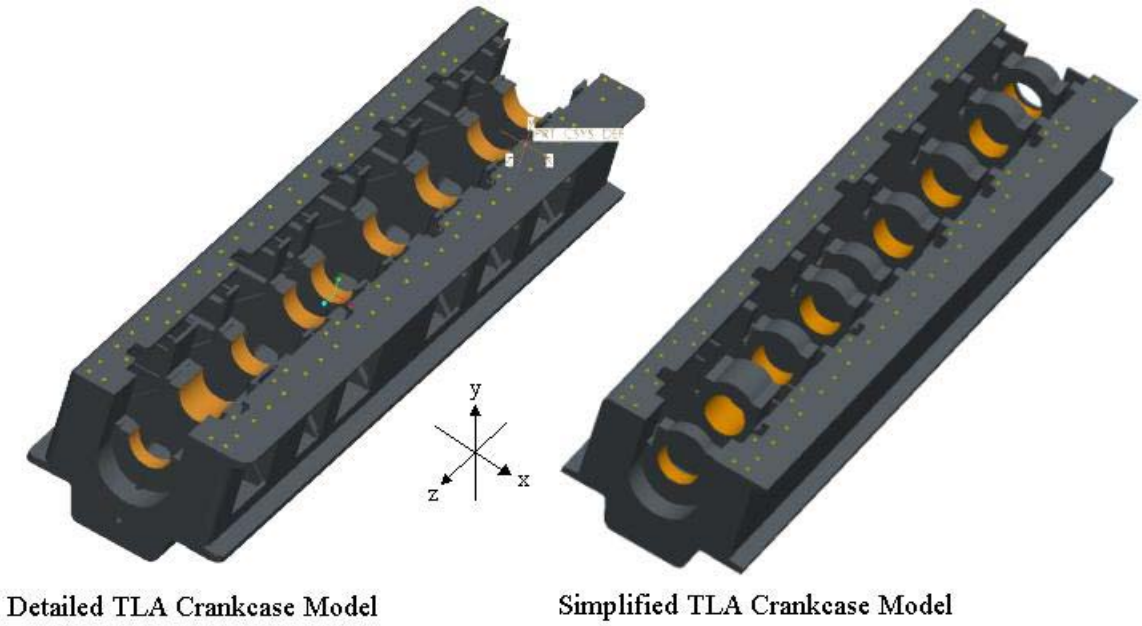

Figure 35 TLA-6 Crankcase modeling comparison

Figure 36 Mesh of the simplified TLA-6 crankcase

	Cylinder Forces (lb) - Nominal						
Run	# 1	# 2	# 3	# 4	# 5	# 6	Notes
1	152,440	4,712	3,752	25,308	5,829	30,506	Cylinder 1 @ P.P.
2	4,712	152,440	25,308	3,752	30,506	5,829	Cylinder 2 @ P.P.
3	5,829	30,506	152,440	4,712	3,752	25,308	Cylinder 3 @ P.P.
4	30,506	5,829	4,712	152,440	25,308	3,752	Cylinder 4 @ P.P.
5	3,752	25,308	5,829	30,506	152,440	4,712	Cylinder 5 @ P.P.
6	25,308	3,752	30,506	5,829	4,712	152,440	Cylinder 6 @ P.P.

Table 6 Force data at individual cylinder peak force locations for the nominal TLA-6

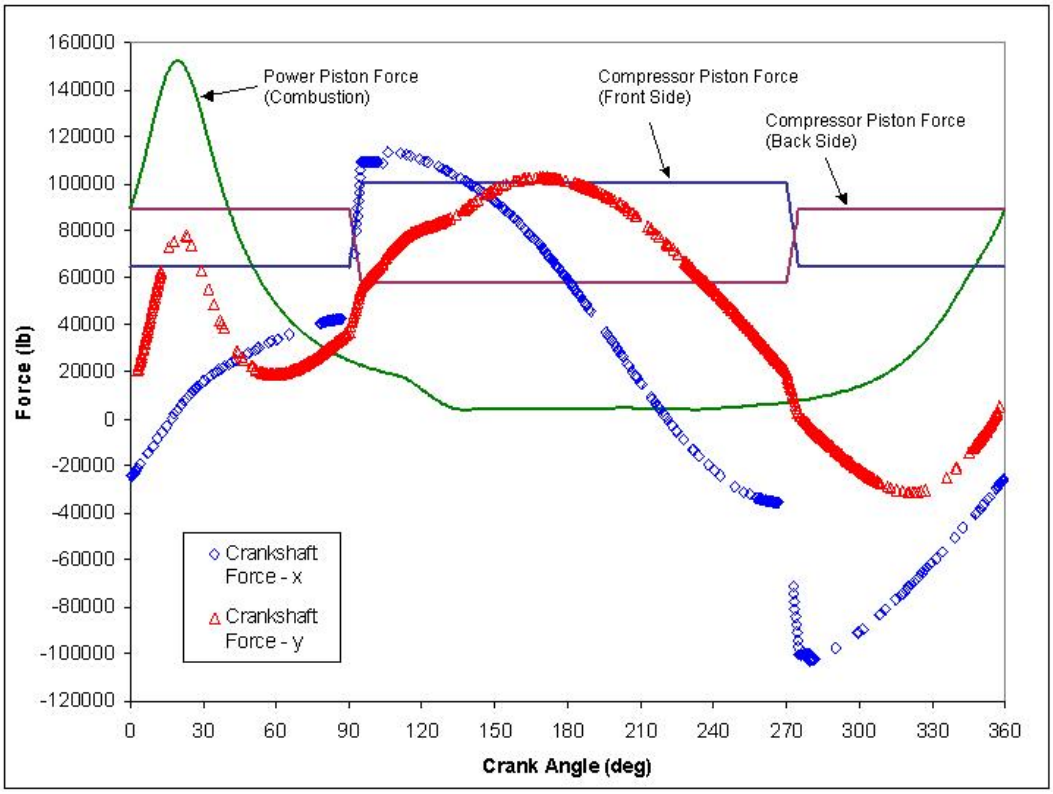

Figure 37 Simulation results of nominal TLA (with compressor) crankshaft bearing forces

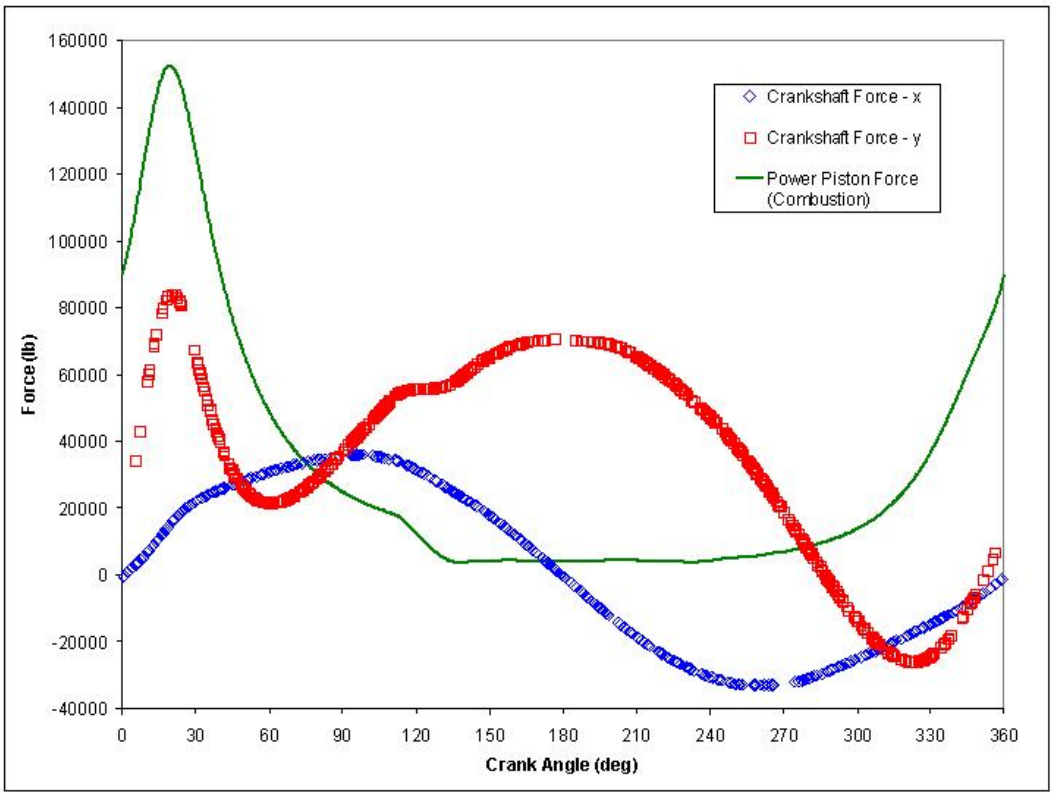

Figure 38 Simulation results of nominal TLA crankshaft bearing forces

Crankcase Bearing Saddle Forces (lb) - Nominal							
	Cylinder 1 w/ Comp.		Cylinder 2		Cylinder 3 w/ Comp.		Notes
Run	x-dir	y-dir	x-dir	y-dir	x-dir	y-dir	
1	-2,000	-75,500	11,700	-69,180	-101,200	-89,410	Cylinder 1 @ P.P.
2	-33,600	-93,820	-13,800	-82,350	74,600	30,900	Cylinder 2 @ P.P.
3	33,580	-34,530	-34,185	-27,960	-2,000	-75,500	Cylinder 3 @ P.P.
4	-40,600	-27,120	33,140	-31,470	-33,600	-93,820	Cylinder 4 @ P.P.
5	-101,200	-89,410	19,250	25,280	33,580	-34,530	Cylinder 5 @ P.P.
6	74,600	30,900	-23,700	-59,100	-40,600	-27,120	Cylinder 6 @ P.P.

Crankcase Bearing Saddle Forces (lb) - Nominal							
	Cylinder 4		Cylinder 5 w/ Comp.		Cylinder 6		Notes
Run	x-dir	y-dir	x-dir	y-dir	x-dir	y-dir	
1	19,250	25,280	33,580	-34,530	-34,185	-27,960	Cylinder 1 @ P.P.
2	-23,700	-59,100	-40,600	-27,120	33,140	-31,470	Cylinder 2 @ P.P.
3	11,700	-69,180	-101,200	-89,410	19,250	25,280	Cylinder 3 @ P.P.
4	-13,800	-82,350	74,600	30,900	-23,700	-59,100	Cylinder 4 @ P.P.
5	-34,185	-27,960	-2,000	-75,500	11,700	-69,180	Cylinder 5 @ P.P.
6	33,140	-31,470	-33,600	-93,820	-13,800	-82,350	Cylinder 6 @ P.P.

Table 7 Working Model dynamic force results for the nominal TLA-6 with compressors

Table 8 lists the forces applied to each of the power pistons, for the uprated condition, at a moment when a piston of interest (e.g. cylinder #1) is at peak pressure (peak force). Figure 39 illustrates the resulting uprated dynamic forces on the crankshaft journal bearings, where these results are also in terms of the forces in the x and y directions. This result includes the effects due to the uprated compressor forces. Figure 40 illustrates the resulting uprated dynamic forces but without the effects due to the compressor forces. Table 9 summarizes the results from the dynamic analysis for the uprated condition. These forces listed in Table 9 are the forces that will be used as the loads for the uprated crankcase stress FEA.

Cylinder Forces (lb) - Uprated							
Run	# 1	# 2	# 3	# 4	# 5	# 6	Notes
1	165,786	4,444	4,201	21,645	4,826	32,980	Cylinder 1 @ P.P.
2	4,444	165,786	21,645	4,201	32,980	4,826	Cylinder 2 @ P.P.
3	4,826	32,980	165,786	4,444	4,201	21,645	Cylinder 3 @ P.P.
4	32,980	4,826	4,444	165,786	21,645	4,201	Cylinder 4 @ P.P.
5	4,201	21,645	4,826	32,980	165,786	4,444	Cylinder 5 @ P.P.
6	21,645	4,201	32,980	4,826	4,444	165,786	Cylinder 6 @ P.P.

Table 8 Force Data at individual cylinder peak force locations for the uprated TLA-6

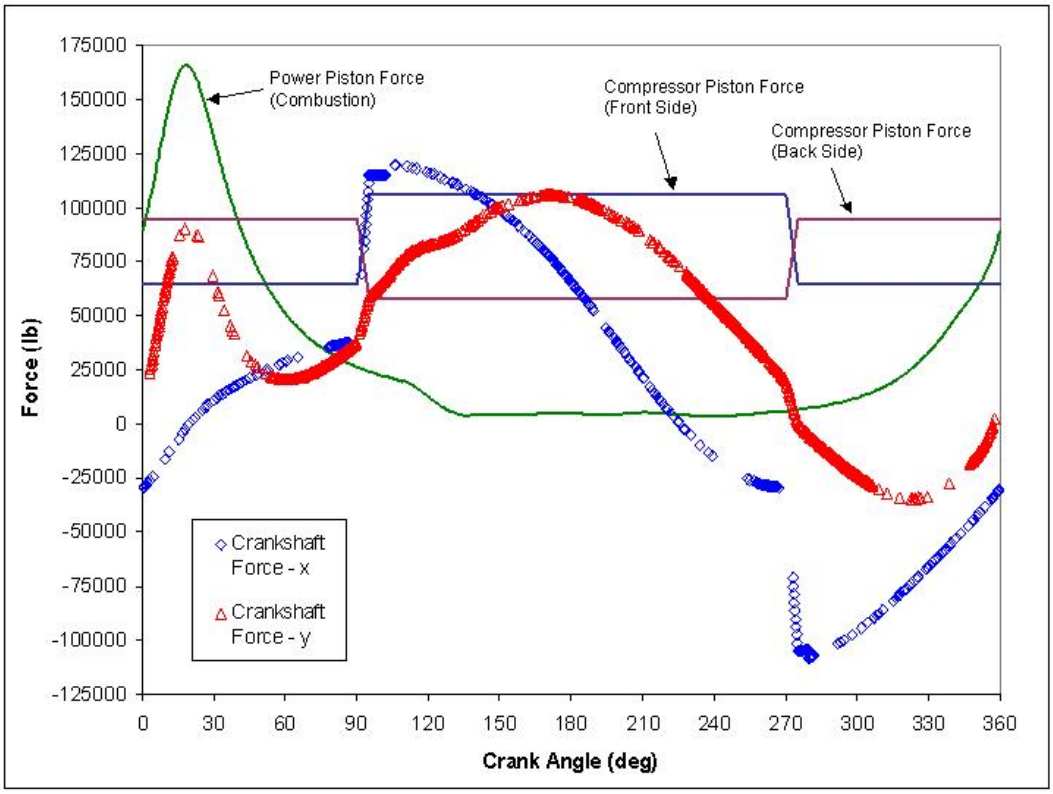

Figure 39 Simulation results of uprated TLA (with compressor) crankshaft bearing forces

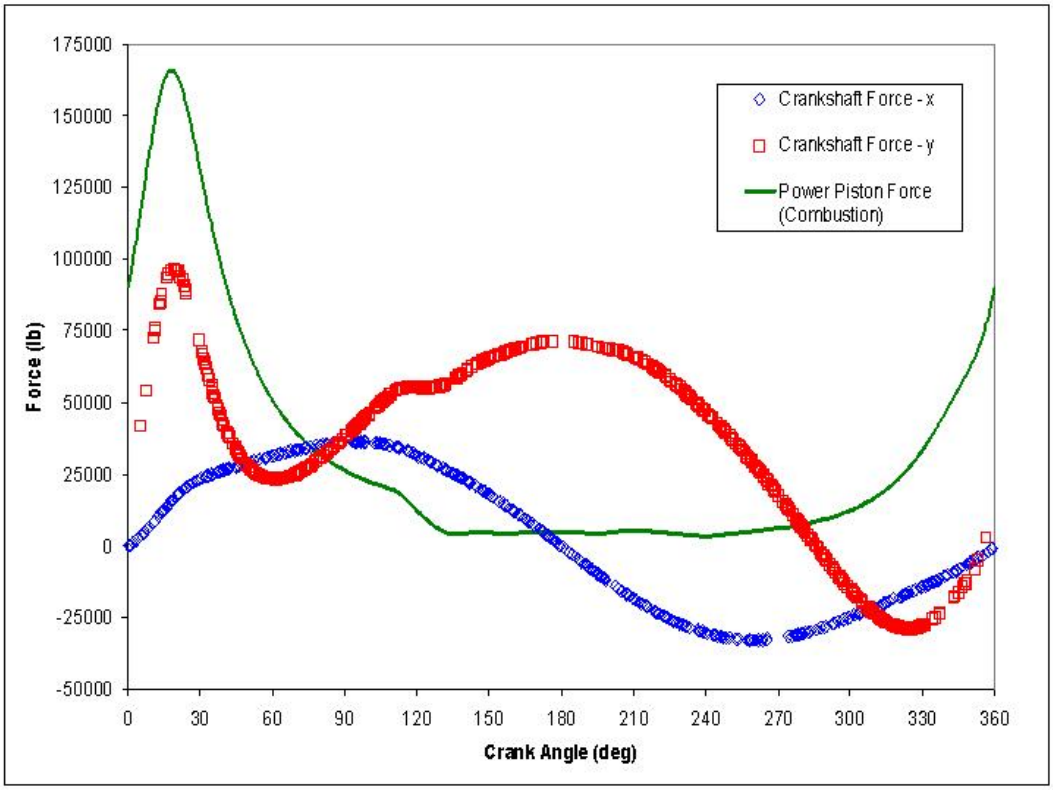

Figure 40 Simulation results of uprated TLA crankshaft bearing forces

Crankcase Bearing Saddle Forces (lb) - Uprated							
	Cylinder 1 w/ Comp.		Cylinder 2		Cylinder 3 w/ Comp.		Notes
Run	x-dir	y-dir	x-dir	y-dir	x-dir	y-dir	
1	2,800	-90,000	11,480	-69,050	-107,500	-92,190	Cylinder 1 @ P.P.
2	-39,900	-96,300	-15,600	-96,380	79,000	34,000	Cylinder 2 @ P.P.
3	27,300	-35,180	-34,900	-29,460	2,800	-90,000	Cylinder 3 @ P.P.
4	-35,550	-27,930	32,860	-30,590	-39,900	-96,300	Cylinder 4 @ P.P.
5	-107,500	-92,190	18,650	27,680	27,300	-35,180	Cylinder 5 @ P.P.
6	79,000	34,000	-23,920	-59,540	-35,550	-27,930	Cylinder 6 @ P.P.

Crankcase Bearing Saddle Forces (lb) - Uprated							
	Cylinder 4		Cylinder 5 w/ Comp.		Cylinder 6		Notes
Run	x-dir	y-dir	x-dir	y-dir	x-dir	y-dir	
1	18,650	27,680	27,300	-35,180	-34,900	-29,460	Cylinder 1 @ P.P.
2	-23,920	-59,540	-35,550	-27,930	32,860	-30,590	Cylinder 2 @ P.P.
3	11,480	-69,050	-107,500	-92,190	18,650	27,680	Cylinder 3 @ P.P.
4	-15,600	-96,380	79,000	34,000	-23,920	-59,540	Cylinder 4 @ P.P.
5	-34,900	-29,460	2,800	-90,000	11,480	-69,050	Cylinder 5 @ P.P.
6	32,860	-30,590	-39,900	-96,300	-15,600	-96,380	Cylinder 6 @ P.P.

Table 9 Working Model dynamic force results for the uprated TLA-6 with compressors

As stated previously, the results listed in Table 7 and Table 9 will be used as the crankcase load-sets for the stress analysis. For each power cylinder and compressor, there are two bearing saddles in the crankcase where the load is applied. Since the sections of the crankshaft corresponding to cylinders 2, 4, and 6 only have a power piston, the loads applied to the corresponding bearing saddles have been determined from the results illustrated in Figure 38 and Figure 40, which were listed in Table 7 and Table 9, for the nominal and uprated condition, respectively. Similarly, the sections of the crankshaft corresponding to cylinders 1, 3, and 5 have the power piston and the compressor loading considerations. The loads applied to the corresponding bearing saddles for these cylinders have been determined from the results illustrated in Figure 37 and Figure 39, which were also listed in Table 7 and Table 9. Figure 41 indicates the locations of each of the crankshaft bearings and their location within the crankcase with respect to the power and compressor cylinders. Again, there are two loading conditions, nominal and uprated. One of the limitations to this method of determining the dynamic loading is that the Working Model software is limited to two-dimensional analysis as opposed to a three-dimensional analysis. Because of this limitation, the dynamic effects due to potential influences of neighboring cylinders and the flywheel have been ignored for this analysis. An example illustrating the crankcase loading can be seen in Figure 42. The loads applied to the crankcase can now be seen as the application of loads from a simply supported section of the crankshaft. It was recognized that from cylinder to cylinder there could be potential dynamic loading effects that were ignored with this

method, especially if crankshaft deflections due to vibrations were to become significant. It should be noted that, although the engine is constrained based upon near-real world engine support schemes, the software treats this as an idealized case and does not account for the degradation of grout pads and other anchoring systems. Other preliminary loads were added to the crankcase model as well, such as the weight of the upper block and the many upper block-anchoring studs that are pre-stressed.

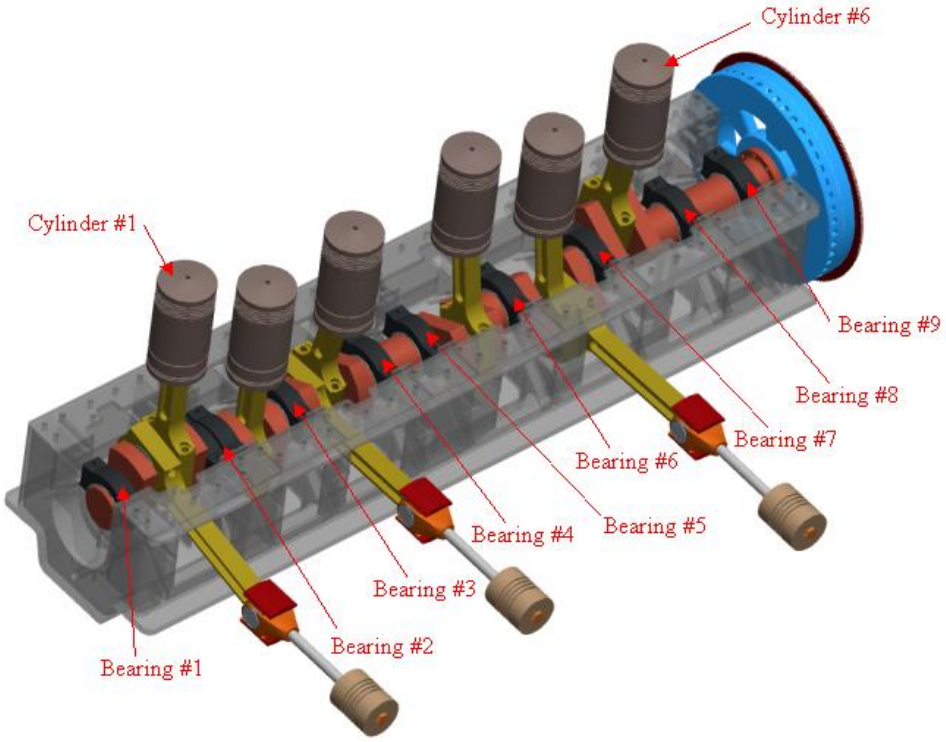

Figure 41 TLA-6 Journal bearing locations to cylinder locations

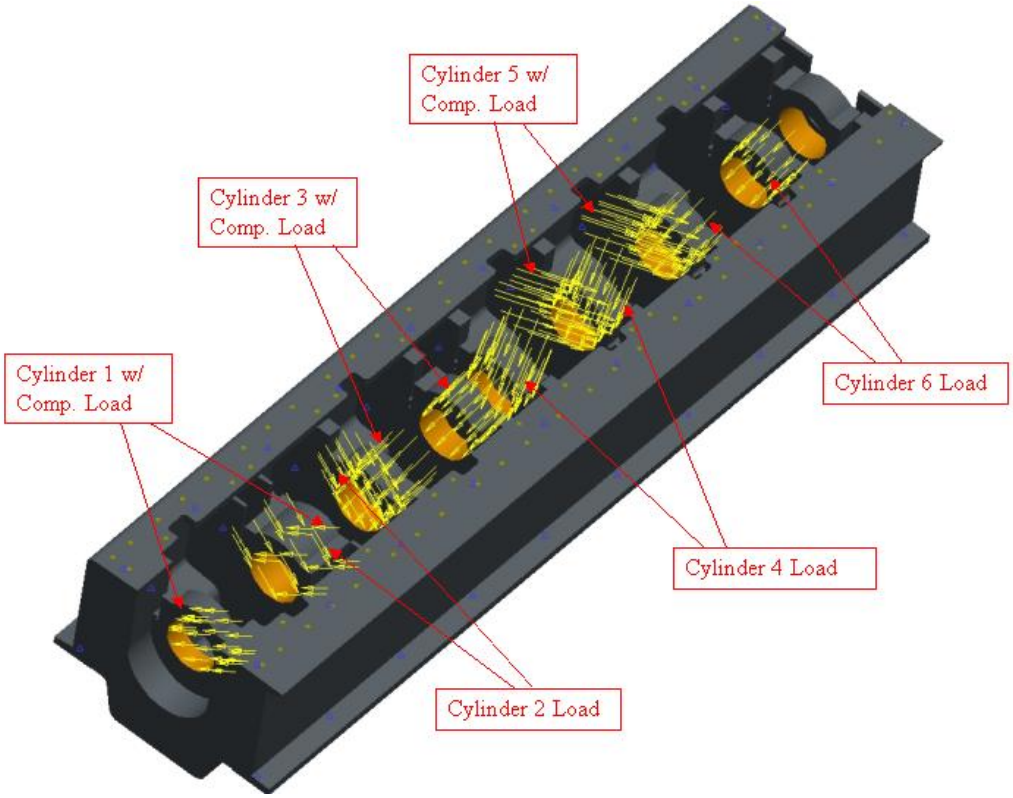

Figure 42 Application of loads to crankcase journal bearings

Finite Element Stress Analysis Results

The results from the stress analysis indicated the stresses did increase in some of the cases analyzed. Table 10 summarizes the results from all twelve cases that were examined. The values of stress indicated are the von Mises stress and the maximum principal stress for the standard condition and uprated condition analyses. The results have considerable variability from one cylinder at peak pressure to another. The maximum stress was a principal stress of -28,543 psi, when cylinder 2 was at peak pressure. The negative sign indicates a direction relative to the world coordinate system within Pro Engineer. Table 11 summarizes the percent difference between the results from the standard condition and the uprated condition. It is interesting to note that due to the dynamic loading condition for cylinders 3 and 4 the overall crankcase stresses actually decreased slightly. The differences between the von Mises stress and the maximum principal stress were negligible for all cases except for cylinder 4 where there was just over a 4% difference between the two types of stresses. The largest difference in stress was associated with cylinders 1 and 2 at almost 14% and just over 11%, respectively. These results can also be seen visually with the fringe plot of the crankcase stresses (see Figure 43 and Figure 44). These two figures were used to illustrate the stress distribution within the crankcase since they illustrated the highest stresses (location and magnitudes) for all cases analyzed. Although these two figures represent stress

results found in the tables for the case when cylinder 2 was at peak pressure, it becomes readily apparent that the increase in the stress distribution is actually quite limited. Since the standard condition stresses ranged from around 6 ksi to almost 26 ksi for the analyzed cases and these engines have been generally operated at the standard condition for decades, it is most probable that any fatigue effects at this stress level are negligible. This is supported by examining most fatigue data for metals where the infinite life point is assumed to be around 10^8 to 10^9 cycles, as can be seen in Figure 45. An engine operating at 300 rpm will exceed the infinite life point if it is run for only 7 continuous months.

The uprated condition that was analyzed indicated a stress range of around 6 ksi to almost 29 ksi. According to the ASM (American Society for Metals) Metals Handbook, gray cast iron has a tensile strength range of 20 ksi to 60 ksi and a compressive strength range of 83 ksi to 188 ksi[ix]. After discussions with an industry expert[x], the mechanical properties of class 30 gray cast iron was used since it is considered to be the most common material for the older generation crankcases. Class 30 gray cast iron also provides a damping effect, which is beneficial for engine applications. Class 30 gray cast iron has an ultimate tensile strength of 31 ksi and an ultimate compressive strength of 109 ksi. For this current modeling, the highest stresses were in compression. Figure 46 illustrates a modified-Mohr failure theory diagram. This diagram can be used for graphically determining an approximate safety factor. For the given ultimate compressive strength of cast iron and the maximum stress for the uprated condition, the safety factor is still (best case) around 3.8 (4.3 for the nominal condition). If endurance limit reduction factors are considered, then the safety factor would be reduced, but the safety factor should still remain greater than 2. Another approach that could be pursued would be to strengthen structural components where high localized stresses occur.

Stress (psi)	Cylinder 1 @ P.P		Cylinder 2 @ P.P		Cylinder 3 @ P.P	
	Std.	Uprated	Std.	Uprated	Std.	Uprated
von Mises	16,108	18,322	20,155	22,420	9,718	9,687
Max. Principal	-20,055	-22,827	-25,645	-28,543	-10,907	-10,863
	Cylinder 4 @ P.P.		Cylinder 5 @ P.P.		Cylinder 6 @ P.P.	
	Std.	Uprated	Std.	Uprated	Std.	Uprated
von Mises	6,143	6,358	15,457	16,321	9,765	10,737
Max. Principal	-7,546	-7,501	-20,034	-21,161	-12,781	-14,037

Table 10 FEA Results for a TLA crankcase

	Percent Increase/Decrease of Stresses					
	Cyl. 1	Cyl. 2	Cyl. 3	Cyl. 4	Cyl. 5	Cyl. 6
von Mises	13.7%	11.2%	-0.3%	3.5%	5.6%	10.0%
Max. Principal	13.8%	11.3%	-0.4%	-0.6%	5.6%	9.8%

Table 11 Percent difference between results from the FEA analyses

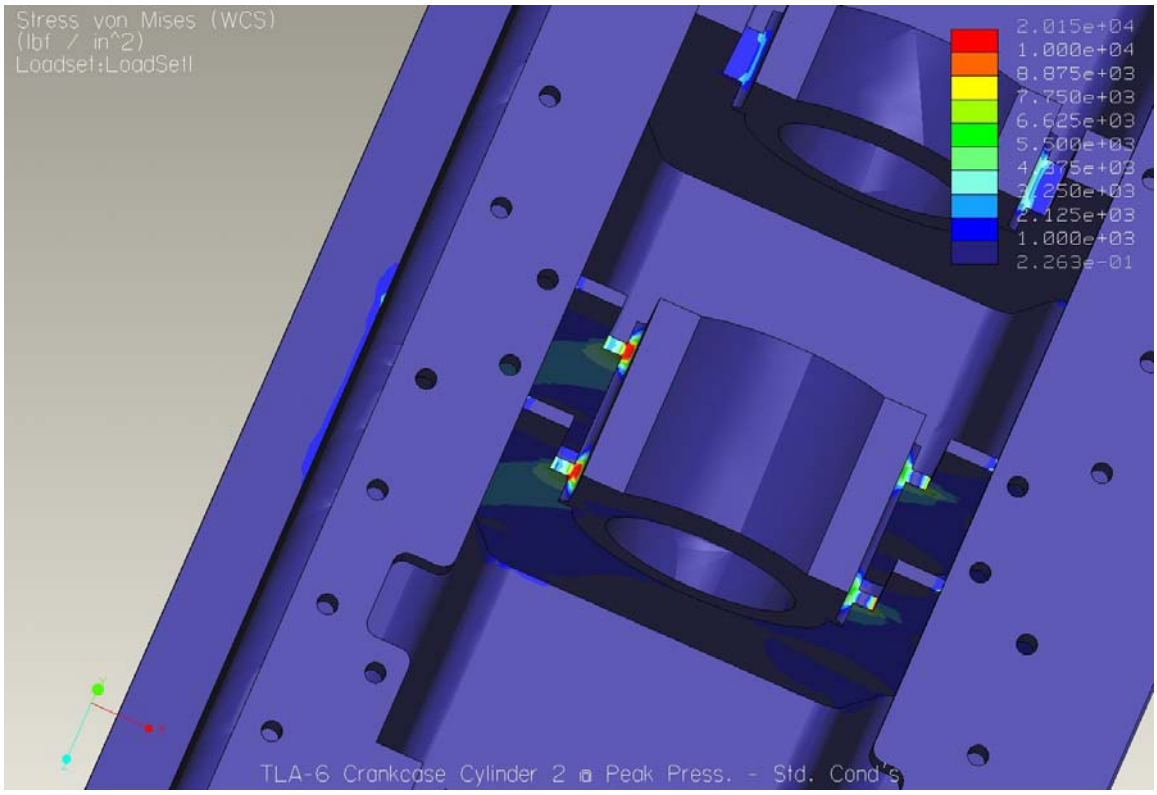

Figure 43 FEA results for bearings 2/3 with cylinder 2 at peak pressure and standard conditions

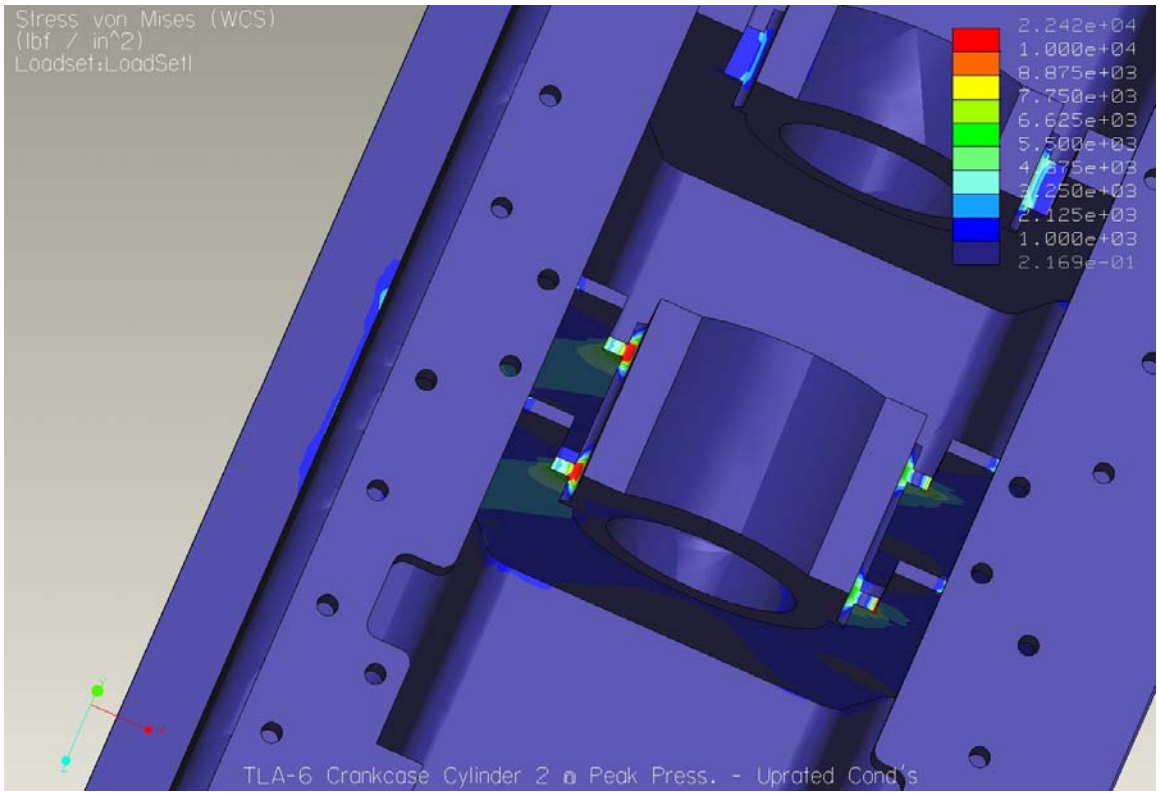

Figure 44 FEA Results for bearings 2/3 with cylinder 2 at peak pressure and uprated conditions

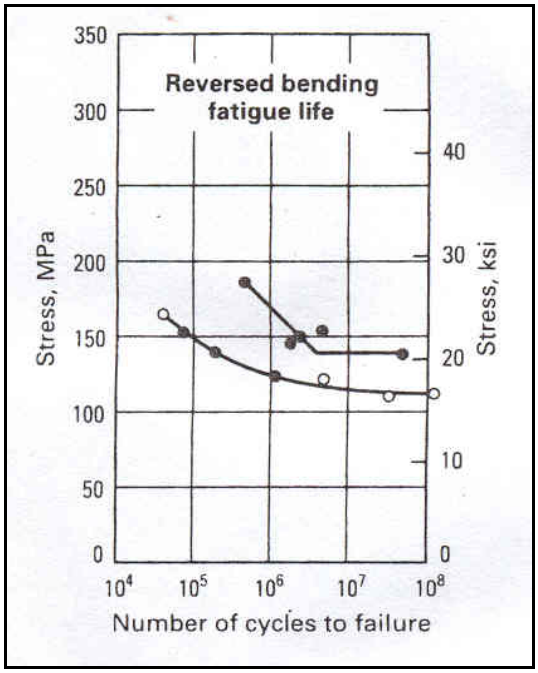

Figure 45 Reversed bending fatigue life of gray cast iron[ix]

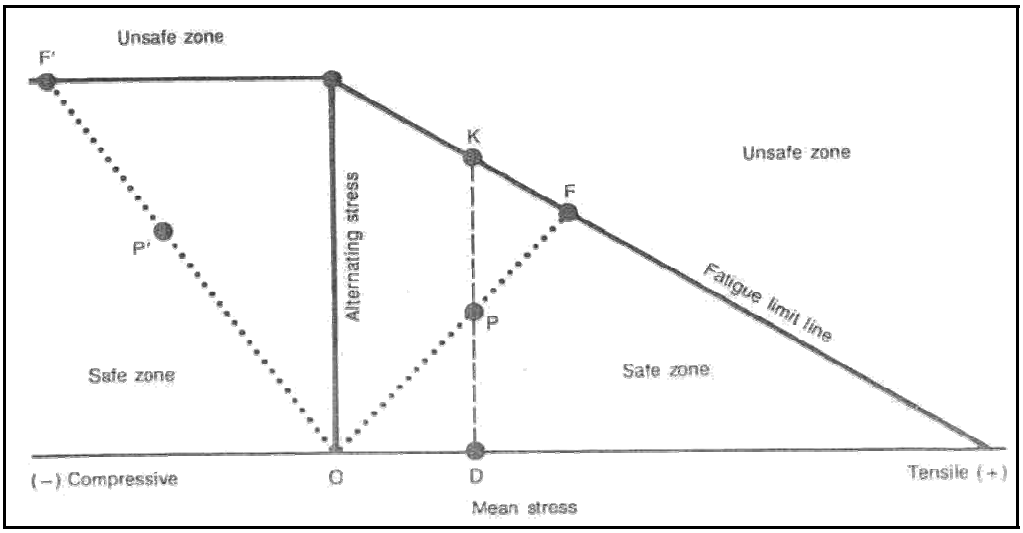

Figure 46 Goodman diagram for indicating safe and unsafe fatigue zones[ix]

2.3 Hydraulically Actuated Mechanical Fuel Injection System

A hydraulically actuated, inwardly opening, mechanical fuel injection valve system was designed for a Clark TLA engine. This design however has potential to be applied to many different engine models. High pressure fuel injection (HPFI) is a technology that is proven to improve efficiency and decrease emissions by enhancing the mixing of fuel and air. HPFI systems currently employed in the field are poppet valves, and contain significant fluid losses due to the flow path created. These systems typically required 500 psi fuel pressure to achieve adequate fuel and air mixing. This new design allows for the introduction of natural gas with jet energy equivalent to commercially available HPFI systems, but with a 80% fuel pressure reduction. The required fuel pressure for the new design is 100 psi. By creating a fuel injection event with equivalent jet energy, the benefits of enhanced mixing are achieved, promoting the extension of the lean limit and associated emissions reductions.

The hydraulically actuated mechanical fuel injection valve body is the OEM fuel injection valve body, with minor modifications. These modifications consist primarily of relatively simple machining operations, most significant of which is the modification of the lower portion of the body to allow for the mounting of a fuel convergent-divergent nozzle body. This nozzle body allows for a much more efficient fuel flow path and provides the seating area for the new fuel valve, which acts more like the typical fuel injection needle (inwardly opening). Images of the original valve design vs. the new valve design can be seen in Figure 47 and Figure 48. Note that the inwardly opening design eliminates regions that can trap fuel, which are present in other converging-diverging nozzles designed to interface with the standard poppet valves.

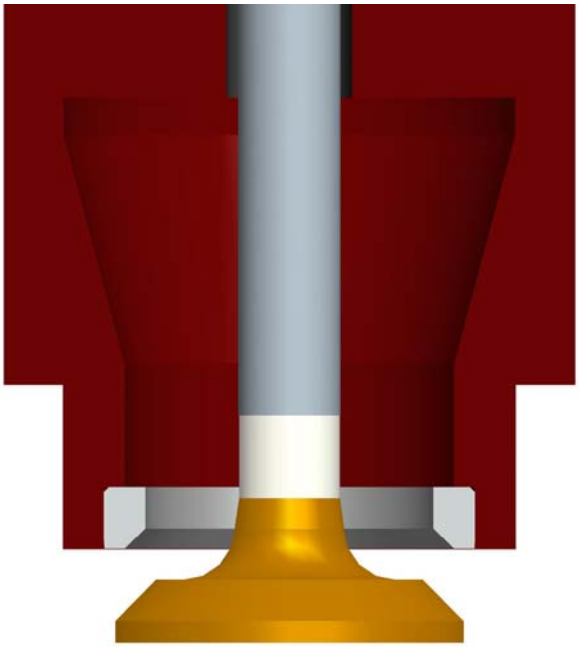

Figure 47 Cross-section view of typical TLA fuel injection valve

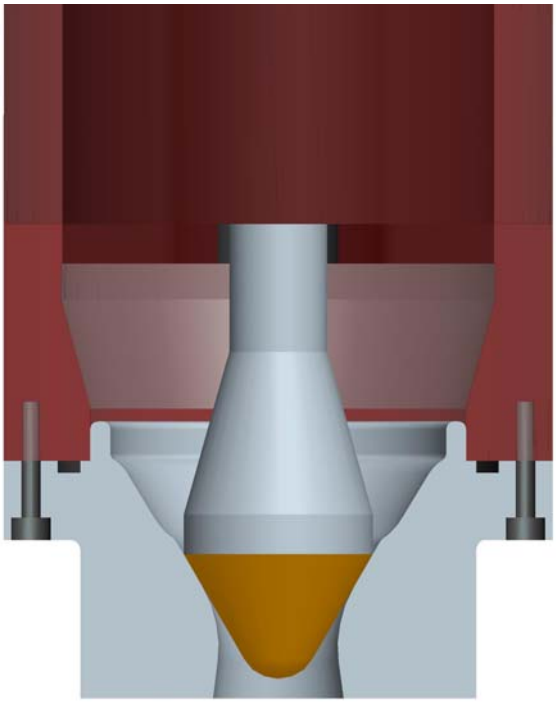

Figure 48 Cross-section view of new fuel injection valve

Fuel injection on a typical TLA is initiated by a fuel cam and rocker arm assembly. Fuel injection with the new hydraulic-mechanical system is initiated by a fuel cam translating a hydraulic cylinder rod, hydraulically coupled to another hydraulic cylinder which opens the fuel valve. Figure 49 and Figure 50 illustrate the concept of the new design. The new system utilizes the engine oil as the hydraulic fluid such that no new fluid needs to be introduced. A pressure relief valve was designed into the new system to allow for removal of air that may be entrained or trapped within the oil. This also facilitates oil circulation for cooling. With each stroke of the fuel injector, a portion of the cam lift profile will over-stroke the hydraulic cylinder attached to the fuel injector. This will cause the pressure relief valve to open, allowing hot oil to pass into the primary engine oil flow to be cooled through the engine oil heat exchanger. New oil is introduced into the fuel injector hydraulic circuit from an engine oil reservoir during non-actuating periods. A circuit schematic of this concept can be seen in Figure 51.

This new design was developed at the CSU EECL in collaboration with Dresser-Rand. Dresser-Rand has expressed interest in developing this technology as a commercially available fuel injection system. An engineering drawing package for this system is provided in Appendix B.

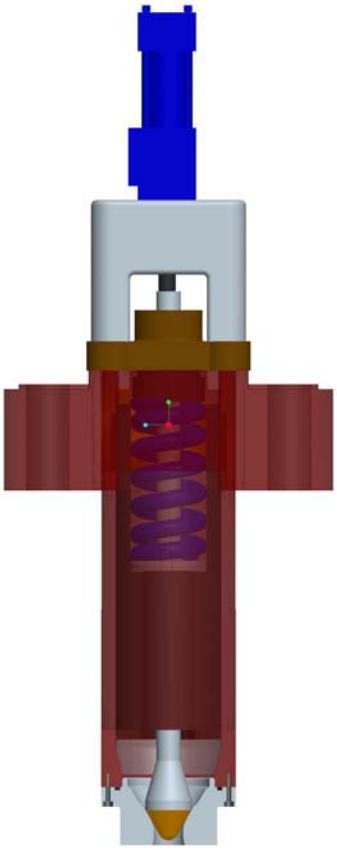

Figure 49 Hydraulically actuated mechanical fuel injection valve assembly

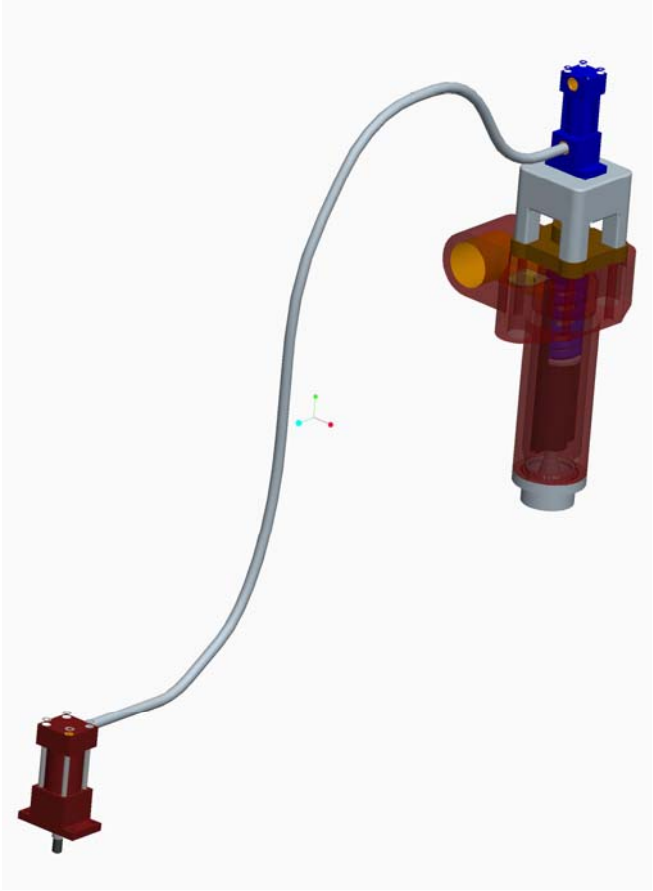

Figure 50 Hydraulically actuated mechanical fuel injection valve system

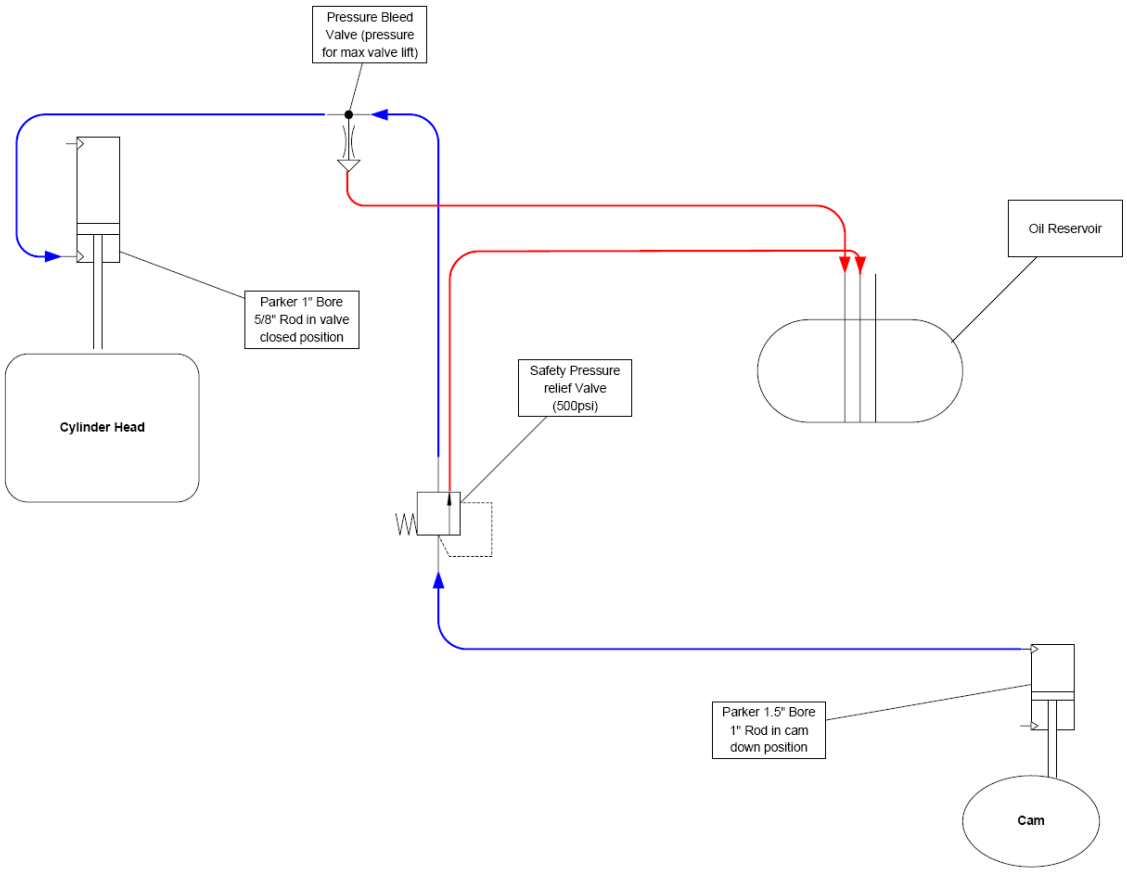

Figure 51 Hydraulic schematic for new fuel valve design

2.4 Uprate Systems Test Plan

The uprate systems test plan has been created and submitted to DOE. This document provides a path for a logical testing procedure. The testing procedures are developed to quantify the engine performance parameters with respect to emissions and power output.

3.0 Conclusions

From the investigations for this project, several key conclusions have been determined. The CFD analysis has indicated significant benefits from high-pressure fuel injection (HPFI). The fuel mixing with the standard mechanical gas admission valve (MGAV) of low-pressure fuel indicates that the fuel gas has a propensity to attach to the surface of the head producing a 'curtain' effect. This does not promote rapid and homogeneous mixing with the air in the combustion chamber. Conversely, the HPFI method injects a high-energy flow of fuel into the combustion chamber and the mixing is significantly improved. Comparing the MGAV results to the HPFI results, there is a high level of mixedness by 60° BTDC with the HPFI system as compared to the MGAV system, which never really achieves the same level of mixing. Additionally, the investigation also provided evidence that modifying the piston crown with a 'sombrero' style surface does not improve mixing compared to the standard TLA combustion chamber piston surface (with HPFI).

A modal analysis of three engine crankshafts was performed using FEA. All three crankshafts had a similar range of results. For a TLA-6 crankshaft the first harmonic was found to be at 59 Hz. An HBA-6 crankshaft was analyzed and its first harmonic was found to be 54 Hz. The third crankshaft analyzed was for a GMV-10 and its first harmonic was found to be at 56 Hz. All of these modal analyses utilized the lumped mass assumption, to account for all of the attached slider crank components, and flywheels were also included. The results from all three analyses were slightly higher than expected, but this method was evaluated for its potential use as a method to give an estimate for a crankshafts natural frequency. Crankshafts are desired to be operated at speeds far away from the natural frequency and the results from these analyses support this goal. The TLA-6, HBA-6, and GMV-10 crankshaft natural frequency speeds were 3,540 rpm, 3,240 rpm, and 3,360 rpm, respectively. Given consideration of their typical operating speed, none of these crankshafts are near a critical order speed when operated at 300 rpm.

FEA results for the TLA crankcase indicate that the strength will be adequate to support the additional stresses due to uprating the engine. The analysis results predict a new maximum stress of less than 23ksi, in compression, which will still provide for a large safety factor of nearly 5. These predicted new stresses are also still within acceptable limits with respect to the fatigue life of gray cast iron. The modeling process developed could be valuable in the investigation of other candidate engines for uprating.

A new hydraulically actuated, inwardly opening, mechanical fuel injection system was designed in cooperation with Dresser-Rand. This new valve design takes advantage of an improved fuel flow path which reduces fluid losses. By reducing fluid losses the natural gas need only be compressed to approximately 100 psi instead of approximately 500 psi necessary for current HPFI systems. This proposed system provides essentially the same high-energy flow as current 500 psi HPFI systems but with an 80% reduction of required natural gas fuel pressure.

4.0 Summary

4.1 Summary of Accomplishments

During this period of research, the following key accomplishments were achieved:

- CFD analysis has shown HPFI significantly improves in-cylinder gas mixing
- Improved in-cylinder gas mixing extends the lean limit of operation, reducing maximum in-cylinder temperatures and hence assists in lowering NO_x generation during combustion
- Modal analysis of three crankshafts completed
- Results for TLA, HBA, and GMV crankshafts indicate sufficient separation between typical operation speed of 300 rpm and a 10^{th} order critical speed range of 320 rpm to 354 rpm
- FEA stress analysis has indicated that an uprated TLA will have a maximum increase in frame stress of approximately 14% for a 20% increase in torque
- FEA stress analysis has also indicated that an uprated TLA will have a maximum stress, in compression, of approximately 23ksi, which maintains a safety factor of almost 5
- FEA stress modeling could be a very effective prediction tool for evaluating potential structural issues for uprate other candidate engines

REFERENCES

[i] Norton, R., *Machine Design: An Integrated Approach 2nd edition* (Upper Saddle River, NJ: Prentice-Hall, 2000), 588-598.

[ii] Heath, A., McNamara, P., "Crankshaft Stress Analysis – Combination of Finite Element and Classical Analysis Techniques," *Journal of Engineering for Gas Turbines and Power* (1990): 268-275.

[iii] Priebsch, H., Affenszeller, J., Gran, S., "Prediction Technique for Stress and Vibration of Nonlinear Supported, Rotating Crankshafts," *Journal of Engineering for Gas Turbines and Power* (1993): 711-720.

[iv] Bargis, E., Vullo, V., Garro, A., "Crankshaft Design and Evaluation – Part 2 –A Modern Design Method: Modal Analysis," *Reliability, Stress Analysis and Failure Prevention Methods in Mechanical Design Conference* (San Francisco, Ca: American Society of Mechanical Engineers, 1980), 203-211.

[v] Dennis W. Schmitt, "Frame Stress and Crankshaft Modal Analysis on Large Bore Natural Gas Engines", Masters Thesis, Colorado State University, Fall 2005.

[vi] Beardmore, Roy. "Coefficients of Friction." *Friction Factors.* 2005. <http://www.roymech.co.uk/Useful_Tables/Tribology/co_of_frict.htm> (Feb. 2005).

[vii] Schmitt, D., Olsen, D., Willson, B., "Systematic Engine Uprate Technology Development and Deployment for Pipeline Compressor Engines," Final Report, GRI Contract #GRI-04/0065, 2004.

[viii] Jeff Clegg, El Paso Corporation at the Colorado Interstate Gas Company-Rawlins, Wyoming Compressor Station. <Jeffrey.Clegg@ElPaso.com> "Compressor Information." July 9, 2004. Research Communication.

[ix] *Metals Handbook 10th edition* (Materials Park, OH: ASM International, 1990), 12-32.

[x] Terry Smith, Gas Industry Consultant, personal communications, February 2005.

Appendix A – OEM Communications

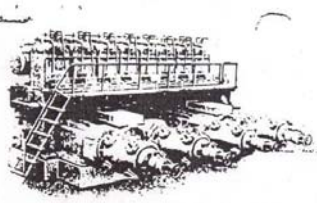

CLARK BROS. CO.

DIVISION OF DRESSER OPERATIONS, INC.

ENGINES - COMPRESSORS - TURBINES

OLEAN · NEW YORK

CLARK

ESTABLISHED 1880

ADDRESS REPLY TO
800 CENTRAL AVENUE
NEW ORLEANS 21, LOUISIANA
PHONE VERNON 3-7277

August 12, 1959

Texaco, Inc.
P.O. Box 7
Harvey, Louisiana

Attention: Mr. J. S. Weatherly

Gentlemen:

Re: RA-6 Unit
Serial # A-21114
Ct. 4181-B
Lafitte Plant

As a result of the recent crankshaft breakage on the Clark, 600 BHP, RA-6, serial no. A-21114, a torsiograph test was run on this engine. This test was to determine if a torsional critical was present in any portion of your operating speed range.

The test results showed that the torsional critical frequency of this crankshaft is 2000 to 2100 cycles per minute. Since the sixth order of running speed is perfect excitation for this engine, the critical frequency will be excited at an engine speed of 340 to 350 RPM. Amplitudes of vibration of 7°, peak to peak, were recorded at 350 RPM. A stress calculation indicated that this is enough to fatigue this shaft at or near the first degree node. This, incidently, is where all three of your crankshafts failed.

This engine has run approximately seven years and did not have any crankshaft failures until approximately three years ago. This coincides exactly with an increase in operating speed which we believe was increased from 300 RPM to approximately 330 RPM. The torsional test showed that the hand tachometer used to set the engine speed consistently set the engine speed 15 to 20 RPM higher We feel that between the 10% engine speed increase and the tachometer inaccuracy, this engine has been running at 340 to 350 RPM, which as indicated before, is at its torsional critical frequency.

.../2

We would like to offer three possibilities in order to prevent any recurrance of this crankshaft breakage. All three possibilities are not necessarily recommended.

1. Clark engine is to be operated at an actual speed of no higher than 320 RPM, and a reasonably accurate tachometer should be used to set the engine speed. This is the simplest solution to this problem.

2. Increase the mass of the flywheel to raise the critical speed. This is not recommended as the flywheel may be heavy enough to break the shaft in bending.

3. Decrease the size of the flywheel to lower the critical speed below operating range. The WR^2 of the existing flywheel would have to be reduced 30 to 40% to accomplish this reduction in critical.

In summary it would appear that the simplest or the easiest method would be to see that the engine would operate no higher than 320 actual RPM in order to keep the engine out of its critical speed. If there are any questions, or if we can give you further information, please let us know.

Very truly yours,

CLARK BROS. CO.

John N. Cooper/BER

John N. Cooper
Branch Manager

JNC/bh

COOPER ENERGY SERVICES

10810 Northwest Freeway
Houston, TX 77092
Phone: 713-354-1900
Fax: 713-354-1923

February 4, 2003

Dominion Transmission, Inc.
445 West Main Street
Clarksburg, WV 26301

Attention: Mr. Ken Gilbert

Reference: GMV Crankshafts / Safe Speeds

Dear Ken,

We recently discussed the over speed shutdown setting on some of your GMV-10 engines with respect to a letter you had that was authored by CES' Jim Caldwell in 1973. I understand that you generally operate the engines at 315 rpm and that with an over speed shutdown setting of 330 rpm you are experiencing some nuisance shutdowns of the engine(s). I have reviewed this situation with our Applied Mechanics engineer who provided the following information:

> For these GMV-10 engines the 7th order critical is right about 255 rpm, the 6th order critical is right about 297 rpm and the 5th order at 357 rpm. The 5th order critical is much stronger and has the potential to do more serious damage than the 6th or 7th and therefore it is desirable to stay much further away from that critical speed.

CES standard practice is to recommend the over speed limit at 10% above the rated speed. Throughout the further evolution of engine designs CES went to great lengths to assure the engines were torsionally safe all the way through that rated times 1.1 point. Unfortunately there were some issues with the early GMV-10's. Due to the placement of the 6th order critical these engines are operated at ~ 315 rpm and while that is satisfactory, adding the *traditional* 10% to this speed puts the setting at 347 rpm and frankly we are just not comfortable with that speed when compared against the 357 rpm of the 5th order critical speed.

The conclusion drawn here was that our recommendation is really to hold the over speed shutdown point at 330 rpm but that stretching that a little will likely provide satisfactory results as well. How much is "a little" is the obvious question and what we can say here is that we certainly would not want to see more than 5 rpm. Is the problem with nuisance trips one of governing capability?

While it would require some expense the safe solution to this problem may well lie with the employment of a more accurate means of governing the engines.

I hope this helps you out and provides some insight as to our concerns for the well being of your equipment. If you would like to discuss this further or need more information please do not hesitate to contact me.

Sincerely,

Chuck Melcher
Manager, Engineered Solutions

Cc: A. Schubert – CES Mount Vernon

cc. Marshall Villers
Paul Dorwith -

Hope this helps.

COOPER-BESSEMER COMPANY

July 5, 1973

Consolidated Gas Supply Corporation
445 West Main Street
Clarksburg, West Virginia 26301

ATTENTION: Mr. E. S. Schwartz, Mechanical Engineer

SUBJECT: GMV-10 Cracked Crankshafts

Dear Ed:

Sorry that I have not answered your May 25th letter before this but it did take some research and I have been out of town recently. As I explained to you in Morgantown, the problem applies only to the GMV-10 cylinder units. In checking your records, I find that you have ten (10) cylinder units with the following cylinder numbers: 41159 listed at McHorter, 41598-9-600-601, 41836-7-8 and 42770 at Clendenon. In order to give you assistance on repair and a mode of operation, I think it would be well to first describe the location of the crack. Please refer to the attached sketch and note that I have located an example in the journal to the left in the elevated view. The corresponding crack in View "RR" starts at Point "X" which is the oil hole in the main bearing journal and travels in a horizontal direction to Point "Y". Referring to the view in elevation the crack then proceeds from Point "Y" down to "Z" where it breaks out into the oil hole. Note by the red mark in the elevated view that there is a triangular plane and as the crack progresses, the plane would propagate to the web to the right. The same phenomenon can happen in the connecting rod bearing journal.

Now as to the reason for the problem. After many years of service, those cracks showed up and it was determined that they were caused by low stress critical speeds. Furthermore, the oil hole was drilled on a diagonal as shown in the elevated view and was drilled from the connecting rod journal down to the main left bearing journal. The same hole was drilled from the connecting rod journal down to the right main bearing journal. Because the 1-1/8" hole was drilled on a diagonal when it breaks out into the journal, it becomes a much larger oblong hole as shown in View "RR". Furthermore, the section of metal at Point "X" is quite thin and when the shaft was first designed, they did not radius them enough at that point. This problem certainly was a low stress proposition because not all shafts broke and the problem did show up after many years of operation.

MOUNT VERNON, OHIO 43050 • PHONE 614/397-0121

COOPER-BESSEMER COMPANY

Page 2
Consolidated Gas Supply Corporation
Attention: Mr. E. S. Schwartz
July 5, 1973

There were several approaches to correction. To begin with, the oil drilling was redesigned and made as shown in Sketch 2. As a matter of fact, if you were to replace one of your shafts by ordering the old part number, you would get the shaft drilled as in Sketch 2. Those shafts that had not broken in the field were radiused at the critical point that I mentioned. Another correction that was made involved operation. Torsional studies were made on all units in the field and they applied no operating bands to the units. In other words, for the subject units, you were told not to run them in the ranges between 250 to 260 RPM and 285 to 310. Maximum RPM should be 320. Of course, that information was based on the fact that the units had ten (10) counterweights, part number GMV-3-2J. There was one exception to the above and that is for Serial Number 42770 which they had ten (10) counterweights, GMV-3-12N. It was not to be operated in the range of 265 to 285 nor above 310 RPM. I would check all the above units to determine that they still have the counterweights on as mentioned above and if they are of that configuration, then I would reissue the above information to the stations. The other correction that we took was to install oscillating counterweights that would allow the engine to be operated at all speeds but according to our records, none of the above units have the oscillating counterweights. I am sorry that I may have confused you on this when discussing it in Morgantown as I thought for sure at that time you had them, so disregard any comments I made about the oscillating counterweights.

PLEASE CHK.

Now as to the correction, please refer to Sketch 1 again and note that if the crack has progressed from Point "X" into the radius of the web, I would scrap the shaft. If it has progressed as shown, then you can drill a 3/16" diameter hole as shown in the right side main bearing journal in the elevated view. In other words, that 3/16" hole is drilled at the end of the crack as shown at Point "Y" in View "RR" and is drilled until it breaks out into the oil hole as shown in the elevated view. There were some shafts that were repaired by metalocking and it was very successful. On the other hand, there are many engines that were drilled at the time of initiation of this fix which was about

COOPER-BESSEMER COMPANY

Page 3
Consolidated Gas Supply Corporation
Attention: Mr. E. S. Schwartz
July 5, 1973

1951 and they are operating today. On the other hand, some cracks have been known to progress past the 3/16" hole and it is satisfactory to redrill or metalock providing that the crack has not gone into the web. I hope that this information will be of assistance to you and if you need any other information, please let me know.

Very truly yours,

Jim

J. H. Caldwell, Manager
Service Training
Customer Services

JHC:dp

Attachments

Note: Cornwell Secondary Cracks.

JWR
MFL
JB

COOPER INDUSTRIES

ENERGY SERVICES GROUP

May 16, 1989

RECEIVED
MAY 17
NATURAL GAS PLANTS DIV.
OKLAHOMA AREA

Texaco U.S.A.
P.O. Box 1560
Tulsa, OK 74102

Attention Mr. M. F. Larkin

Subject: Speed Uprate on Cooper-Bessemer GMV-6

Dear Mike:

Cooper Industries/Energy Services Group is pleased to submit our proposal to provide Engineering Services. The scope of the proposed study is to perform a torsional study of your Cooper-Bessemer GMV-6 Integral Engine/Compressor to evaluate the possibility of a speed increase.

The report generated as a result of this study will indicate those modifications that need to be made to the engine in order to operate at the higher speed. If no changes are required, Texaco will receive our approval to uprate the speed to 330 RPM and new nameplates to this effect will be issued.

If the report indicates that modifications are required, at your option, we will quote you those items required to uprate the engine to 330 RPM. After the required modifications have been made, new nameplates will be issued indicating the uprated speed capability.

Please note that the study is much more than a "records search to verify components." The records search is the first step in the study. After the records are searched to indicate component part numbers, weights, sizes, and materials, the pertinent data is provided to our Analytical Engineering Group. This group will computer model the system, calculating stress levels, critical speeds, etc. This data is then analyzed to ensure that no dangerously high stress levels are encountered in the proposed operating speed range. If high stresses are indicated, recommendations are made to reduce stress levels. Finally, a formal report is prepared and submitted.

4405 South 74 East Avenue
P.O. Box 470383
Tulsa, Oklahoma 74147-0383
(918) 622-4670 Telex: 49-7528

We trust that you will find this information to be useful. Please do not hesitate to call if you have questions or comments. We look forward to working with you on this project.

Sincerely,

Randy Bissey

Randy Bissey
Senior Sales Engineer

PRB:rc

Enclosure

cc: C. W. Melcher, Grove City
M. C. Wymore, Tulsa

COOPER ENERGY SERVICES GROUP

COOPER-BESSEMER RECIPROCATING PRODUCTS

APPLIED MECHANICS REPORT

AM-3291-JK

TEXACO, INCORPORATED

GMV-6 SN-41827, 41833, and 42200

GMVL-6 SN-44785

SO-1153 Balance Study

Inertia balance and torsional results are presented for these engines.

SUBMITTED BY

R. W. HARVEY

NOVEMBER 7, 1989

NGP&L DIVISION
OKLAHOMA AREA

DEC 01 '89

NOTE COPY HANDLE

JWH		
MFL		
JB		
File		
Arkoma		
Enville		
Hardy		
Kellyville		
Maysville		
Velma		

ENERGY SERVICES GROUP

November 29, 1989

Texaco U.S.A.
Maysville Gas Plant
Post Office Box 846
Maysville, Oklahoma 73057

Attention: Mr. C. D. Jackson

Subject: GMV-6 Torsional Study
Your P.O. #HL545191

Dear Chris:

Cooper Industries/Energy Services Group is pleased to submit our completed report. We appreciate your order.

If you should have comments or questions, please do not hesitate to call.

Sincerely,

Randy Bissey

Randy Bissey
Senior Sales Engineer

RECEIVED
DEC 13 1989
NATURAL GAS PLANTS DIV.
ENGINEERING SERVICES

PRB:cdl

CC: Mr. Mike Larkin - Texaco, U.S.A.
P.O. Box 1650
Tulsa, OK 74102

Mike Wymore - Tulsa
Chuck Melcher - G.C.

Overspeed setting?
Weights of Rods?
If comp cyl weights/balance counter
are reasonable GMV-6 can
be run at 330 RPM Talked w/ Randy 12/18
w/ no Rods

4405 South 74 East Avenue
P.O. Box 470383
Tulsa, Oklahoma 74147-0383
(918) 622-4670 Telex: 49-7528

AJAX® COBERRA® COOPER-BESSEMER® EN-TRONIC® CONTROLS PENN™ SUPERIOR®

Cooper submits the following Engineering Study to Texaco based on the assumption the units in question are in excellent physical condition, have received proper maintenance, have not been modified in any way without Cooper's approval, and have not been operated in a manner for which they were not designed. The results which follow are only an opinion, presented as an advisory nature, the use of which is done at the sole discretion of Texaco. Due to the fact that the units being studied are in unknown condition, may not have received proper maintenance, may have been used for purposes other than those for which they were originally designed, and may have been modified in some way without the knowledge of Cooper-Bessemer, Cooper can not take any responsibility for the structural soundness of, or ultimate suitability for, the units' ability to operate satisfactorily at the proposed higher speed. Texaco must make that judgment and accept that responsibility. This study does not carry with it any guarantee as to the specific units' ability to perform at the higher speed in an acceptable manner. Cooper will not accept any liability for loss or damages, consequential, incidental, loss of anticipated profits, loss of use of equipment, installation, system, or facility arising out of the failure of a unit to operate at a level for which it was not originally designed.

AM-3291-JK
11-07-89

The customer wishes to increase the operating speed of a group of older GMV-6 engines from 300 to 330 RPM. Representative engines are:

CASE	ENGINE	LOCATION
A	GMV-6 SN-42200	Eunice, II
B	GMV-6 SN-41833	Criner #4
C	GMVL-6 SN-44785	Criner #3
D	GMV-6 SN-41827	Antioch #8

These engines are believed to have the compressor cylinders and balance equipment listed in Tables 1 to 4. Please report any discrepancies between these Tables and the engines.

The predicted inertia unbalance at 330 RPM is:

	Eunice # CASE A	Criner #4 CASE B	Criner #3 CASE C	Antioch #8 CASE D
Horizontal primary force, kip	2.6	0.9	0.8	10.9
Vertical primary force, kip	0.0	0.0	0.4	0.0
Horizontal primary couple, kip-ft	194	203	164	205
Vertical primary couple, kip-ft	39	39	28	39
Horizontal secondary force, kip	0.5	0.2	0.2	2.3
Vertical secondary force, kip	0.0	0.0	0.0	0.0
Horizontal secondary couple, kip-ft	43	44	39	44
Vertical secondary couple, kip-ft	8	8	8	8

The inertia balance of Cases A, B and C is satisfactory for a GMV-6 engine mounted on a good, firm earth foundation. The 10.9 kip of horizontal primary force unbalance of Case D should be reduced by adding reciprocating weight to Throw 2. The recommended Modified Case D equipment is listed in Table 5, and the predicted inertia unbalance at 330 RPM is:

	MODIFIED CASE D
Horizontal primary force, kip	2.6
Vertical primary force, kip	0.0
Horizontal primary couple, kip-ft	205
Vertical primary couple, kip-ft	39
Horizontal secondary force, kip	0.5
Vertical secondary force, kip	0.0
Horizontal secondary couple, kip-ft	44
Vertical secondary couple, kip-ft	8

The calculated first mode torsional natural frequencies are:

CASE	FREQUENCY, CPM	CRITICALS NEAR 330 RPM
A	2744	8th at 343 RPM & 9th at 305 RPM
B	2739	8th at 342 RPM & 9th at 304 RPM
C	3128	9th at 348 RPM & 10th at 313 RPM
D	2757	8th at 344 RPM & 9th at 306 RPM
Modified D	2744	8th at 343 RPM & 9th at 305 RPM

At 330 RPM and speeds below 330 RPM the torsional responses will be acceptable. Therefore, the Case A, B, C & Modified D engines appear to be satisfactory for 330 RPM operation.

Submitted by,

R. W. Harvey
R. W. Harvey
Analytical Engineer

Approved by,

John M. Horne, Manager
Analytical and Compressor Engineering

Attachments

CC w/att: C. W. Melcher (4)
AM-3291, Packet #35

:jld
11/07/89

Table 1, Case A Engine

Texaco, Eunice II

GMV-6 SN-42200 SO-1153 Study

1. Compressor Cylinders

Throw	Cylinder	Piston Material
1	14-1/2" C5B-14	CI
2	21-1/2" CE-14	AI
3	21-1/2" CE-14	AI

Flywheel End

2. Crankshaft Counterweights and Flywheel

Web	Counterweight
1 forward	GMV-3-9D
1 aft	GMV-3-9D
2 forward	GMV-3-9D
2 aft	GMV-3-9D
3 forward	GMV-3-9D
3 aft	GMV-3-9D

GMV-6-26A Flywheel

3. Reciprocating Parts

Throw	Crosshead	Crosshead Shoe	Scavenging Piston
1	GMV-38-2C	GMV-38-2B	GMV-38-1F
2	GMV-38-2C	GMV-38-2B	GMV-38-1F
3	GMV-38-2C	GMV-38-2B	GMV-38-1F

NOTE: The GMV-6, SN-42337 engine at Eunice II has GMV-38-4A scavenging pistons instead of the listed GMV-38-1F. The effect on inertia balance and torsional results will be very small.

Table 2, Case B Engine

Texaco, Criner #4

GMV-6 SN-41833 SO-1153 Study

1. Compressor Cylinders

Throw	Cylinder	Piston Material
1	14-3/4" C5B-14	CI
2	20" CE-14	CI
3	20" CE-14	CI

Flywheel End

2. Crankshaft Counterweights and Flywheel

Web	Counterweight
1 forward	GMV-3-2D
1 aft	GMV-3-2D
2 forward	GMV-3-2D
2 aft	GMV-3-2D
3 forward	GMV-3-2D
3 aft	GMV-3-9D

GMV-6-26A Flywheel

3. Reciprocating Parts

Throw	Crosshead	Crosshead Shoe	Scavenging Piston
1	GMV-38-2C	GMV-38-2B	GMV-38-1F
2	GMV-38-2C	GMV-38-2B	GMV-38-1F
3	GMV-38-2C	GMV-38-2B	GMV-38-1F

Table 3, Case C Engine

Texaco, Criner #3

GMVL-6 SN-44785 SO-1153 Study

1. Compressor Cylinders

Throw	Cylinder	Piston Material
1	14-3/4" C5B-14	CI
2	20" CE-14	CI
3	20" CE-14	CI

Flywheel End

2. Crankshaft Counterweights and Flywheel

Web	Counterweight
1 forward	GMVA-3-L
1 aft	GMVA-3-L
2 forward	GMVA-3-P
2 aft	--------
3 forward	GMVA-3-L
3 aft	GMVA-3-L

GMVA-6-A Flywheel

3. Reciprocating Parts

Throw	Crosshead	Crosshead Shoes
1	GMVA-38-1A	GMVA-38-1C
2	GMVA-38-1A	GMVA-38-1C
3	GMVA-38-1A	GMVA-38-1C

Table 4, Case D Engine

Texaco, Antioch #8

GMV-6 SN-41827 SO-1153 Study

1. Compressor Cylinders

Throw	Cylinder	Piston Material
1	14" C5B-14	CI
2	Blank	--
3	25" CE-14	CI

Flywheel End

2. Crankshaft Counterweights and Flywheel

Web	Counterweight
1 forward	GMV-3-2D
1 aft	GMV-3-2D
2 forward	GMV-3-2D
2 aft	GMV-3-2D
3 forward	GMV-3-2D
3 aft	GMV-3-9D

GMV-6-26A Flywheel

3. Reciprocating Parts

Throw	Crosshead	Crosshead Shoe	Scavenging Piston
1	GMV-38-2C	GMV-38-2B	GMV-38-1F
2	GMV-38-2C	GMV-38-2B	GMV-38-1F
3	GMV-38-2C	GMV-38-2B	GMV-38-1F

Table 5, Modified Case D Engine

Texaco, Antioch #8

GMV-6 SN-41827 SO-1153 Study

1. Compressor Cylinders

Throw	Cylinder	Piston Material
1	14" C5B-14	CI
2	Blank	--
3	25" CE-14	CI

Flywheel End

2. Crankshaft Counterweights and Flywheel

Web	Counterweight
1 forward	GMV-3-2D
1 aft	GMV-3-2D
2 forward	GMV-3-2D
2 aft	GMV-3-2D
3 forward	GMV-3-2D
3 aft	GMV-3-9D

GMV-6-26A Flywheel

3. Reciprocating Parts

Throw	Crosshead	Crosshead Shoe	Scavenging Piston
1	GMV-38-2C	GMV-38-2B	GMV-38-1F
2	GMV-38-2C	GMV-38-2B	GMV-38-6A* with two GMV-38-6C#2 balancing weights
3	GMV-38-2C	GMV-38-2B	GMV-38-1F

* Replaces existing GMV-38-1F scavenging piston.

4. Needed Parts, Ref: GMV-38-6

Part	Description	Quantity
GMV-38-6A	Scavenging piston	1
GMV-38-6C#2	Balancing weight	2
1-03F-001-048-073	3/4-10 stud	4
CSA-343-048	3/4-10 Drake nut	4

Appendix B – Hydraulically Actuated Mechanical Fuel Injection Valve

Original Valve Design

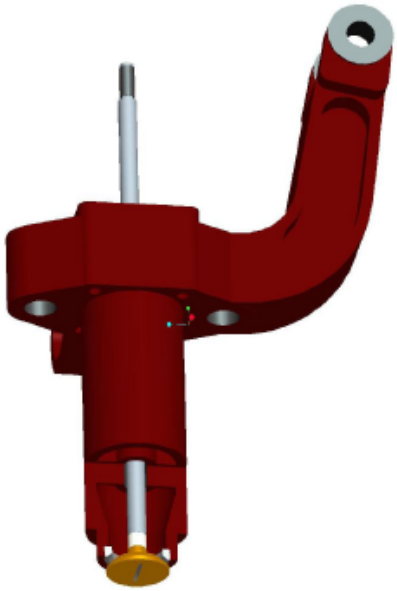

Original Valve Design

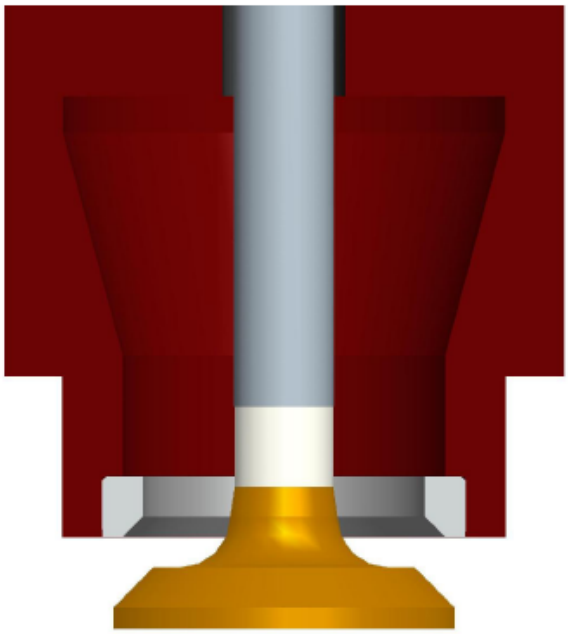

New Valve Design

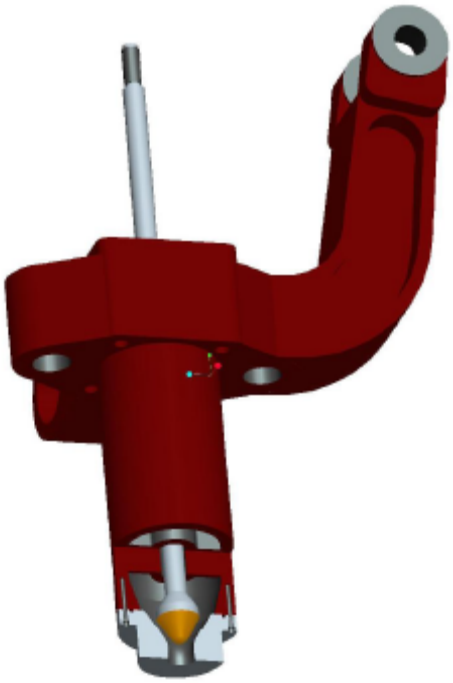

New Valve Design

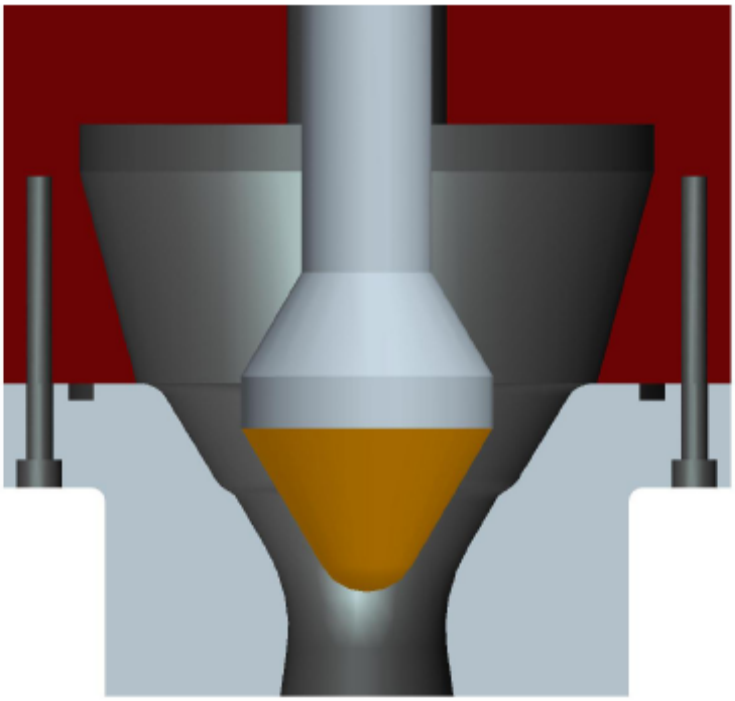

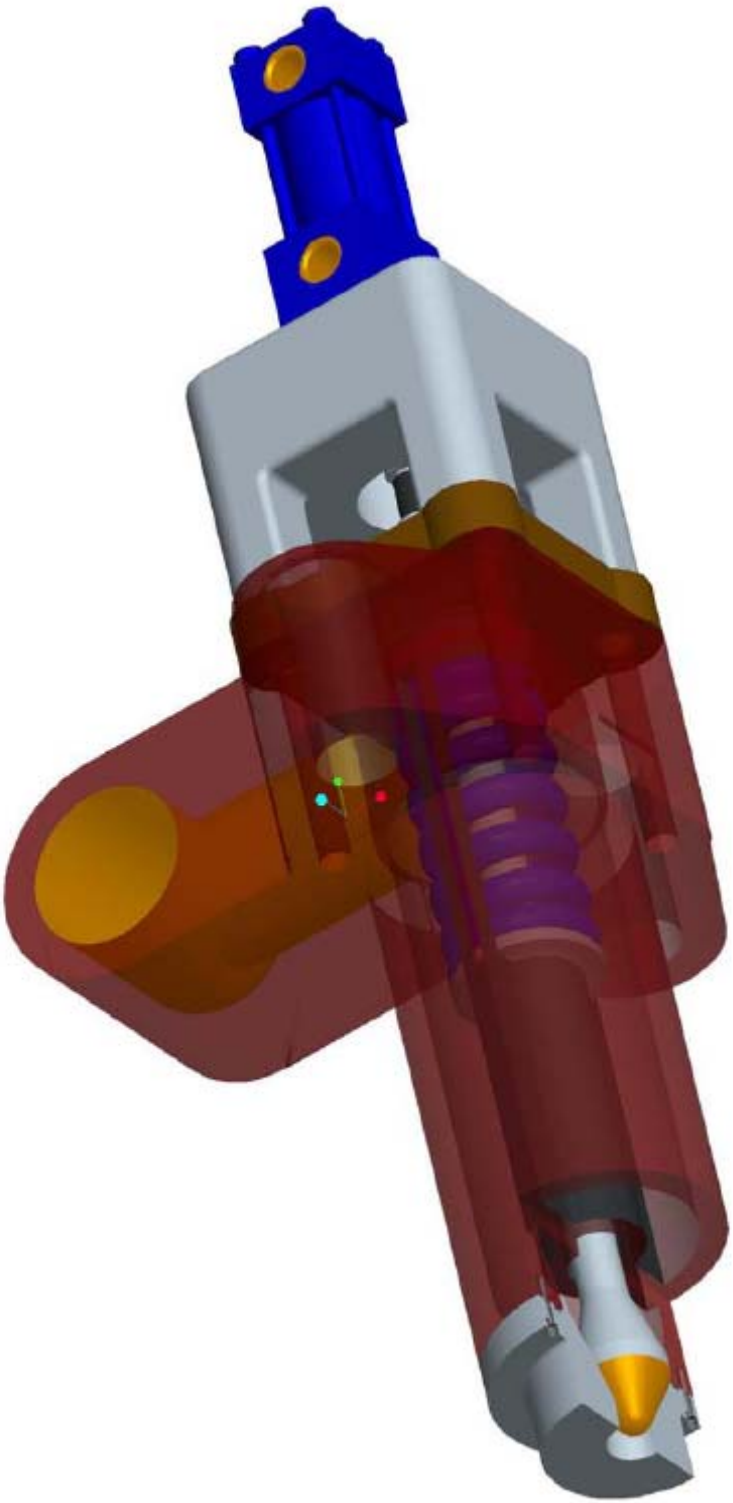

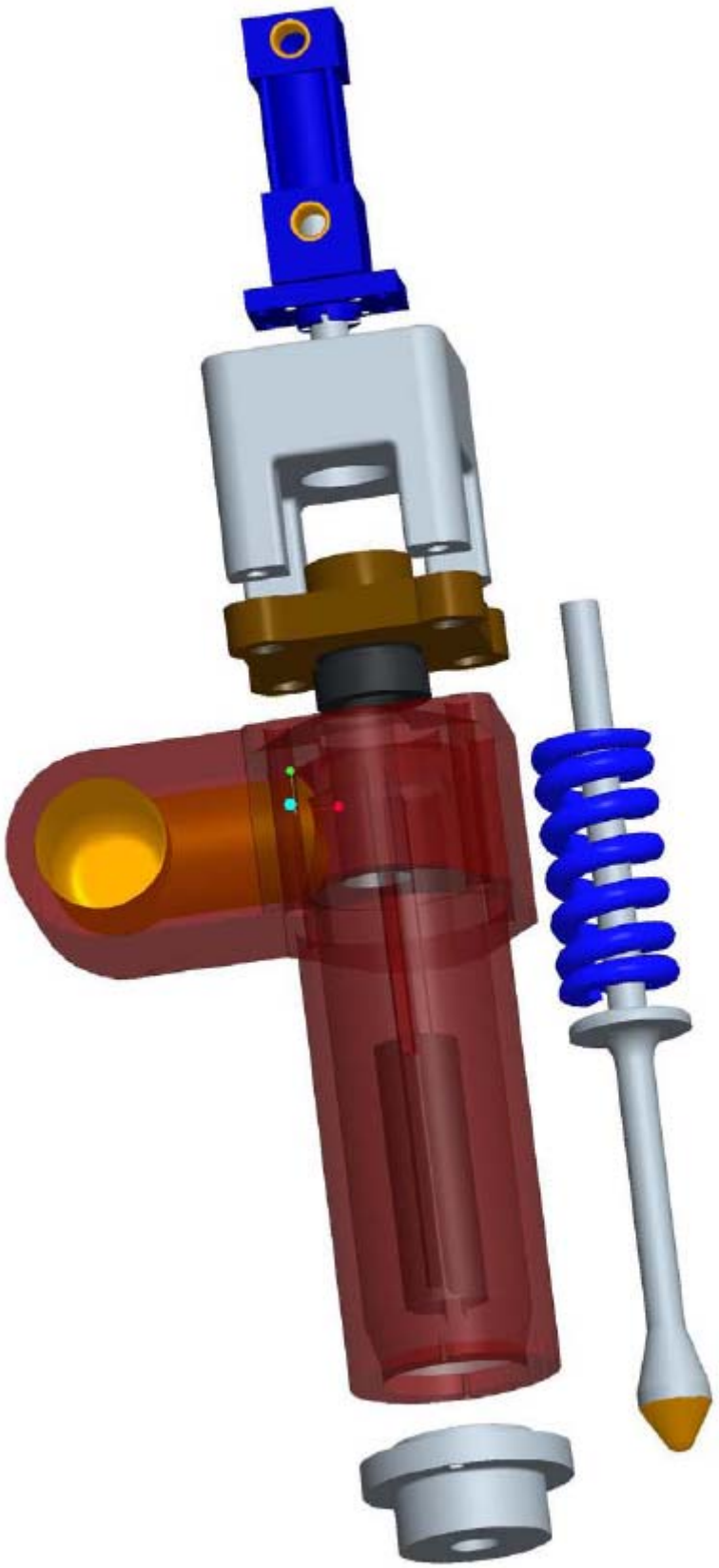

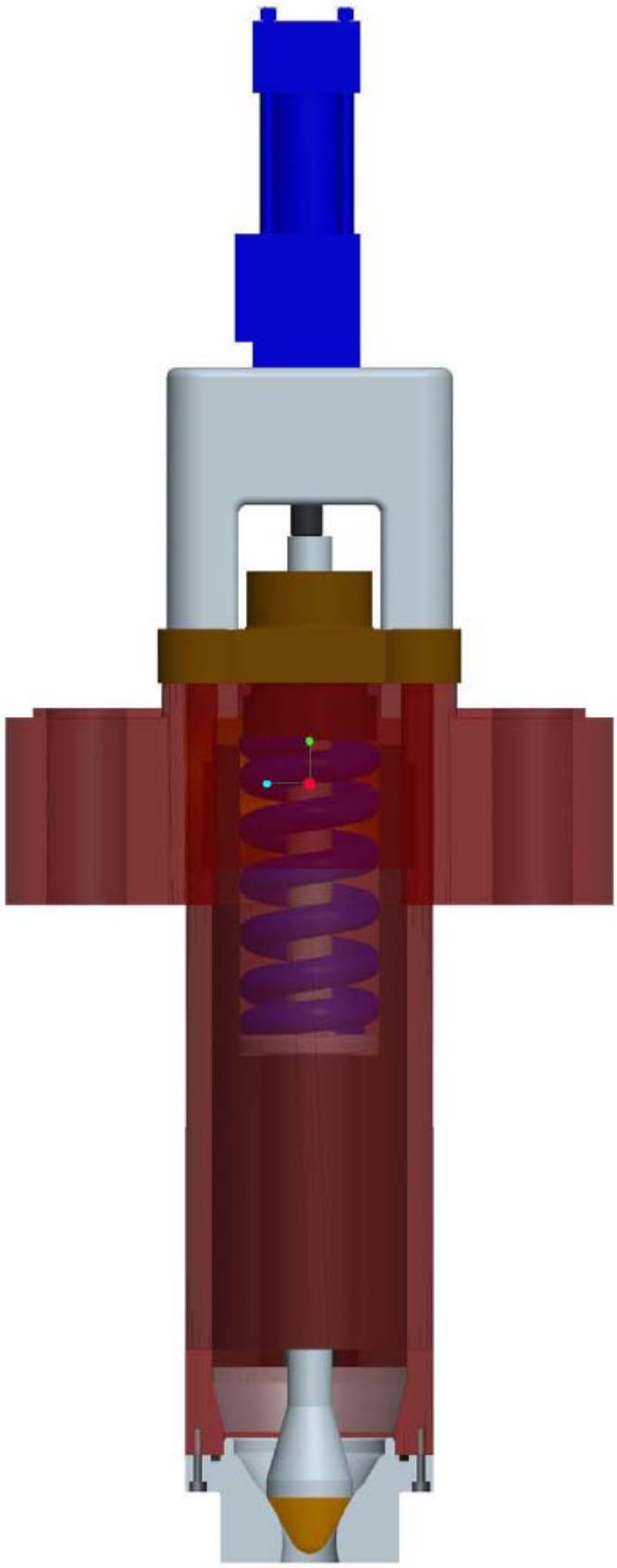

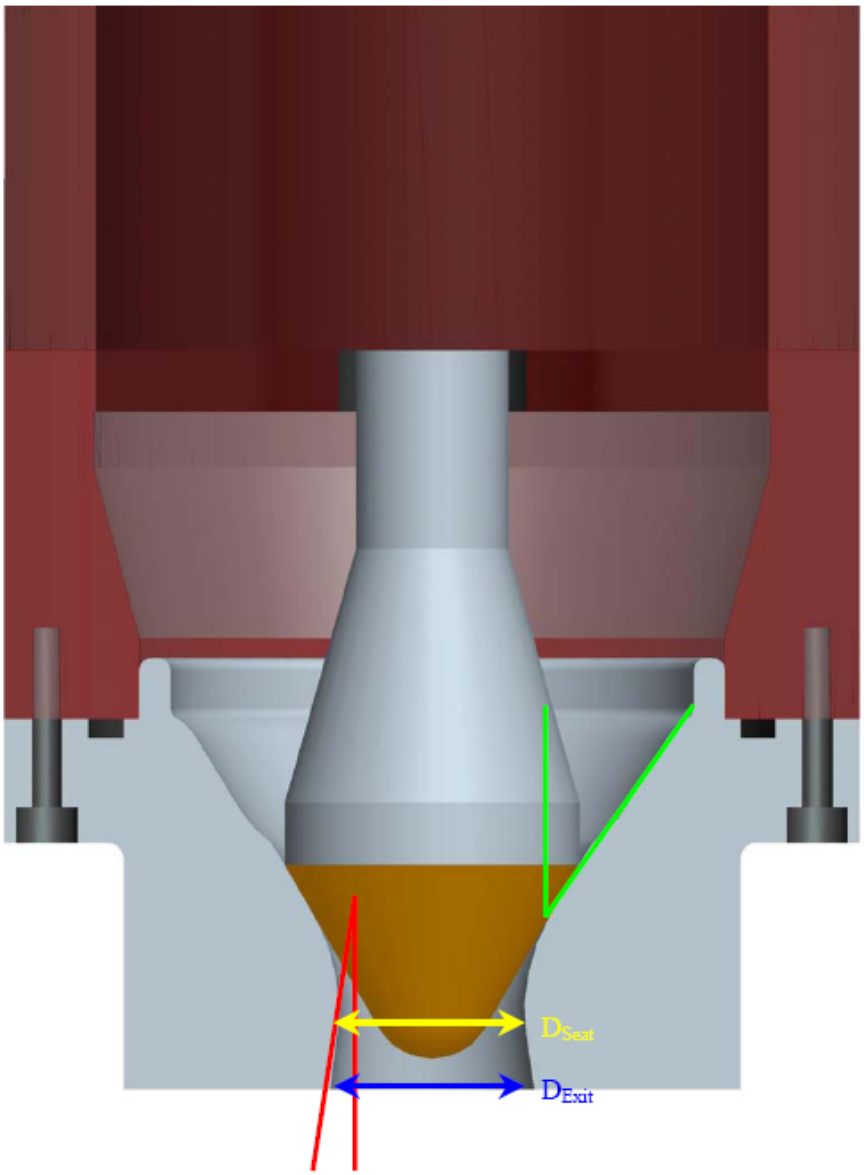

Mach #	Cd	At (in2)	Dseat (in)	Aexit (in2)	Dexit (in2)
1.66	0.75	0.445	0.755	0.593	0.869
1.74	0.85	0.393	0.667	0.558	0.843
1.81	0.95	0.351	0.596	0.529	0.821

Lift (in)	0.375
Cam Duration (deg)	34
FVO ATDC (deg)	245

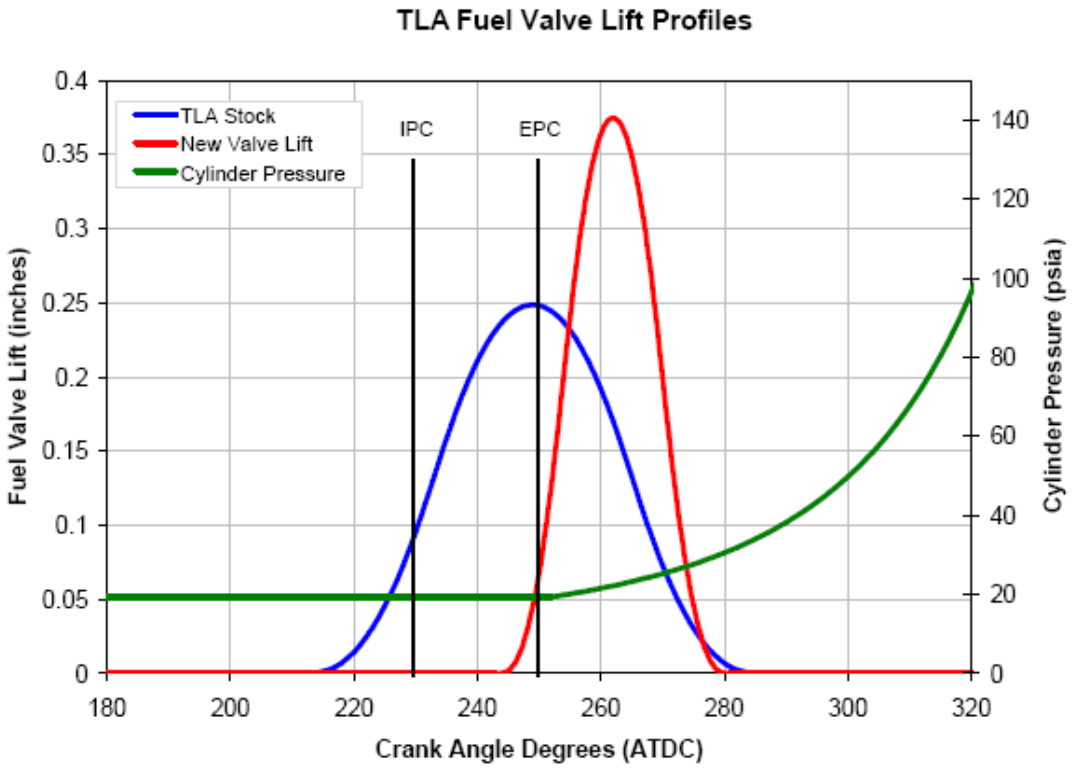
TLA Fuel Valve Lift Profiles
TLA Stock
New Valve Lift
Cylinder Pressure
IPC
EPC
Fuel Valve Lift (inches)
Cylinder Pressure (psia)
Crank Angle Degrees (ATDC)
0.4
0.35
0.3
0.25
0.2
0.15
0.1
0.05
0
140
120
100
80
60
40
20
0
180
200
220
240
260
280
300
320

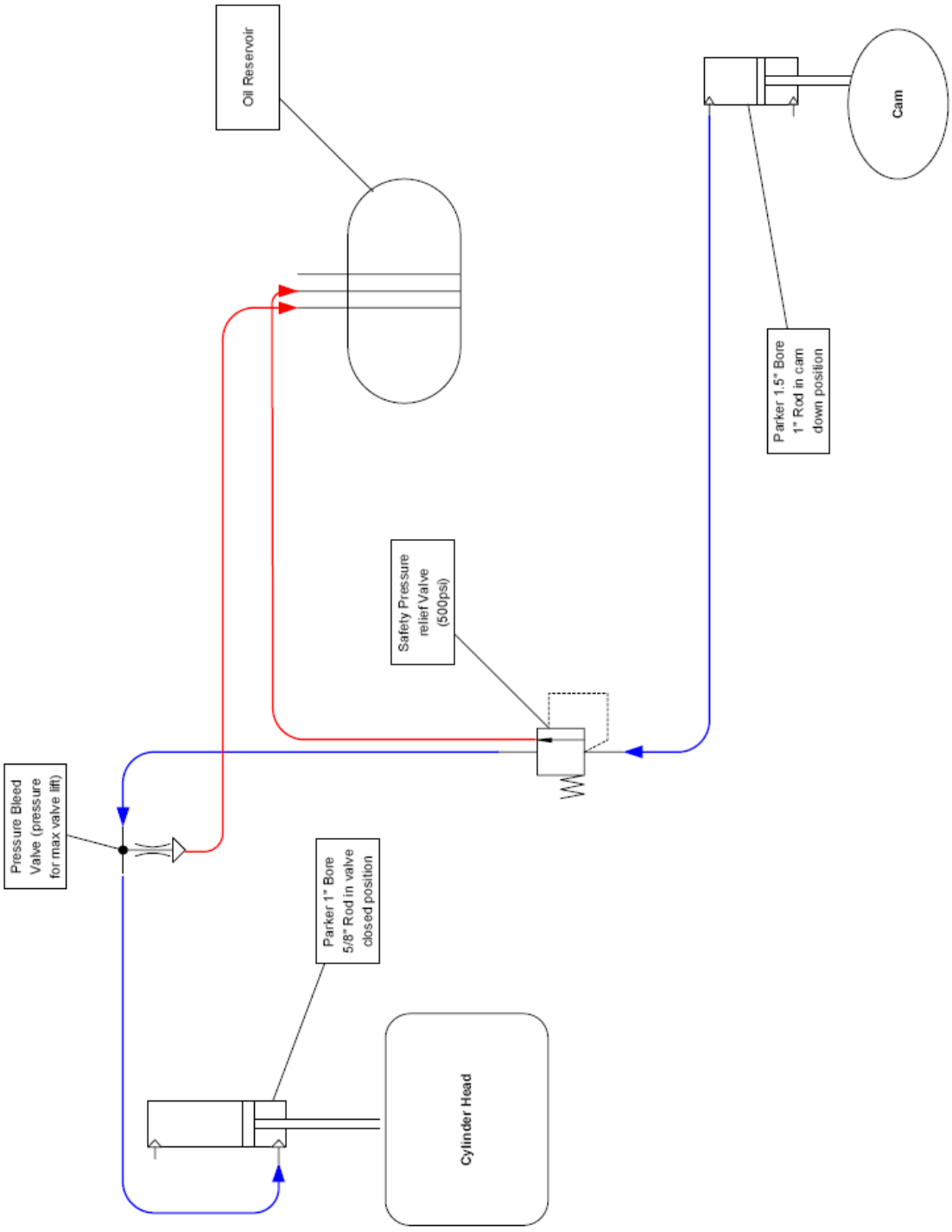
Oil Reservoir
Cam
Parker 1.5" Bore
1" Rod in cam
down position
Safety Pressure
relief Valve
(500psi)
Pressure Bleed
Valve (pressure
for max valve lift)
Parker 1" Bore
5/8" Rod in valve
closed position
Cylinder Head

Valve Calculations for Hydraulic Cylinders

Injector Side

$D1_{bore} := 1in$ $D1_{rod} := \frac{5}{8}in$

$A1_{bore} := \pi \cdot \left(\frac{D1_{bore}}{2}\right)^2$ $A1_{rod} := \pi \cdot \left(\frac{D1_{rod}}{2}\right)^2$

$A1 := A1_{bore} - A1_{rod}$

$A1 = 0.479\,in^2$

Needed A2 $A2_{needed} := 2A1$

$A2_{needed} = 0.957\,in^2$

Camshaft Side

$D2_{bore} := 1.5in$ $D2_{rod} := 1in$

$A2_{bore} := \pi \cdot \left(\frac{D2_{bore}}{2}\right)^2$ $A2_{rod} := \pi \cdot \left(\frac{D2_{rod}}{2}\right)^2$

$A2 := A2_{bore} - A2_{rod}$

$A2 = 0.982\,in^2$

Lift Ratio

$n_{lift} := \frac{A2}{A1}$ $n_{lift} = 2.051$

Based on a desired lift ratio = 2 a Parker Series 3L 1" and 1.5" bore cylinders were selected, each with 1" stroke

Spring Calculations

$D_{tmax} := .755in$ Throat Diameter of Nozzle

$A_{tmax} := \pi \cdot \left(\frac{D_{tmax}}{2}\right)^2$

Estimated Pressures and Safety Factor

$P_{cylinder\_max} := 1500psi$ $P_{hyd\_line} := 50psi$ $SF := 2$

$P_{design} := SF \cdot (P_{hyd\_line} + P_{cylinder\_max})$

$F_{design} := A_{tmax} \cdot P_{design}$

$F_{design} = 6173.506\ N$ $F_{design} = 1387.8594\ lbf$

Injector Hydraulic Pressure

$$P_{Injector} := \frac{F_{design}}{A1}$$

$P_{Injector} = 2899.819\ psi$

Spring Data From Century Springs

Spring Stock Number: D-1478

Hole size: 2.00in

Rod size: 1.00in

Wire dia: .460in

$Rate := 3816 \frac{lbf}{in}$ $Lift := .375in$

Preload Distance

$$\delta_{PL} := \frac{F_{design}}{Rate}$$

$\delta_{PL} = 0.364\ in$

Valve Cover Interference

$\delta_{VC} := 0.81in$ $L_{drill} := 5in$

$L_{pl} := L_{drill} - \delta_{VC}$

$L_{free} := L_{pl} + \delta_{PL}$

$L_{free} = 4.554\ in$

Total Deflection

$\delta_{Total} := \delta_{PL} + Lift$

$\delta_{Total} = 0.739\ in$

Service Life for Springs

$\delta_{max} := .25 \cdot L_{free}$ $\delta_{long\_life} := .15 \cdot L_{free}$

$\delta_{max} = 1.138\ in$ $\delta_{long\_life} = 0.683\ in$

$L_{afterPL} := L_{free} - \delta_{PL}$

$L_{afterPL} = 4.19\ in$

Given

$C_0 = 0$

$0 = C_0 + C_1 \cdot (1) + C_2 \cdot (1)^2 + C_3 \cdot (1)^3 + C_4 \cdot (1)^4 + C_5 \cdot (1)^5 + C_6 \cdot (1)^6 + C_7 \cdot (1)^7$

$h = C_0 + C_1 \cdot (.5) + C_2 \cdot (.5)^2 + C_3 \cdot (.5)^3 + C_4 \cdot (.5)^4 + C_5 \cdot (.5)^5 + C_6 \cdot (.5)^6 + C_7 \cdot (.5)^7$

$0 = C_1$

$0 = C_1 + 2 \cdot C_2 \cdot (1) + 3 \cdot C_3 \cdot (1)^2 + 4 \cdot C_4 \cdot (1)^3 + 5 \cdot C_5 \cdot (1)^4 + 6 \cdot C_6 \cdot (1)^5 + 7 \cdot C_7 \cdot (1)^6$

$0 = C_2$

$0 = 2 \cdot C_2 + 6 \cdot C_3 \cdot (1) + 12 \cdot C_4 \cdot (1)^2 + 20 \cdot C_5 \cdot (1)^3 + 30 \cdot C_6 \cdot (1)^4 + 42 \cdot C_7 \cdot (1)^5$

$0 = 6 \cdot C_3 + 24 \cdot C_4 \cdot (1) + 60 \cdot C_5 \cdot (1)^2 + 120 \cdot C_6 \cdot (1)^3 + 210 \cdot C_7 \cdot (1)^4$

$$\text{Find}(C_0, C_1, C_2, C_3, C_4, C_5, C_6, C_7) \rightarrow \begin{pmatrix} 0 \\ 0 \\ 0 \\ 128. \cdot h \\ -512. \cdot h \\ 768. \cdot h \\ -512. \cdot h \\ 128. \cdot h \end{pmatrix}$$

$N := 400 \quad i := 0 .. N \quad \theta_i := \frac{(i \cdot 2 \cdot \pi)}{N} \quad \beta := 36\text{deg}$

$i' := 0 .. N \cdot \frac{\beta}{2 \cdot \pi} \quad i'' := \text{round}\left(N \cdot \frac{\beta}{2 \cdot \pi}\right) + 1 .. N \quad h := .1875$

$C_0 := 0 \quad C_1 := 0 \quad C_2 := 0 \quad C_3 := 128 \cdot h \quad C_4 := -512 \cdot h \quad C_5 := 768 \cdot h \quad C_6 := -512 \cdot h \quad C_7 := 128 \cdot h$

$$S_{i'} := 1\left[C_0 + C_1\cdot\frac{\theta_{i'}}{\beta} + C_2\cdot\left(\frac{\theta_{i'}}{\beta}\right)^2 + C_3\cdot\left(\frac{\theta_{i'}}{\beta}\right)^3 + C_4\cdot\left(\frac{\theta_{i'}}{\beta}\right)^4 + C_5\cdot\left(\frac{\theta_{i'}}{\beta}\right)^5 + C_6\cdot\left(\frac{\theta_{i'}}{\beta}\right)^6 + C_7\cdot\left(\frac{\theta_{i'}}{\beta}\right)^7\right]$$

$$V_{i'} := \frac{1}{\beta}\left[C_1 + 2\cdot C_2\cdot\left(\frac{\theta_{i'}}{\beta}\right) + 3\cdot C_3\cdot\left(\frac{\theta_{i'}}{\beta}\right)^2 + 4\cdot C_4\cdot\left(\frac{\theta_{i'}}{\beta}\right)^3 + 5\cdot C_5\cdot\left(\frac{\theta_{i'}}{\beta}\right)^4 + 6\cdot C_6\cdot\left(\frac{\theta_{i'}}{\beta}\right)^5 + 7\cdot C_7\cdot\left(\frac{\theta_{i'}}{\beta}\right)^6\right]$$

$$A_{i'} := \frac{1}{\beta^2}\left[2\cdot C_2 + 6\cdot C_3\cdot\left(\frac{\theta_{i'}}{\beta}\right) + 12\cdot C_4\cdot\left(\frac{\theta_{i'}}{\beta}\right)^2 + 20\cdot C_5\cdot\left(\frac{\theta_{i'}}{\beta}\right)^3 + 30\cdot C_6\cdot\left(\frac{\theta_{i'}}{\beta}\right)^4 + 42\cdot C_7\cdot\left(\frac{\theta_{i'}}{\beta}\right)^5\right]$$

$$J_{i'} := \frac{1}{\beta^3}\left[6\cdot C_3 + 24\cdot C_4\cdot\left(\frac{\theta_{i'}}{\beta}\right) + 60\cdot C_5\cdot\left(\frac{\theta_{i'}}{\beta}\right)^2 + 120\cdot C_6\cdot\left(\frac{\theta_{i'}}{\beta}\right)^3 + 210\cdot C_7\cdot\left(\frac{\theta_{i'}}{\beta}\right)^4\right]$$

$S_{i''} := 0 \qquad V_{i''} := 0 \qquad A_{i''} := 0 \qquad J_{i''} := 0$

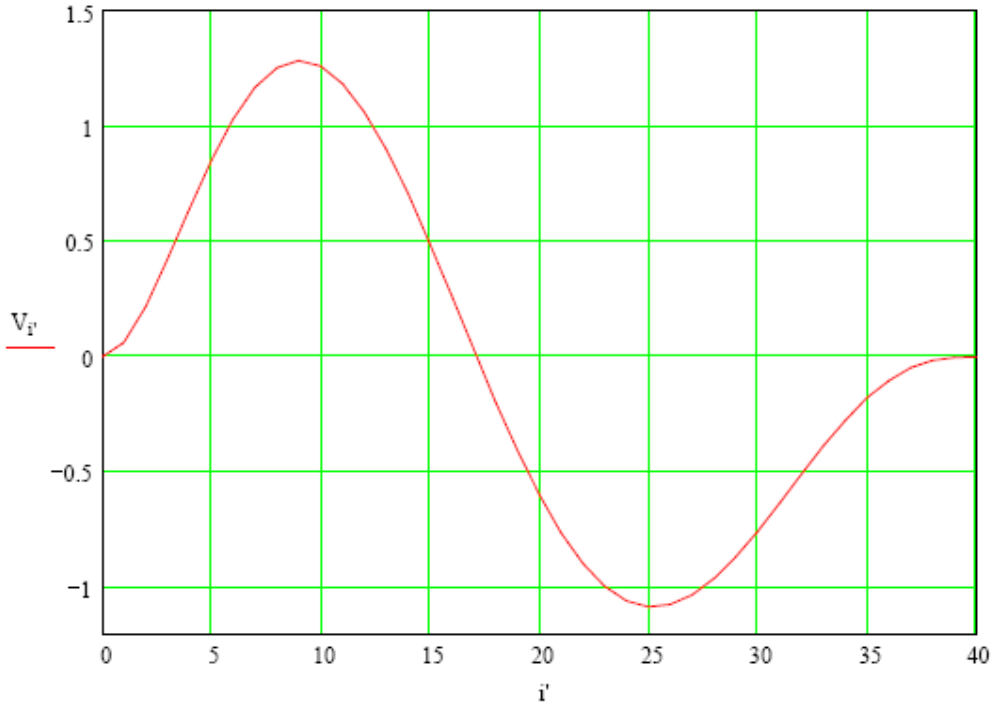
1.5
1
0.5
0
−0.5
−1
$V_{i'}$
0
5
10
15
20
25
30
35
40
i'

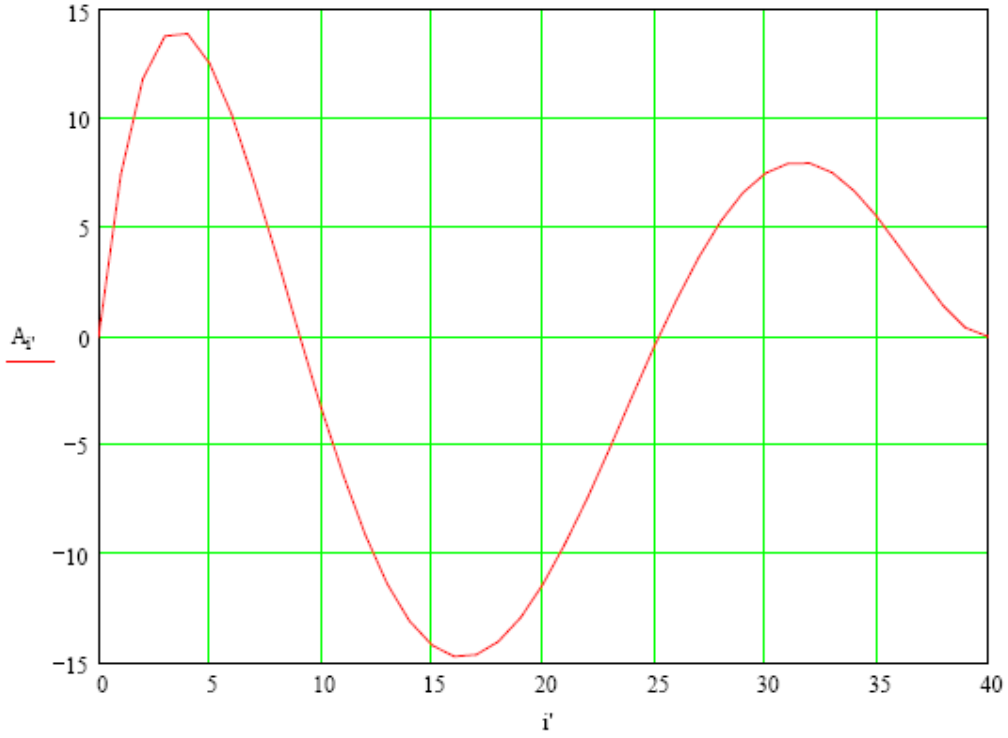
15
10
5
0
−5
−10
−15
$A_{i'}$
0
5
10
15
20
25
30
35
40
i'

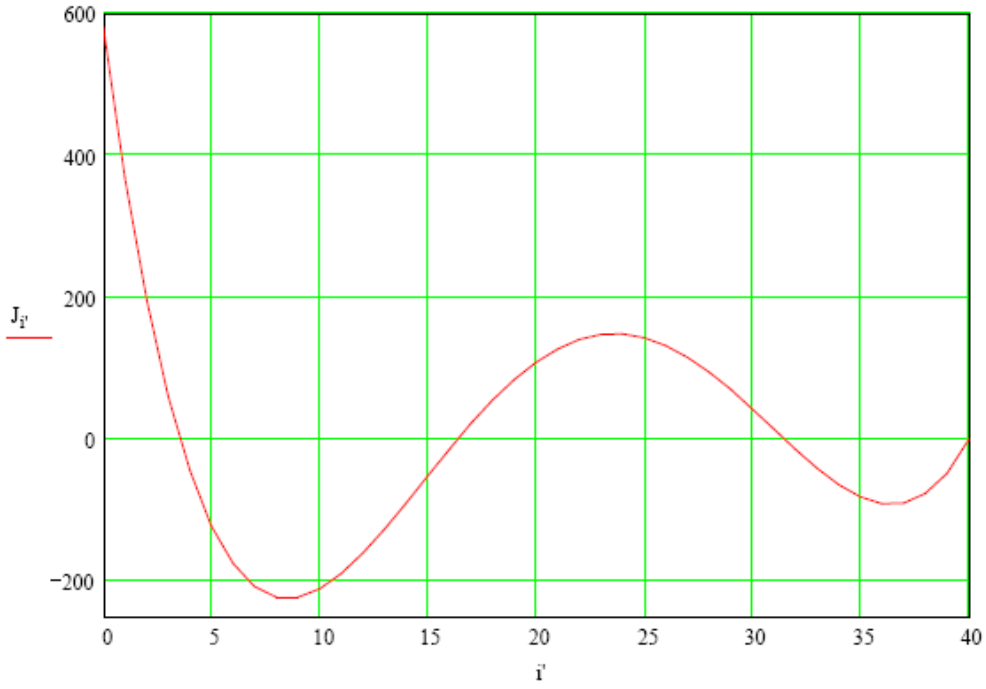
600
400
200
0
−200
$J_{i'}$
0
5
10
15
20
25
30
35
40
i'

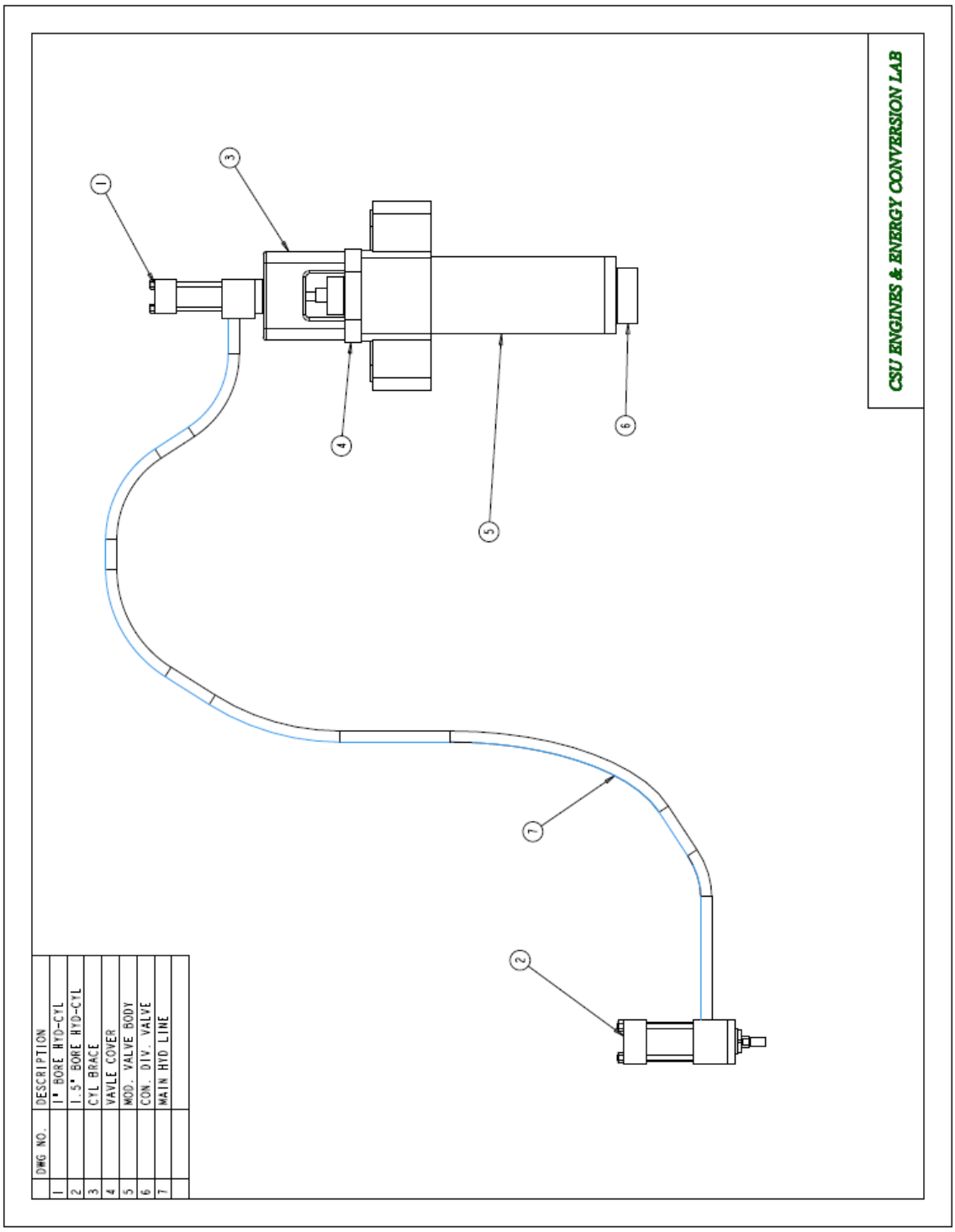
CSU ENGINES & ENERGY CONVERSION LAB
DWG NO.
DESCRIPTION
1" BORE HYD-CYL
1.5" BORE HYD-CYL
CYL BRACE
VAVLE COVER
MOD. VALVE BODY
CON. DIV. VALVE
MAIN HYD LINE
1
2
3
4
5
6
7

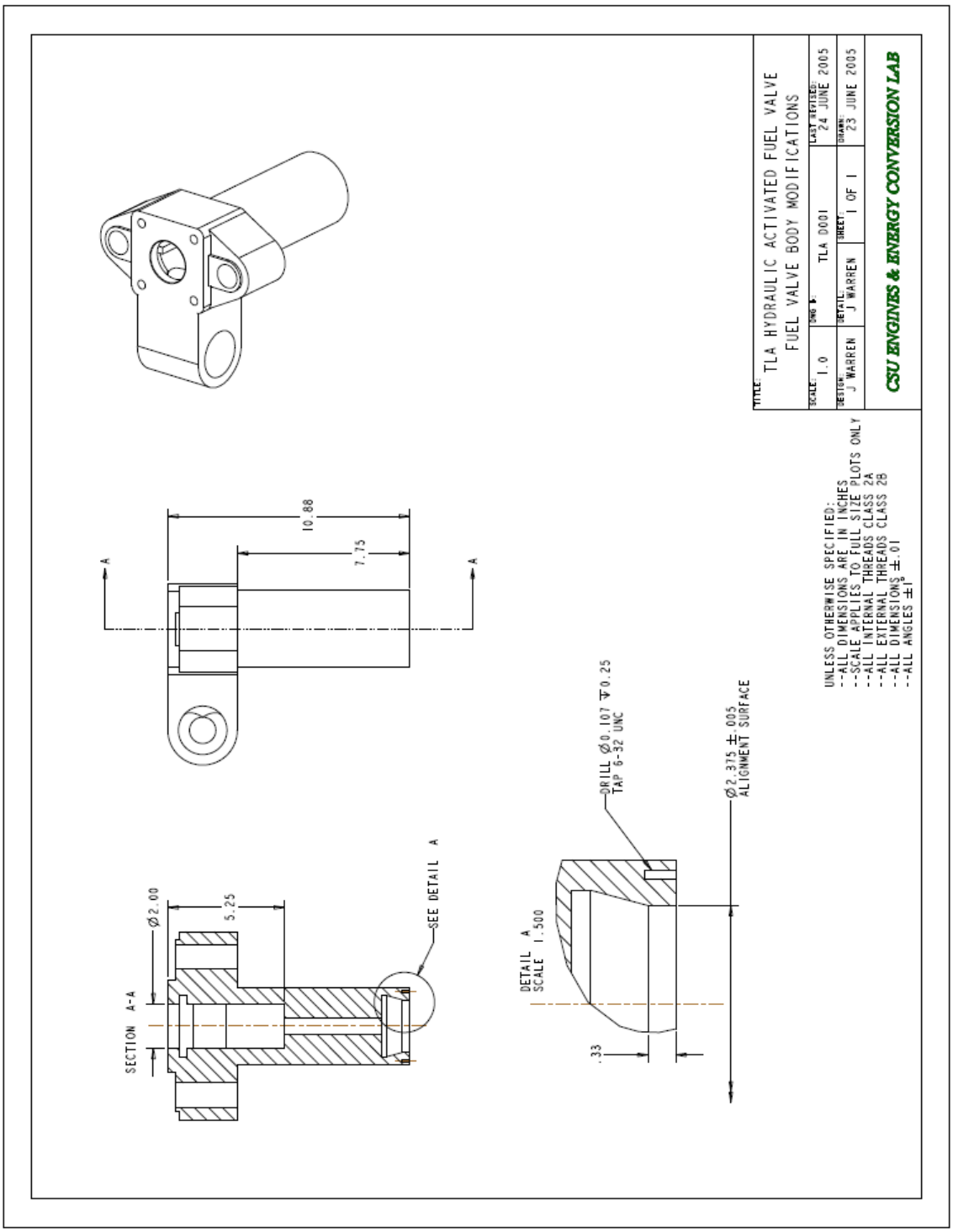
TLA HYDRAULIC ACTIVATED FUEL VALVE
FUEL VALVE BODY MODIFICATIONS
SCALE: 1.0
SIZE: B
DWG #: TLA 0001
LAST REVISED: 24 JUNE 2005
DESIGN: J WARREN
DETAIL: J WARREN
SHEET: 1 OF 1
DRAWN: 23 JUNE 2005
CSU ENGINES & ENERGY CONVERSION LAB
UNLESS OTHERWISE SPECIFIED:
--ALL DIMENSIONS ARE IN INCHES
--SCALE APPLIES TO FULL SIZE PLOTS ONLY
--ALL INTERNAL THREADS CLASS 2A
--ALL EXTERNAL THREADS CLASS 2B
--ALL DIMENSIONS ±.01
--ALL ANGLES ±1°
10.88
7.75
A
A
SECTION A-A
Ø2.00
5.25
SEE DETAIL A
DETAIL A
SCALE 1.500
DRILL Ø0.107 ∓0.25
TAP 6-32 UNC
Ø2.375 +.005 -.000
ALIGNMENT SURFACE
.33

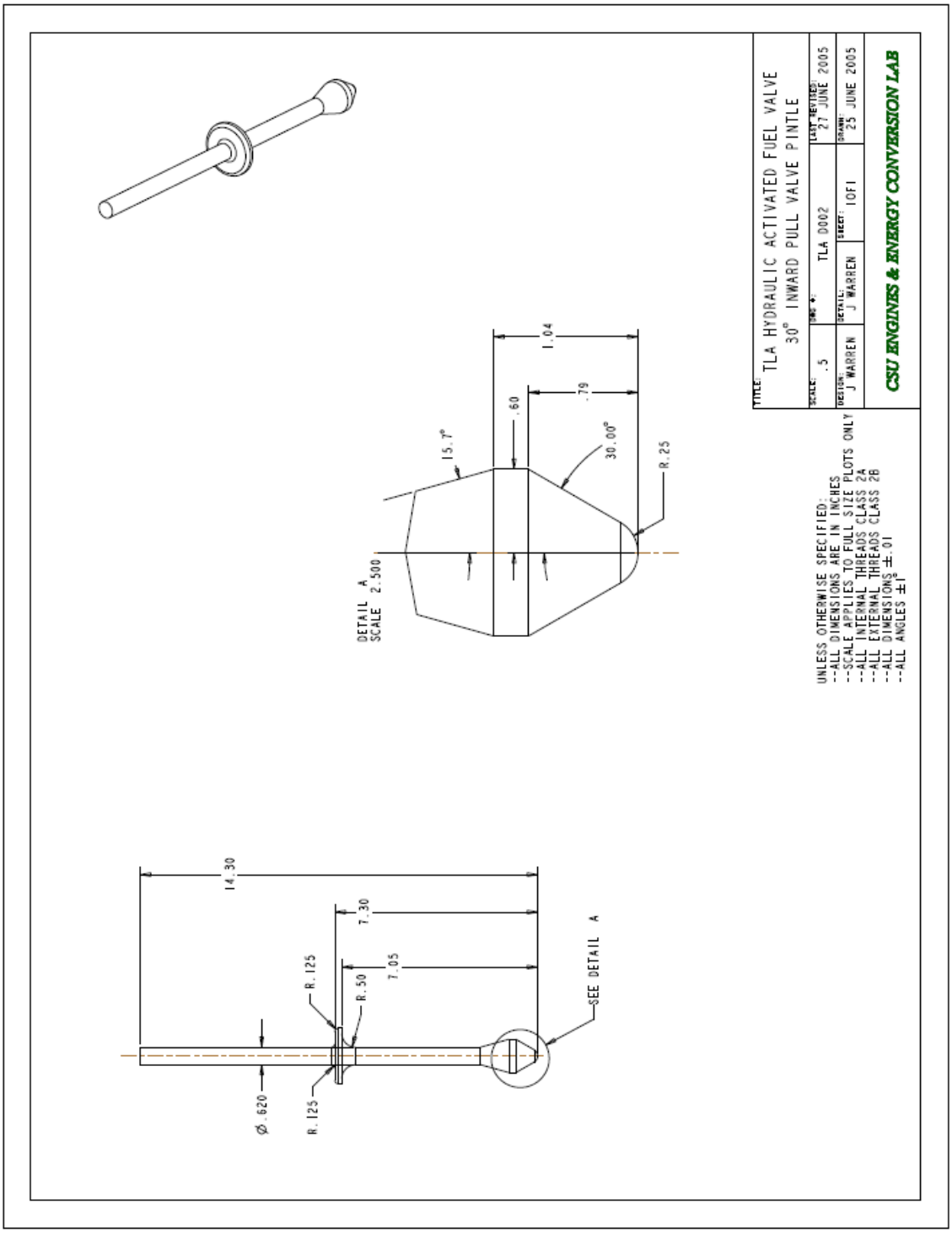
TLA HYDRAULIC ACTIVATED FUEL VALVE
30° INWARD PULL VALVE PINTLE
TLA 0002
27 JUNE 2005
25 JUNE 2005
J WARREN
1 OF 1
CSU ENGINES & ENERGY CONVERSION LAB
UNLESS OTHERWISE SPECIFIED:
--ALL DIMENSIONS ARE IN INCHES
--SCALE APPLIES TO FULL SIZE PLOTS ONLY
--ALL INTERNAL THREADS CLASS 2A
--ALL EXTERNAL THREADS CLASS 2B
--ALL DIMENSIONS ±.01
--ALL ANGLES ±1°
DETAIL A
SCALE 2.500
15.7°
.60
.79
1.04
30.00°
R.25
14.30
7.30
7.05
R.125
R.50
R.125
Ø.620
SEE DETAIL A

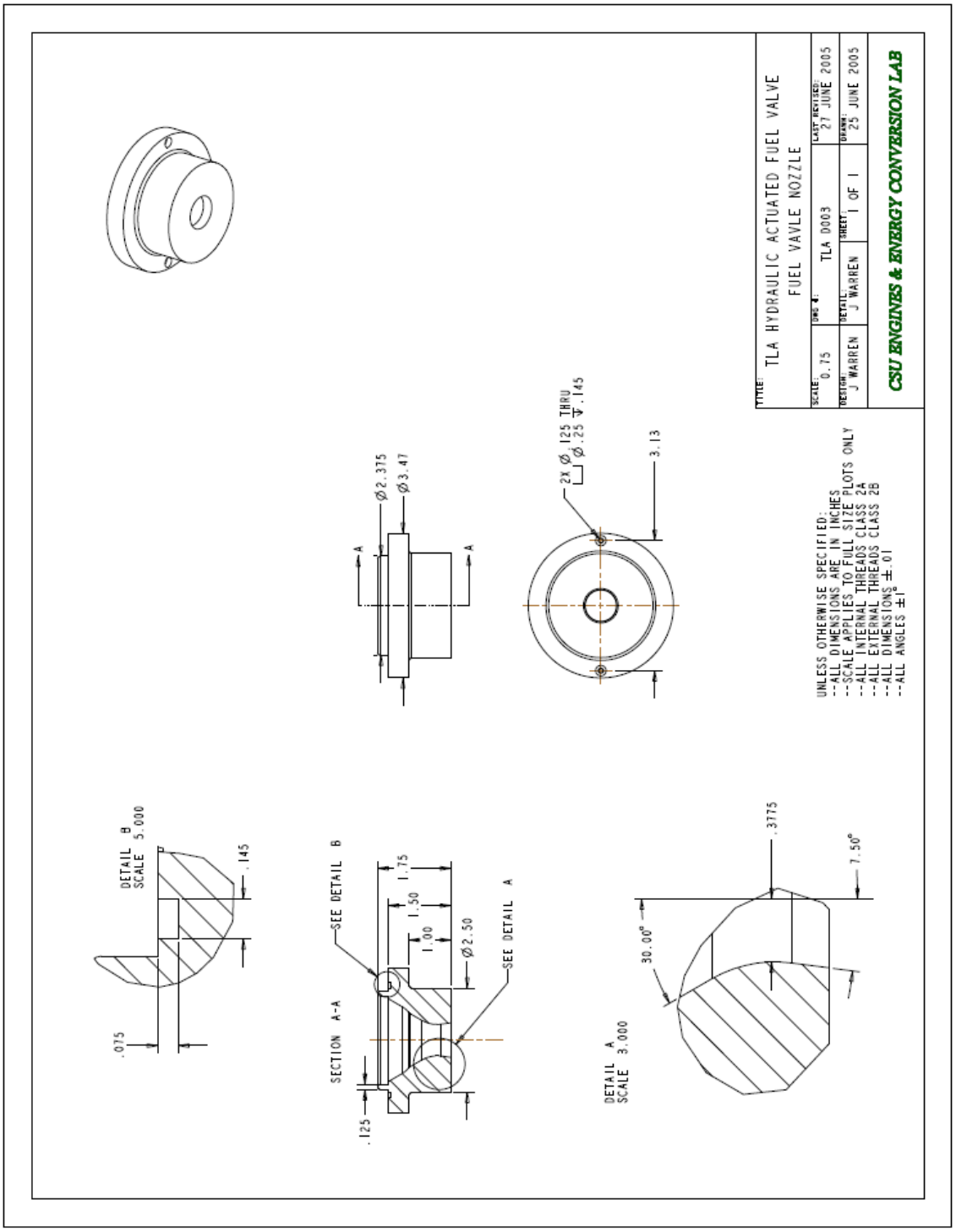
TLA HYDRAULIC ACTUATED FUEL VALVE
FUEL VAVLE NOZZLE
TLA 0003
SCALE: 0.75
SHEET 1 OF 1
DRAWN: J WARREN
DETAIL: J WARREN
LAST REVISED: 27 JUNE 2005
DRAWN: 25 JUNE 2005
CSU ENGINES & ENERGY CONVERSION LAB
UNLESS OTHERWISE SPECIFIED:
--ALL DIMENSIONS ARE IN INCHES
--SCALE APPLIES TO FULL SIZE PLOTS ONLY
--ALL INTERNAL THREADS CLASS 2A
--ALL EXTERNAL THREADS CLASS 2B
--ALL DIMENSIONS ±.01
--ALL ANGLES ±1°
Ø2.375
Ø3.47
2X Ø.125 THRU
Ø.25 ↧.145
3.13
DETAIL B
SCALE 5.000
.145
.075
SECTION A-A
SEE DETAIL B
SEE DETAIL A
1.75
1.50
1.00
Ø2.50
.125
DETAIL A
SCALE 3.000
.3775
7.50°
30.00°

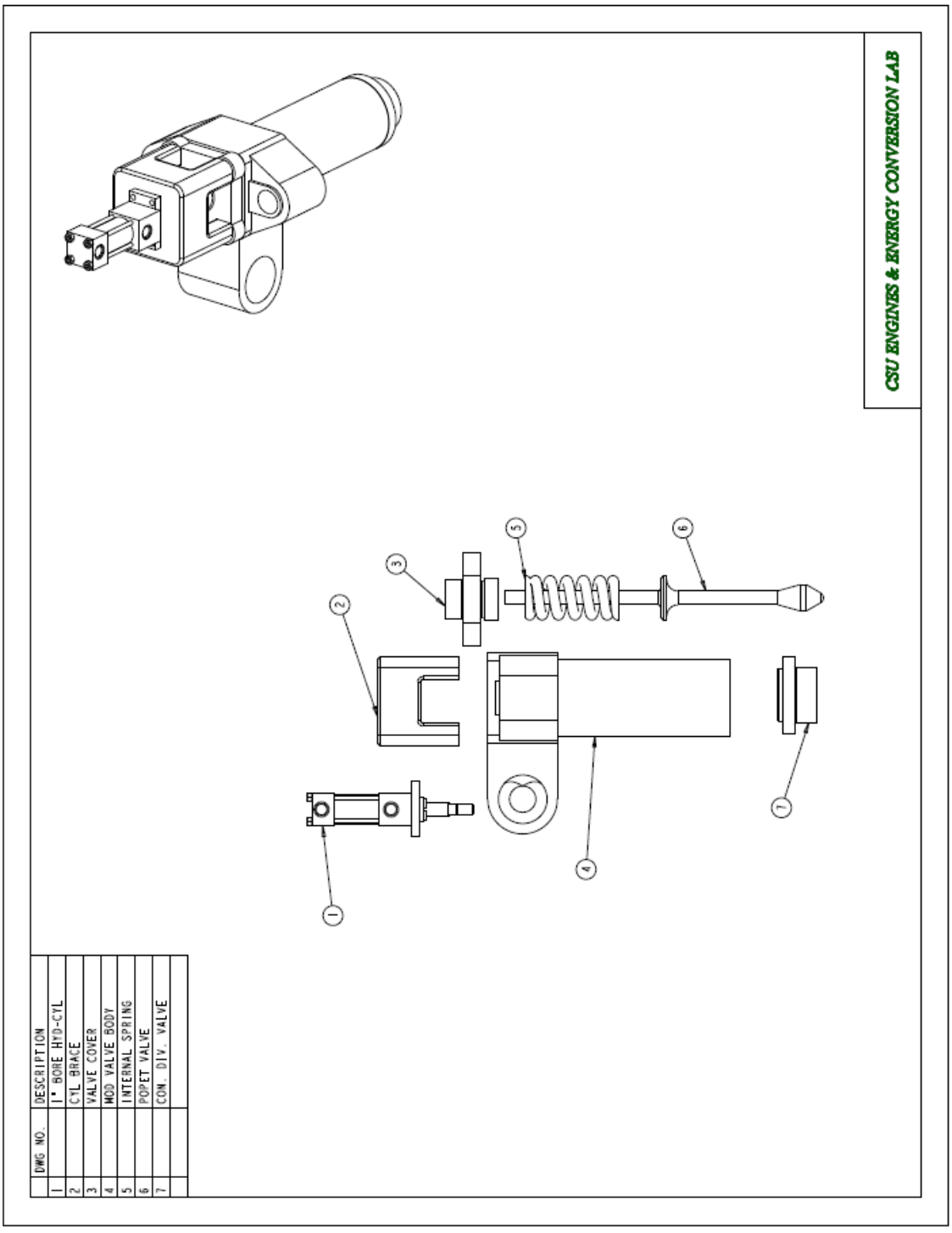
CSU ENGINES & ENERGY CONVERSION LAB
DWG NO.
DESCRIPTION
1" BORE HYD-CYL
CYL BRACE
VALVE COVER
MOD VALVE BODY
INTERNAL SPRING
POPET VALVE
CON. DIV. VALVE
1
2
3
4
5
6
7

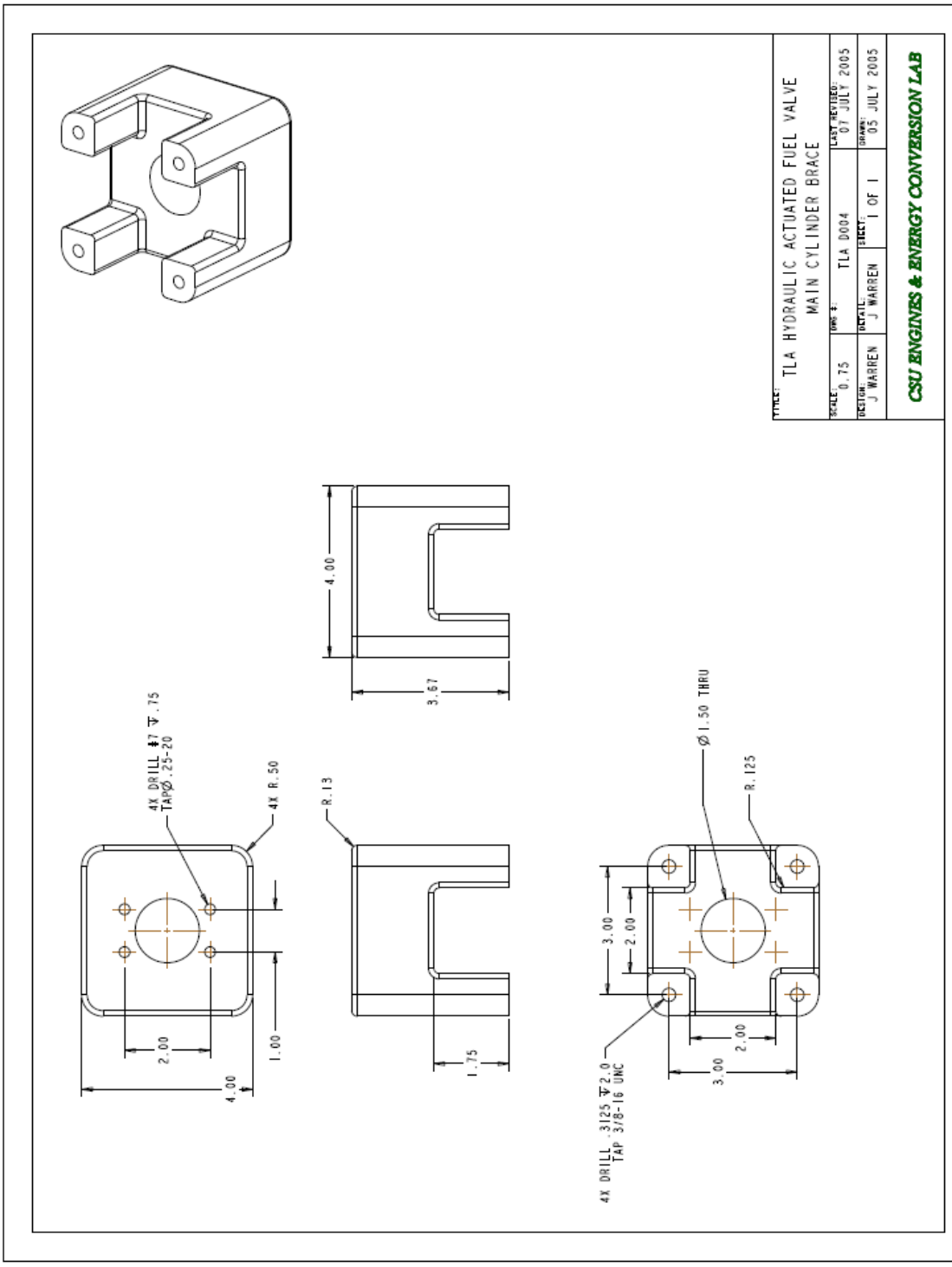
TLA HYDRAULIC ACTUATED FUEL VALVE
MAIN CYLINDER BRACE
SCALE: 0.75
DWG #: TLA 0004
LAST REVISED: 07 JULY 2005
DESIGN: J WARREN
DETAIL: J WARREN
SHEET: 1 OF 1
DRAWN: 05 JULY 2005
CSU ENGINES & ENERGY CONVERSION LAB
4X DRILL #7 ↧.75
TAPØ.25-20
4X R.50
2.00
1.00
4.00
R.13
4.00
3.67
1.75
Ø1.50 THRU
R.125
3.00
2.00
2.00
3.00
4X DRILL .3125 ↧2.0
TAP 3/8-16 UNC

Tie Rod and Rectangular Flange Mountings 1" to 6" Bore Sizes

Series 3L Medium Duty Hydraulic Cylinders

Tie Rods Extended
Style TB
(NFPA Style MX3)

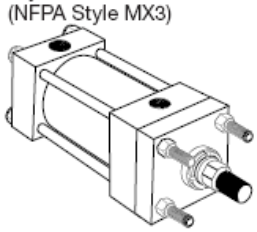

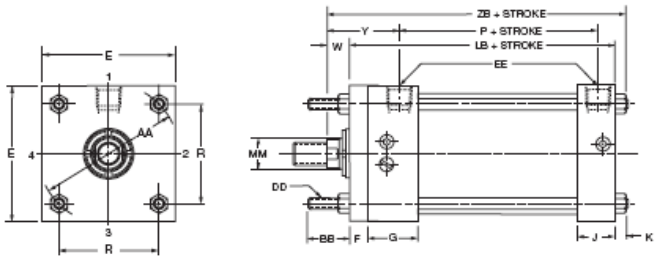

Style TB (NFPA MX3) Head Tie Rods Extended, Illustrated; Style TC (NFPA MX2), Cap Tie Rods Extended; and Style TD (NFPA MX1), Both Ends Tie Rods Extended are also available. All "T" styles can be dimensioned from Style TB drawing at right. Basic Mounting (T) — NFPA MX0 — no tie rods extended can be supplied upon request.

Head Rectangular Flange
Style J
(NFPA Style MF1)

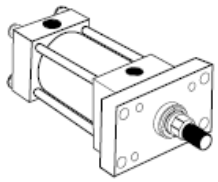

For Style "J" Mount

Bore Size	Max. PSI - Push* Rod Code 1	2	3	4
1	1900	1500	–	–
1 1/2	1400	850	–	–
2	1050	450	900	–
2 1/2	700	350	500	–
3 1/4	1300	900	1300	1000
4	900	700	900	900
5	600	400	700	600
6	700	450	700	700

Bore Size	5	6	7	8
1	–	–	–	–
1 1/2	–	–	–	–
2	–	–	–	–
2 1/2	–	–	700	–
3 1/4	–	–	–	–
4	–	–	900	–
5	450	–	600	900
6	650	600	700	–

*Maximum pressure rating — push application.

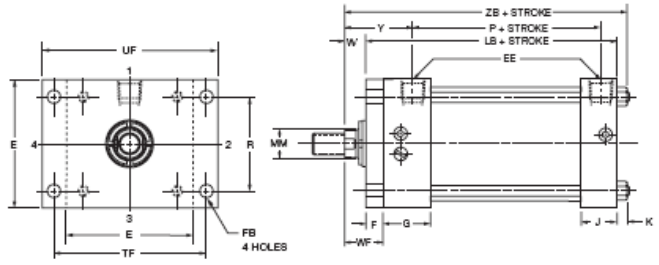

Cap Rectangular Flange
Style H
(NFPA Style MF2)

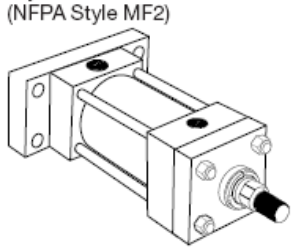

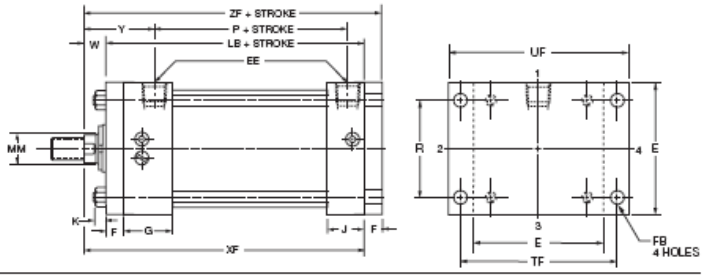

Rod End Dimensions—see table 2

Thread Style 4
(NFPA Style SM)
Small Male

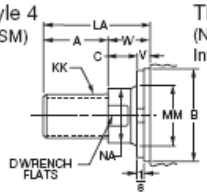

Thread Style 8
(NFPA Style IM)
Intermediate Male

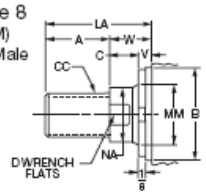

Thread Style 9
(NFPA Style SF)
Small Female

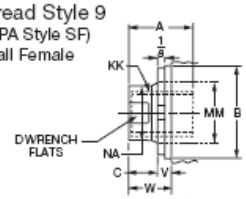

Straight Thread Port Adapters

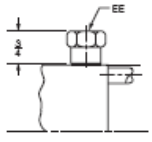

Used on 1½" bore cap end. Also used on 1½" bore with Code 2 rod head end.

A high strength rod end stud is supplied on thread style 4 through 2" diameter rods and on thread style 8 through 1¾" diameter rods. Larger sizes or special rod ends are cut threads. Style 4 rod ends are recommended where the workpiece is secured against the rod shoulder. When the workpiece is not shouldered, style 4 rod ends are recommended through 2" piston rod diameters and style 8 rod ends are recommended on larger diameters. Use style 9 for applications where female rod end threads are required. If rod end is not specified, style 4 will be supplied.

"Specials" Thread Style 3

To order, specify "Style 3" and give desired dimensions for CC or KK, A and LA. If otherwise special, furnish dimensional sketch.

For additional information – call your local Parker Cylinder Distributor.

Series 3L
Medium Duty Hydraulic Cylinders

Tie Rod and Rectangular Flange Mountings 1" to 6" Bore Sizes

Table 1—Envelope and Mounting Dimensions

Bore	AA	BB	DD	E	EE NPTF⊖	EE SAE*	F	FB	G	J	K	R	TF	UF	Add Stroke LB	Add Stroke P
1‡	1.53	3/4	10-24	■	1/4†	6#	3/8	1/4	1 1/2	1	3/16	1.08	2	2 1/2	3 7/8	2 1/8
1 1/2	2.02	1	1/4-28	2	3/8†	6#	3/8	5/16	1 1/2	1	1/4	1.43	2 3/4	3 3/8	4	2 1/4
2	2.6	1 1/8	5/16-24	2 1/2	3/8†	6	3/8	3/8	1 1/2	1	5/16	1.84	3 3/8	4 1/8	4	2 1/4
2 1/2	3.1	1 1/8	5/16-24	3	3/8†	6	3/8	3/8	1 1/2	1	5/16	2.19	3 7/8	4 5/8	4 1/8	2 3/8
3 1/4	3.9	1 3/8	3/8-24	3 3/4	1/2	10	5/8	7/16	1 3/4	1 1/4	3/8	2.76	4 11/16	5 1/2	4 7/8	2 5/8
4	4.7	1 3/8	3/8-24	4 1/2	1/2	10	5/8	7/16	1 3/4	1 1/4	3/8	3.32	5 7/16	6 1/4	4 7/8	2 5/8
5	5.8	1 13/16	1/2-20	5 1/2	1/2	10	5/8	9/16	1 3/4	1 1/4	7/16	4.10	6 5/8	7 5/8	5 1/8	2 7/8
6	6.9	1 13/16	1/2-20	6 1/2	3/4	12	3/4	9/16	2	1 1/2	7/16	4.88	7 5/8	8 5/8	5 3/4	3 1/8

⊖ NPTF ports will be furnished as standard unless SAE straight thread ports are specified.

* SAE straight thread ports are indicated by port number.

‡ Cushion adjusting needle valve for 1" bore projects beyond sides of head and cap.

† On 1", 1 1/4", 2" and 2 1/2" bore sizes, the head end (only) pipe thread is not full depth on cylinders with No. 2 rods. Minimum of 3 full threads available.

■ 1" bore 3L heads are rectangular — see page 20.

Straight thread ports on 1 1/4" bore cap end, and head end with Code 2 rod, require an adapter fitting. (See "Straight Thread Port Adapter" drawing on opposite page.) Adapters are furnished as standard.

Table 2—Rod Dimensions

Bore	Rod No.	Rod Dia. MM	Thread Style 8 CC	Thread Style 4 & 9 KK	Rod Extensions and Pilot Dimensions A	+.000 -.002 B	C	D	LA	NA	V	W
1	1(Std.)	1/2	7/16-20	5/16-24	5/8	.999	3/8	3/8	1 1/4	7/16	1/4	5/8
	2	5/8	1/2-20	7/16-20	3/4	1.124	3/8	1/2	1 3/8	9/16	1/4	5/8
1 1/2	1(Std.)	5/8	1/2-20	7/16-20	3/4	1.124	3/8	1/2	1 3/8	9/16	1/4	5/8
	2	1	7/8-14	3/4-16	1 1/8	1.499	1/2	7/8	2 1/8	15/16	1/2	1
2	1(Std.)	5/8	1/2-20	7/16-20	3/4	1.124	3/8	1/2	1 3/8	9/16	1/4	5/8
	2	1 3/8	1 1/4-12	1-14	1 5/8	1.999	5/8	1 1/8	2 7/8	1 5/16	5/8	1 1/4
	3	1	7/8-14	3/4-16	1 1/8	1.499	1/2	7/8	2 1/8	15/16	1/2	1
2 1/2	1(Std.)	1	7/8-14	3/4-16	1 1/8	1.499	1/2	7/8	2 1/8	15/16	1/2	1
	2	1 3/4	1 1/2-12	1 1/4-12	2	2.374	3/4	1 1/2	3 1/2	1 11/16	3/4	1 1/2
	3	1 3/8	1 1/4-12	1-14	1 5/8	1.999	5/8	1 1/8	2 7/8	1 5/16	5/8	1 1/4
	7	5/8	1/2-20	7/16-20	3/4	1.124	3/8	1/2	1 3/8	9/16	1/4	5/8
3 1/4	1(Std.)	1	7/8-14	3/4-16	1 1/8	1.499	1/2	7/8	1 7/8	1 5/16	1/4	3/4
	2	2	1 3/4-12	1 1/2-12	2 1/4	2.624	7/8	1 11/16	3 5/8	1 15/16	1/2	1 3/8
	3	1 3/8	1 1/4-12	1-14	1 5/8	1.999	5/8	1 1/8	2 5/8	1 5/16	3/8	1
	4	1 3/4	1 1/2-12	1 1/4-12	2	2.374	3/4	1 1/2	3 1/4	1 11/16	1/2	1 1/4
4	1(Std.)	1 3/8	1 1/4-12	1-14	1 5/8	1.999	5/8	1 1/8	2 5/8	1 5/16	3/8	1
	2	2 1/2	2 1/4-12	1 7/8-12	3	3.124	1	2 1/16	4 5/8	2 3/8	5/8	1 5/8
	3	1 3/4	1 1/2-12	1 1/4-12	2	2.374	3/4	1 1/2	3 1/4	1 11/16	1/2	1 1/4
	4	2	1 3/4-12	1 1/2-12	2 1/4	2.624	7/8	1 11/16	3 5/8	1 15/16	1/2	1 3/8
	7	1	7/8-14	3/4-16	1 1/8	1.499	1/2	7/8	1 7/8	1 5/16	1/4	3/4
5	1(Std.)	1 3/4	1 1/2-12	1 1/4-12	2	2.374	3/4	1 1/2	3 1/4	1 11/16	1/2	1 1/4
	2	3 1/2	3 1/4-12	2 1/2-12	3 1/2	4.249	1	3	5 1/8	3 3/8	5/8	1 5/8
	3	2	1 3/4-12	1 1/2-12	2 1/4	2.624	7/8	1 11/16	3 5/8	1 15/16	1/2	1 3/8
	4	2 1/2	2 1/4-12	1 7/8-12	3	3.124	1	2 1/16	4 5/8	2 3/8	5/8	1 5/8
	5	3	2 3/4-12	2 1/4-12	3 1/2	3.749	1	2 5/8	5 1/8	2 7/8	5/8	1 5/8
	7	1	7/8-14	3/4-16	1 1/8	1.499	1/2	7/8	1 7/8	1 5/16	1/4	3/4
	8	1 3/8	1 1/4-12	1-14	1 5/8	1.999	5/8	1 1/8	2 5/8	1 5/16	3/8	1
6	1(Std.)	1 3/4	1 1/2-12	1 1/4-12	2	2.374	3/4	1 1/2	3 1/8	1 11/16	3/8	1 1/8
	2	4	3 3/4-12	3-12	4	4.749	1	3 3/8	5 1/2	3 7/8	1/2	1 1/2
	3	2	1 3/4-12	1 1/2-12	2 1/4	2.624	7/8	1 11/16	3 1/2	1 15/16	3/8	1 1/4
	4	2 1/2	2 1/4-12	1 7/8-12	3	3.124	1	2 1/16	4 1/2	2 3/8	1/2	1 1/2
	5	3	2 3/4-12	2 1/4-12	3 1/2	3.749	1	2 5/8	5	2 7/8	1/2	1 1/2
	6	3 1/2	3 1/4-12	2 1/2-12	3 1/2	4.249	1	3	5	3 3/8	1/2	1 1/2
	7	1 3/8	1 1/4-12	1-14	1 5/8	1.999	5/8	1 1/8	2 1/2	1 5/16	1/4	7/8

Table 3—Envelope and Mounting Dimensions

Bore	WF	Y	Add Stroke XF	Add Stroke ZB	Add Stroke ZF
1	1	1 15/16	4 1/2	4 11/16	4 7/8
	1	1 15/16	4 1/2	4 11/16	4 7/8
1 1/2	1	1 15/16	4 5/8	4 7/8	5
	1 3/8	2 5/16	5	5 1/4	5 3/8
2	1	1 15/16	4 5/8	4 15/16	5
	1 5/8	2 9/16	5 1/4	5 9/16	5 5/8
	1 3/8	2 5/16	5	5 5/16	5 3/8
2 1/2	1 3/8	2 5/16	5 1/8	5 7/16	5 1/2
	1 7/8	2 13/16	5 5/8	5 15/16	6
	1 5/8	2 9/16	5 3/8	5 11/16	5 3/4
	1	1 15/16	4 3/4	5 1/16	5 1/8
3 1/4	1 3/8	2 7/16	5 5/8	6	6 1/4
	2	3 1/16	6 1/4	6 5/8	6 7/8
	1 5/8	2 11/16	5 7/8	6 1/4	6 1/2
	1 7/8	2 15/16	6 1/8	6 1/2	6 3/4
4	1 5/8	2 11/16	5 7/8	6 1/4	6 1/2
	2 1/4	3 5/16	6 1/2	6 7/8	7 1/8
	1 7/8	2 15/16	6 1/8	6 1/2	6 3/4
	2	3 1/16	6 1/4	6 5/8	6 7/8
	1 3/8	2 7/16	5 5/8	6	6 1/4
5	1 7/8	2 15/16	6 3/8	6 13/16	7
	2 1/4	3 5/16	6 3/4	7 3/16	7 3/8
	2	3 1/16	6 1/2	6 15/16	7 1/8
	2 1/4	3 5/16	6 3/4	7 3/16	7 3/8
	2 1/4	3 5/16	6 3/4	7 3/16	7 3/8
	1 3/8	2 7/16	5 7/8	6 5/16	6 1/2
	1 5/8	2 11/16	6 1/8	6 9/16	6 3/4
6	1 7/8	3 1/16	6 7/8	7 5/16	7 5/8
	2 1/4	3 7/16	7 1/4	7 11/16	8
	2	3 3/16	7	7 7/16	7 3/4
	2 1/4	3 7/16	7 1/4	7 11/16	8
	2 1/4	3 7/16	7 1/4	7 11/16	8
	2 1/4	3 7/16	7 1/4	7 11/16	8
	1 5/8	2 13/16	6 5/8	7 1/16	7 3/8

For Cylinder Division Plant Locations – See Page II.

Parker Cylinder

Series 3L Model Numbers – How to Develop Them – How to "Decode" Them

Parker Series 3L cylinders can be completely and accurately described by a model number consisting of coded symbols. To develop a model number, select only those symbols that represent the cylinder required, and place them in the sequence indicated below.

Note: Page numbers with a letter prefix, ie: C77, are located in section C of this catalog.

Feature	Description	Page No.	Symbol
Bore*	Specify in inches	—	—
Cushion-Head	Used only if cushion required	6	C
Double-Rod	Used only if double-rod cylinder is required	32	K
Mounting* Style	Head Tie Rods Extended	8 & 22	TB
	Cap Tie Rods Extended	8 & 22	TC
	Both End Tie Rods Extended	8 & 22	TD
	Head Rectangular Flange	8	J
	Cap Rectangular Flange	8	H
	Head Square Flange	10 & 22	JB
	Cap Square Flange	10 & 22	HB
	Side Lugs	12 & 24	C†
	Centerline Lugs	12 & 24	E
	Side Tapped	14 & 24	F†
	Side End Lugs	14 & 26	G†
	Head Trunnion	16 & 28	D
	Cap Trunnion	16 & 28	DB
	Intermediate Fixed Trunnion‡	16 & 28	DD
	Cap Fixed Clevis	18 & 26	BB
	Cap Detachable Clevis	18	BC
	Spherical Bearing	30 & 31	SB
	Head Rectangular	20	JJ
Mounting Modifications	Used only for Thrust Key (Styles C, F & G)	C93	P
	Used only for Manifold Port O-Ring Seal (Style C)	C91	M
Combination Mounting Style	Any Practical Mounting Style	–	AS
	Listed Above	–	listed above
		–	
Series*	Used in all 3L Model Numbers	–	–3L
Piston	Ring packed piston is standard.	–	C
	Use only for Lipseal® Piston.	6 & 7	L
Ports*	SAE Straight Thread O-Ring Port	C89	T
	Used only for NPTF (Dry Seal Pipe Thread)	C89	U
	Used only for BSP (Parallel Thread ISO 228)	C89	R
	Used only for BSPT (Taper Thread)	C89	B
	Used only for Metric Thread	C89	G
	Used only for Metric Thread per ISO 6149	C89	Y
Common Modifications	High Water Content Fluid	C83	J
	Nut Retained Piston	7	F
	Fluorocarbon Seals	C83	V
	Water Service	C83	W
	EPR Seals	C83	X
Special Modifications	Used only if special Modifications are required: Oversize Ports	C91	S
	Port Position Change	C89	
	Rod End Bellows	C104	
	Special Seals	C83	
	Stop Tube*	C95	
	Stroke Adjuster	C93	
	Tie Rod Supports	C93	
Piston Rod* Number	For Single Rod Cylinders, select one only.	–	1
	Refer to Rod number listing, Table 2,	–	2
	Catalog Pages 8 through 27.	–	3
	See chart in Section C, page 83 for	–	4
	minimum piston rod diameter	–	5
		–	6
		–	7
		–	8
		–	9
		–	0
Piston* Rod End	Select:		
	Style 4 Small Male	C92	4
	Style 7 Female Thread for Spherical Rod Eye	B30, 31	7
	Style 8 Intermediate Male	C92	8
	Style 9 Short Female	C92	9
	Style 55 Rod End for Flange Coupling	C19	55
	Style 3 Special (Specify)	C92	3
Piston Rod Alternate Thread	Used only for stud two times longer than standard.	C92	2
Piston Rod* Threads	UNF Standard	C92	A
	BSF (British Fine)	C92	W
	Metric	C92	M
Cushion-Cap	Used only if cushion required	6	C
Stroke**	Specify in inches	C96	–

6" C K F P TB –3L L T V S 1 4 2 A C 12"

Use Symbol S to designate any special modification except piston rod end.

Styles 4, 8, and 9 are catalog standards
Specify Style 3 for any special piston rod end.

Double Rod Cylinders
For double rod cylinders, specify rod number and rod end symbols for both piston rods. A typical double rod model number would be:
6" KJ-3LU14A/14AX12"

Cylinder serial numbers are factory production record numbers and are assigned to each cylinder, in addition to the model number.

*Required for Basic Cylinder Model Number
*In case of Stop Tube, call out Gross Stroke Length

†Cylinders with these mounting styles should have a minimum stroke length equal to or greater than their bore size.

Dark Arrows Indicate Basic Minimum Model Number

‡Specify XI dimension

For Cylinder Division Plant Locations – See Page II.

Parker Cylinder

1-800-237-5225
Fax (213) 749-3802
www.centuryspring.com

DIE SPRINGS

Century Spring offers a complete line of die springs in both oil-tempered and chrome-alloy materials. Die springs are used primarily in die machinery. They are, however, well-suited for many applications where high-static or shock-load stresses are required, or when maximum cycle-life is important.

Selecting a Die Spring:

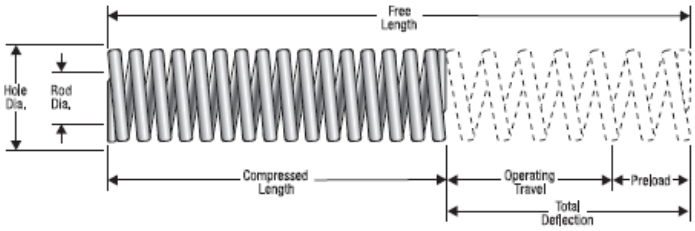

- If the application is for a die set, always use as many springs as the die will accommodate to produce the required load and cause the least amount of deflection. This will increase the service-life and reduce the chances of early failure.
- Decide if the springs will be used for short or long runs, average or high-frequency cycling, or high stress in order to select the duty-level capability found in the following pages of inventory.
- The higher the rate of cycling, the higher the rate of fatigue-caused failures. In slow-oscillating dies or fixtures, it is possible to get good performance with springs operating near maximum deflection. As the working speed increases, the life expectancy of the spring at that deflection decreases.

The following figure indicates how the load-carrying capability of the die spring increases by scanning through the color code range of the 3-inch long spring's increasing duty capability.

Note the suggested maximum deflections expressed as percentages of free length. These guideline limits are important for extended service-life.

RATE-POUNDS PER INCH OF DEFLECTION

Hole Size	Rod Size	Free Length	LD (Blue)	MD (Red)	HD (Gold)	XHD (Green)
3/8"	3/16"	3"	180	30	42	65
1/2"	9/32"	3"	40	57	74	90
5/8"	11/32"	3"	56	100	144	180
3/4"	3/8"	3"	96	144	312	405
1"	1/2"	3"	152	232	544	736
1-1/4"	5/8"	3"	240	512	952	1184
1-1/2"	3/4"	3"	336	624	1224	2312
2"	1"	3"	768	960	1856	3120
High Cycle Life Range % of Length			25% to 35%	20% to 25%	15% to 20%	15%
Suggested Maximum Deflection % of Length			50%	37%	30%	25%

1-800-237-5225
Fax (213) 749-3802
www.centuryspring.com

Spring Characteristics

Holes and Rod Diameter

The die-spring-containment-hole diameter sizes tabulated in the following pages of inventory must be considered to eliminate possible spring-to-wall friction-caused heat, wear due to fabrication tolerances, and interference from the spring-diameter growth due to compression. If the spring is long for its diameter, an internal supporting rod may be required to eliminate spring buckling.

Heat

Thermal effects are frequently ignored in spring-failure or load-loss analysis. The maximum rated service temperature for chrome-alloy steel is about 440° F. The following table reflects the approximate load losses due to heat that can be expected with die springs.

Stress Determination

The die wire stress can be estimated with the rectangular wire equation:

$$S = \frac{PD}{bt\sqrt{bt}}\ \beta \qquad \text{(p.s.i.)}$$

Where: **P** = Load, Lbs.
D = Mean coil diameter, (O.D.-d) inches
b = Wire width (radially), inches
t = Wire thickness, inches
β = Stress-correction factor, see below

LOAD LOSS DUE TO TEMPERATURE

STRESS P.S.I.	CARBON STEEL SAE-1070				CHROME ALLOY STEEL				
	Approximate Percent Loss of Load				Approximate Percent Loss of Load				
	Degrees Fahrenheit				Degrees Fahrenheit				
	250	300	350	400	250	300	350	400	450
120,000	10	12	13	18	6	7	9	10	13
110,000	7	9	12	14	4	6	7	8	12
100,000	5	7	10	11	3	4	5	6	11
90,000	4	6	8	9	2	3	4	5	10
80,000	3	5	6	8	2	2	3	4	9
70,000	3	4	6	7	2	2	3	4	8
60,000	3	4	5	6	1	1	3	4	7
50,000	2	3	4	5	1	1	3	3	6
40,000	2	3	4	5	1	1	2	3	5

Stress Factor β for rectangular wire (b and t as shown)

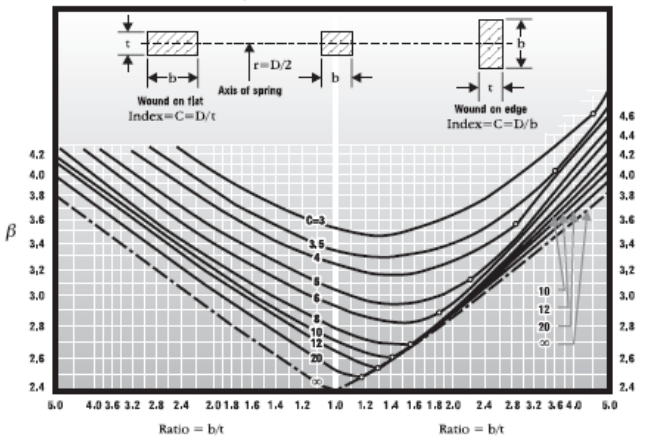

Material

All of our die springs are fabricated from the most efficient wire cross section, which is rectangular with rounded corners. The oil-tempered die springs are offered for die sets and general use at a reduced cost. A very long service life may be expected from oil-tempered springs if their maximum deflection is held to about 25 percent of their length. The highest grade of electrically-furnaced, shot-peened and preset chrome-alloy steel die springs are offered for unsurpassed quality.

Material certification available only with custom-made die springs manufactured to print or specifications.

Finish

Die springs of oil-tempered material are available as unfinished only. A color-coding system is employed for our chrome-alloy line for instant visual identification of the spring's work range and to prevent errors in spring selection and installation. The color coding is a light coating of water-based paint.

COLOR	RANGE
Blue	Light duty
Red	Medium duty
Gold	Heavy duty
Green	Extra heavy duty

1-800-237-5225
Fax (213) 749-3802
www.centuryspring.com

DIE SPRINGS *EXTRA HEAVY-DUTY CHROME ALLOY (GREEN)*

CENTURY STOCK NUMBER	HOLE SIZE (Inches)	ROD SIZE (Inches)	WIRE DIA (Inches)	FREE LENGTH (Inches)	RATE (Lbs./In.)	APPROX. MAX. DEFLECTION* 25% OF FREE LENGTH FORCE LBS.	DEFL. IN.	DEFLECTION FOR AVERAGE LIFE 17% OF FREE LENGTH FORCE LBS.	DEFL. IN.	DEFLECTION FOR LONG LIFE 15% OF FREE LENGTH FORCE LBS.	DEFL. IN.
D-1401				1.00	220	55	.25	44	.20	33	.15
D-1402				1.25	170	53	.31	43	.25	32	.19
D-1403	3/8	3/16	.080	1.50	125	54	.38	44	.30	33	.23
D-1404			X	1.75	115	50	.44	40	.35	30	.26
D-1405	.375	.187	.059	2.00	100	50	.50	40	.40	30	.30
D-1406				2.50	80	50	.63	40	.50	30	.38
D-1407				3.00	65	49	.75	39	.60	29	.45
D-1408				12.00	15	45	3.00	36	2.40	27	1.80
D-1409				1.00	320	80	.25	64	.20	48	.15
D-1410				1.25	240	75	.31	60	.25	45	.19
D-1411				1.50	200	75	.38	60	.30	45	.23
D-1412	1/2	9/32	.097	1.75	170	74	.44	60	.35	45	.26
D-1413			X	2.00	140	70	.50	56	.40	42	.30
D-1414	.500	.281	.084	2.50	115	72	.63	58	.50	43	.38
D-1415				3.00	90	68	.75	54	.60	41	.45
D-1416				3.50	80	70	.88	56	.70	42	.53
D-1417				12.00	25	75	3.00	60	2.40	45	1.80
D-1418				1.00	630	158	.25	126	.20	95	.15
D-1419				1.25	470	147	.31	118	.25	88	.19
D-1420				1.50	380	143	.38	114	.30	86	.23
D-1421				1.75	320	140	.44	112	.35	84	.26
D-1422	5/8	11/32	.126	2.00	290	145	.50	116	.40	87	.30
D-1423			X	2.50	220	138	.63	110	.50	83	.38
D-1424	.625	.344	.110	3.00	180	135	.75	108	.60	81	.45
D-1425				3.50	160	140	.88	112	.70	84	.53
D-1426				4.00	135	135	1.00	108	.80	81	.60
D-1427				12.00	45	135	3.00	108	2.40	81	1.80
D-1428				1.00	1400	350	.25	280	.20	210	.15
D-1429				1.25	1100	344	.31	275	.25	207	.19
D-1430				1.50	890	334	.38	267	.30	200	.23
D-1431				1.75	750	329	.44	263	.35	197	.26
D-1432				2.00	635	318	.50	254	.40	191	.30
D-1433	3/4	3/8	.165	2.50	500	313	.63	250	.50	188	.38
D-1434			X	3.00	405	304	.75	243	.60	182	.45
D-1435	.750	.375	.135	3.50	345	302	.88	242	.70	181	.53
D-1436				4.00	300	300	1.00	240	.80	180	.60
D-1437				4.50	265	298	1.13	239	.90	179	.68
D-1438				5.00	235	294	1.25	235	1.00	176	.75
D-1439				5.50	215	296	1.38	237	1.10	177	.83
D-1440				6.00	195	293	1.50	234	1.20	176	.90
D-1441				12.00	95	285	3.00	228	2.40	171	1.80
D-1442				1.50	1848	693	.38	554	.30	416	.23
D-1443				2.00	1160	580	.50	464	.40	348	.30
D-1444				2.50	896	560	.63	448	.50	336	.38
D-1445	1	1/2	.225	3.00	736	552	.75	442	.60	331	.45
D-1446			X	3.50	624	546	.88	437	.70	328	.53
D-1447	1.000	.500	.188	4.00	552	552	1.00	442	.80	331	.60
D-1448				4.50	488	549	1.13	439	.90	329	.68
D-1449				5.00	432	540	1.25	432	1.00	324	.75
D-1450				6.00	360	540	1.50	432	1.20	324	.90
D-1451				12.00	176	528	3.00	422	2.40	317	1.80
D-1452				2.00	1920	960	.50	768	.40	576	.30
D-1453				2.50	1440	900	.63	720	.50	540	.38
D-1454				3.00	1184	888	.75	710	.60	533	.45
D-1455				3.50	1008	882	.88	706	.70	529	.53
D-1456	1-1/4	5/8	.295	4.00	840	840	1.00	672	.80	504	.60
D-1457			X	4.50	784	882	1.13	706	.90	529	.68
D-1458	1.250	.625	.225	5.00	680	850	1.25	680	1.00	510	.75
D-1459				6.00	560	840	1.50	672	1.20	504	.90
D-1460				8.00	416	832	2.00	666	1.60	499	1.20
D-1461				10.00	336	840	2.50	672	2.00	504	1.50
D-1462				12.00	264	792	3.00	634	2.40	475	1.80
D-1463				2.00	3760	1880	.50	1504	.40	1128	.30
D-1464				2.50	2944	1840	.63	1472	.50	1104	.38
D-1465				3.00	2312	1734	.75	1387	.60	1040	.45
D-1466				3.50	1960	1715	.88	1372	.70	1029	.53
D-1467	1-1/2	3/4	.350	4.00	1712	1712	1.00	1370	.80	1027	.60
D-1468			X	4.50	1480	1665	1.13	1332	.90	999	.68
D-1469	1500	.750	.300	5.00	1360	1700	1.25	1360	1.00	1020	.75
D-1470				6.00	1104	1656	1.50	1325	1.20	994	.90
D-1471				8.00	808	1616	2.00	1293	1.60	970	1.20
D-1472				10.00	672	1680	2.50	1344	2.00	1008	1.50
D-1473				12.00	544	1632	3.00	1306	2.40	979	1.80
D-1474				2.50	3816	2385	.63	1908	.50	1431	.38
D-1475				3.00	3120	2340	.75	1872	.60	1404	.45
D-1476				3.50	2544	2226	.88	1781	.70	1336	.53
D-1477				4.00	2200	2200	1.00	1760	.80	1320	.60
D-1478	2	1	.460	4.50	1888	2124	1.13	1699	.90	1274	.68
D-1479			X	5.00	1728	2160	1.25	1728	1.00	1296	.75
D-1480	2.000	1.000	.365	6.00	1416	2124	1.50	1699	1.20	1274	.90
D-1481				8.00	1000	2000	2.00	1600	1.60	1200	1.20
D-1482				10.00	840	2100	2.50	1680	2.00	1260	1.50
D-1483				12.00	712	2136	3.00	1709	2.40	1282	1.80

* Loads near solid lengths for reference only; overstressed condition.